UNIVERSIDAD AUTÓNOMA DE MADRID

Facultad de Ciencias

Departamento de Biología Molecular

Design and construction of synthetic adhesins driving the specific attachment of *Escherichia coli* to target surfaces, cells, and tumors

Doctoral Thesis

Carlos Piñero Lambea

Madrid 2014

Tesis presentada por D. Carlos Piñero Lambea para optar al grado de Doctor en Ciencias por la Universidad Autónoma de Madrid.

Directores de la Tesis Doctoral:

Dr. Luis Ángel Fernández Herrero, Investigador Científico del Consejo Superior de Investigaciones Científicas.

Dr. Gustavo Bodelón González, Investigador contratado del Consejo Superior de Investigaciones Científicas.

Este trabajo ha sido realizado en el Departamento de Biotecnología Microbiana del Centro Nacional de Biotecnología del Consejo Superior de Investigaciones Científicas (CNB-CSIC), gracias a una beca de formación de personal investigador (BES-2009-024051) y a la financiación de distintos proyectos de investigación recibida del Ministerio de Economía y Competitividad (BIO2011-26689), la Comunidad Autónoma de Madrid (S2010-BMD-2312) y el *European Research Council* (ERC-2012-ADG_20120314).

AGRADECIMIENTOS

Hace casi cinco años desde la primera vez que pise el CNB, han sido unos años increíbles que me han permitido crecer tanto en el plano personal como en el científico, y sin duda todo eso tengo que agradecérselo a la gente que he tenido la oportunidad de conocer estos años, porque sin ellos esta tesis no habría sido posible.

En primer lugar, a mi director de tesis, Luis Ángel Fernández, que confió en mi y me dio la oportunidad de trabajar en un proyecto increíble que tardó cinco minutos en “venderme”. Eres un científico con ideas brillantes, pero sobre todo eres un gran jefe y una mejor persona, siempre con una buena cara y una frase con la que animar. Si algo me llevo de ti es el gusto por las cosas bien hechas. Te mereces que todo te vaya muy bien. Muchas gracias por todo.

Evidentemente a mi codirector de tesis, Gustavo Bodelón, al que siempre he considerado un compañero. Con él di mis primeros pasos en el laboratorio, y por tanto de él he aprendido la inmensa mayoría de lo que sé. La Ciencia necesita de gente como tú, con esa capacidad de trabajo y sobre todo esa ilusión y ese optimismo.

A mis compañeros antiguos (Ana, Elvira, Carmen) y actuales (David, Vally, Massiel, Carmen Bea y Yago), así como a todos los que transitoriamente han pasado por el 241 (Alberto, Lorenza, Ari e Isabel). En el 241 los problemas son de todos, y poder solucionarlos entre todos es un lujo. Ha sido un placer compartir estos años y poder aprender de cada uno de vosotros, no tengo duda de que cuando salgáis del CNB os espera un gran futuro.

A la gente del laboratorio 280 (Álvaro, Juanjo, Diana, Estel), por su ayuda y por siempre sonreír ante la enésima petición de una P24. A la gente del antiguo del 211 (Noelia, Coloma, Alexandro, Couce, Claudia, Elva, Jasmina), por tener ese ambiente tan propenso a la discusión científica. A Paolo y Cris del 217 y Alejandra del 212, por no quedarse en el protocolario saludo de pasillo.

A toda la gente que trabaja en el CNB y hace que todo sea mas fácil (Yolanda, Juancar, Angelines etc.). No les agradecemos lo suficiente su predisposición a ayudar y su buena cara. Mención aparte merecen Sylvia del servicio de Confocal por su infinita ayuda, y Javi de Animalario, siempre dispuesto a echar una mano cuando me veía agobiado.

A Luis Álvarez Vallina y todo su equipo del Hospital Puerta de Hierro, en especial a Ángel Cuesta y Rodrigo Fernández, porque con ellos di mis primeros pasos en experimentos *in vivo* y fueron grandes maestros.

A Jean-Marc Ghigo y Christophe Beloin, que me dieron la oportunidad de visitar durante tres meses su laboratorio en el Institut Pasteur, y aprender como funcionan las cosas mas allá del CNB. A toda la gente con la que coincidí allí y me hicieron sentir tan cómodo (Chantal, Fanny, Chizu, David, Bianca, Fran, Sylvie y Ashwini). A Marta, Joaquín y Jose, que "me adoptaron", me sacaron del bucle residencia-laboratorio y me enseñaron a disfrutar Paris.

Al servicio de Genómica del CNB, la Genopole del Institut Pasteur y al grupo del Dr. José Antonio Bengoechea, por su colaboración en algunos de los experimentos de esta tesis.

A todos mis compañero de carrera (Rincho, Hugo, Pablulu, Manolo, Carol, Ainhoa, Paloma, Ana, Paula, Pauli, Isa, Maribel, Almu, Gon, Jaime) y alguno más que seguro me olvido, por ser gente entrañable a la que veo menos de lo que me gustaría porque se me van muy lejos. Da igual donde estemos, en las casas rurales se seguirán creando esas atmosferas de euforia colectiva. De este grupo de compañeros han quedado excluidos intencionadamente Djordje y Jero. Tener la oportunidad de trabajar a diez metros de dos de tus mejores amigos es algo que todo el mundo debería experimentar, no tiene precio y lo recordaré siempre.

A mis amigos no biólogos (Sara, Irene, Ana, Alba, Carmen, Juanan, Miguel Ángel y Adrián), por hacerme ver lo entretenido que es mi trabajo cuando uno pierde la perspectiva.

A mis padres, que siempre han confiado en mi y me han dado la libertad de hacer lo que he querido, sin vuestro apoyo esta tesis no habría sido posible. Os admiro y me siento muy orgulloso de vosotros. A mi hermano, que siempre ha sido un ejemplo que seguir, me has enseñado mas cosas de las que puedas imaginar. A Otto, que ha sufrido como el que más los días que llegaba de mal humor porque algo no salía. Al resto de mi familia (tíos/tías, primos/primas, yaya), por siempre mostrar interés en eso que estaba haciendo aunque no lo entendieran muy bien.

Por ultimo, pero no por ello menos importante, a Alicia, porque esta tesis es mitad mía y mitad tuya, porque la hemos sufrido los dos. Gracias por estar siempre a mi lado, ya fuera estando en Madrid o en Brescia siempre te sentí muy cerca. Por entenderme mejor de lo que yo mismo lo hago. En definitiva gracias por ser tu. No sé que nos depara el futuro, pero contigo cerca no puede ser nada malo.

TABLE OF CONTENTS

LIST OF FIGURES

LIST OF TABLES

ABBREVIATIONS

aa	amino-acid
Ab	Antibody
Ap	Ampicillin
APEx	Anchored periplasmic expression
AT	Autotransporter
BAM	β-barrel assembly machinery
BCA	Bicinchoninic acid
BDEPT	Bacterial-directed enzyme prodrug therapy
bp	base pair
CD	Cytosine deaminase
CDR	Complementarity determining region
CH	Constant domain of the heavy chain of an immunoglobulin
CL	Constant domain of the light chain of an immunoglobulin
Cm	Chloramphenicol
DAPI	4',6-diamidino-2-fenindol
DEPC	Diethylpyrocarbonate
DMEM	Dulbecco´s modified Eagle´s medium
DNA	Deoxyribonucleic acid
DNAse	DNA ribonuclease
EDTA	Ethylenediaminetetraacetic acid
EGFR	Epidermal growth factor receptor
EHEC	Enterohaemorrhagic *Escherichia coli*
ELISA	Enzyme-linked immunosorbent assay
EPEC	Enteropathogenic *Escherichia coli*
FACS	Fluorescence activated cell sorting
FBS	Fetal bovine serum
Fc	Crystallizable constant fragment of Ab
Fib	Human Fibrinogen
Fv	Variable fragment of an Ab
GFP	Green fluorescent protein
h	hour
HCAb	Heavy chain only Ab
Ig	Immunoglobulin

IM	Inner membrane
IPTG	Isopropylthio-β-D-galactoside
kDa	kiloDalton
Km	Kanamycin
LB	Luria-Bertani medium
LPS	Lipopolysaccharide
mAb	Monoclonal Ab
mRNA	messenger RNA
μg	microgram
μl	microliter
μm	micrometer
μM	micromolar
mg	milligram
ml	milliliter
mm	millimeter
mM	millimolar
min	minute
MOI	Multiplicity of infection
nm	nanometer
OD_{600}	Optical density at 600nm
OMV	Outer membrane vesicle
ORF	Open reading frame
PAGE	Polyacrylamide gel electrophoresis
PBS	Phosphate buffered saline
PCR	Polymerase chain reaction
PG	Peptidoglycan
POD	Peroxidase
RBS	Ribosome binding site
RNA	Ribonucleic acid
RNAse	RNA ribonuclease
rpm	revolutions per minute
rRNA	ribosomal RNA
SA	Synthetic adhesin
scFv	single chain fragment variable
sdAb	single domain antibody
SDS	Sodium dodecyl sulphate

shRNA	Short hairpin RNA
siRNA	Small interfering RNA
T5SS	Type V secretion system
TE	Tris-EDTA
TEM	Transmission electron microscopy
Tir	Translocated intimin receptor
TirM	Extracellular domain of Tir
TK	Thymidine kinase
tm	transmembrane
TNF	Tumor necrosis factor
TRAIL	Tumor necrosis factor-related apoptosis-inducing ligand
tRNA	transfer RNA
VH	Variable domain of the heavy chain of an Ig
VHH	Variable domain of the heavy chain of a HCAb, also termed Nanobody
VL	Variable domain of the light chain of an Ig
WT	Wild type

SUMMARY

One of the aims of genetic engineering and synthetic biology is the design of microorganisms with novel capabilities that could be beneficial for humans, including their use of vaccines, diagnostic sensors, and therapeutic applications for major diseases such as cancer. In this regard, the availability of genetic elements able to program the adhesion of the engineered bacterium to different targets would be extremely useful.

This work reports the development of synthetic adhesins (SAs) that enable to precisely program the adhesion properties of *Escherichia coli* bacteria to different target surfaces, including tumor cells. The structural organization of these novel SAs is defined by a domain that anchors the SA to the bacterial outer membrane, which is derived from the N-terminal fragment of Intimin comprising residues 1-659, and an adhesive domain based on the smallest antibody fragments known to date, termed VHHs. This modular organization allows the modification of the binding specificity of the SA by the exchange of the VHH sequence. We demonstrate that SAs are efficiently displayed on the surface of *E. coli* and are able to drive bacterial adhesion to antigen-coated abiotic surfaces and to target tumor cells expressing on their surface the antigen recognized by SAs. SAs are constitutively and stably expressing from the chromosome of an engineered *E. coli* strain lacking a conserved set of natural adhesins (i.e. type 1 fimbriae, Antigen 43 and mat fimbriae) and constitutively expressing the *lux* operon as bioluminescent reporter. Using tumor xenograft mouse models we have demonstrated that engineered *E. coli* strains carrying SAs colonize efficiently solid tumors expressing the cognate antigen recognized by the SA using two order of magnitude lower doses of systemically administered bacteria compared to control strains with SAs binding an unrelated antigen or the wild type *E. coli* strain. In addition, we observed that the engineered strains were cleared faster from non-target organs (e.g. liver and spleen) probably due to the deletion of natural adhesins.

The fast and specific adhesion mediated by SAs was also employed to characterize the influence of both, flagella and YcgR protein in the adhesion process, as well as to investigate the short-term transcriptional response of *E. coli* upon adhesion to tumor cells. Our results indicate that, whereas active bacterial motility mediated by flagella is important for an efficient adhesion to target cells, the lack of YcgR protein does not affect the ability of bacteria to adhere to target cells, suggesting that the arrest of bacterial motility upon adhesion is independent of YcgR protein. In addition, we analyzed by RNAseq the global transcriptional response of *E. coli* bacteria upon adhesion (15 min) to target tumor cells. Our results indicate a common transcriptional response upon adhesion regardless of the cellular receptor recognized. Genes involved in sulfur uptake and its metabolism were upregulated upon adhesion, whereas genes involved in the transport of intermediates of the tricarboxylic acid cycle and tryptophan

synthesis were downregulated. We found that the activity of gene fusions between the chromosomal *yeeE* promoter region and the mCherry reporter gene were upregulated in response to bacterial adhesion.

Lastly, we have also demonstrated that SAs can drive the specific adhesion of non-live bacterial derived nanoparticles toward target tumor cells expressing a therapeutically relevant cell surface receptor (i.e. EGFR).

RESUMEN

Uno de los objetivos de la ingeniería genética y de la biología sintética es la creación de microorganismos con capacidades no existentes en la naturaleza para su posible aplicación en el desarrollo de vacunas, biosensores o en terapias frente a determinadas enfermedades como el cáncer. En este contexto, sería extremadamente valiosa la disponibilidad de un sistema que permitiese programar la adhesión de bacterias genéticamente modificadas hacia distintas dianas con el fin de poder localizar la acción terapéutica de estos microorganismos en un determinado punto. Para ello, en esta tesis nos propusimos generar adhesinas sintéticas (SAs en sus siglas en inglés) que permitiesen dirigir la adhesión de *Escherichia coli* (*E. coli*) hacia cualquier superficie o célula deseada. Las SAs tienen una organización estructural inspirada en la encontrada en muchas adhesinas naturales de *E. coli,* consistente en un dominio de anclaje a la membrana externa y un dominio adhesivo expuesto en la superficie de la bacteria con estructura tipo inmunoglobulina (Ig). Como dominio de anclaje seleccionamos la región N-terminal de la Intimina (residuos 1-659), una adhesina natural que se encuentra en las cepas enterohemorrágicas y enteropatógenas de *E. coli* (EPEC y EHEC, respectivamente) y que se inserta en la membrana externa bacteriana a través de una región plegada como un barril β muy estable a la desnaturalización y a la acción de proteasas. Como dominio adhesivo seleccionamos los fragmentos de anticuerpo más pequeños conocidos hasta la fecha, denominados VHHs o nanobodies (12-14 kDa), que presentan afinidades por sus antígeno similares a la de los anticuerpos convencionales y, además, tienen buenas propiedades de solubilidad, estabilidad a la desnaturalización y resistencia a proteasas. Los VHHs o nanobodies están basados en los únicos dominio variables encontrados en unos anticuerpos que sólo contienen cadena pesada encontrados en especies pertenecientes a la familia Camelidae (dromedarios, camellos, llamas, alpacas, guanacos y vicuñas). Esta organización modular de las SAs permite modificar su especificidad mediante un simple cambio del dominio adhesivo que, al estar basado en fragmentos recombinantes VHH, puede dirigirse frente a una gran variedad de antígenos seleccionando un clon de VHH con la especificidad deseada desde repertorios clonados en *E. coli* y sus fagos.

La fácil modificación de la especificidad de las SAs queda evidenciada en esta tesis mediante el desarrollo de SAs que reconocen cuatro antígenos distintos: La proteína verde fluorescente (GFP en sus siglas en inglés) de *Aequorea victoria*, el Fibrinógeno humano, la región extracelular del receptor translocado de Intimina (TirM en sus siglas en inglés) y el domino extracelular del receptor para el factor de crecimiento epidérmico humano (EGFR en sus siglas

en inglés). Hemos demostrado que las SAs se expresan de manera efectiva en la superficie de *E. coli* y que su expresión permite dirigir la adhesión bacteriana de manera específica hacia superficies recubiertas de antígeno (GFP y Fibrinógeno). Una vez evidenciado el potencial de las SAs para dirigir la adhesión de *E. coli*, se empleó un sistema de modificación genética que nos permitió reemplazar adhesinas naturales de *E. coli* por SAs o sistemas de biodetección (operón *lux*), en un solo paso. Esta estrategia hizo posible, no sólo crear cepa bacterianas que carecen de un grupo de adhesinas naturales conservadas (fimbrias tipo 1, Antigeno 43 y Fimbrias Mat), si no también obtener una expresión constitutiva y no tóxica de los genes de interés (SAs y operón *lux*) que permite su expresión estable durante múltiples generaciones (al menos 55) sin necesidad de inductores o antibióticos que ejerzan una presión selectiva.
Estas cepas modificadas fueron utilizadas para demostrar la eficacia de las SAs en el control de la adhesión bacteriana a células tumorales que expresan en su superficie un antígeno (p.ej. GFP, TirM o EGFR) que es reconocido por las SAs. La gran especificidad y efectividad observada en los ensayos de adhesión *in vitro* de estas cepas sobre células tumorales nos llevo a investigar la utilidad de las SAs en experimentos de colonización de tumores *in vivo*, dado que la colonización de tumores por bacterias es una de las terapias bacterianas que más se está desarrollando en los últimos años. Los resultados de nuestros experimentos con ratones con tumores implantados, demuestran que la cepa modificada de *E. coli* coloniza con mayor eficacia tumores sólidos que expresan en la superficie de sus células el antígeno reconocido por las SAs de modo más eficiente que las cepas control (cepa sin modificar, y cepa que expresa SAs frente a un antígeno no relacionado). Esta mayor eficacia en la colonización de tumores permite una reducción significativa (alrededor de dos órdenes de magnitud) en la dosis de bacterias necesarias para conseguir la colonización *in vivo* de los tumores sólidos. Además, probablemente debido a la deleción de las adhesinas naturales (fimbrias tipo 1, Antígeno 43 y fimbrias Mat), observamos que las cepas modificas de *E. coli* se acumulan en menor medida y por menos tiempo en órganos que no son diana, como el hígado o el bazo. Por tanto, en esta tesis se demuestra la utilidad de las SAs en terapias bacterianas destinadas al tratamiento de tumores.

La adhesión de *E. coli* con SAs a las células diana se utilizó para caracterizar la influencia del flagelo en el proceso de adhesión bacteriano, así como para investigar la respuesta transcripcional que tiene lugar en *E. coli* inmediatamente después de su adhesión a una célula tumoral. Nuestros datos sugieren que, al menos in vitro, la motilidad bacteriana mediada por el flagelo es necesaria para obtener una adhesión rápida y eficaz, dado que el número de bacterias adheridas a células tumorales a distintos tiempos fue siempre mucho mayor (unas 30 veces para un tiempo de adhesión de 15 minutos) en el caso de las cepas que expresaba un flagelo funcional que en el caso de la cepa que carecía de dos componentes principales del

filamento del flagelo (FliC y FliD). Además, estudiamos si la proteína YcgR, que se ha propuesto que está implicada en la inhibición de la motilidad bacteriana tras la adhesión a superficies, jugaba algún papel en una parada de la motilidad que observábamos en las bacterias *E. coli* con SAs adheridas a sus células diana. Nuestros resultados indican que la ausencia de la proteína YcgR no afecta a la capacidad de las bacterias para adherirse a las células diana, lo que sugiere que la inhibición de la motilidad bacteriana observada en nuestros experimentos es independiente de la acción de YcgR, y que por tanto otros mecanismos adicionales deben estar controlando esta transición.

En esta tesis también se ha estudiado la respuesta transcripcional desarrollada por *E. coli* inmediatamente después (15 min) de su adhesión a células tumorales. Estudios anteriores se centraban en la adaptación transcripcional llevada a cabo por *E. coli* tras su adhesión durante varias horas o incluso días sobre superficies abióticas durante el proceso de formación de biopelículas bacterianas. El rápido fenotipo de adhesión conferido por la expresión de SAs y la posibilidad de programarlas frente a antígenos presentes en la superficie de células tumorales permitieron, por primera vez, estudiar la respuesta transcripcional llevada a cabo por *E. coli* tras su adhesión a células tumorales y a un tiempo post-adhesión muy corto, nunca estudiado. La adaptación transcripcional de *E. coli* tras la adhesión fue analizada mediante secuenciación masiva de RNA (RNAseq) en dos modelos experimentales distintos que implicaban adhesión a células tumorales que expresan en su superficie dos marcadores diferentes (EGFR y GFP). Nuestros resultados indican que *E. coli* genera una respuesta transcripcional similar, independientemente del receptor reconocido. Entre los genes de *E. coli* cuya expresión se ve incrementada en respuesta a la adhesión encontramos fundamentalmente genes implicados en la captación de azufre y su asimilación en forma de aminoácidos (*cysD, cysP, yeeE*). Por otra parte, encontramos una disminución en la tasa de transcripción de genes relacionados con el transporte de carbohidratos *(rbsA, ugpE*), aminoácidos (*mtr*) e intermediarios del ciclo de Krebs (*dctA*). Además, los resultados obtenidos por RNAseq fueron confirmados mediante una técnica distinta (DNA *microarrays*).

El hallazgo de que la expresión de ciertos genes de *E. coli* se ve incrementada en respuesta a la adhesión a células tumorales, nos motivó a intentar generar un sistema genético que nos permitiese acoplar un estimulo (adhesión) a una respuesta (producción de una proteína con fines terapéuticos o de biodetección). Para ello, basándonos en la cepa que expresa SAs contra EGFR, se construyeron cepas en las que el gen de la proteína roja fluorescente mCherry estaba integrado en el cromosoma bajo control de distintos promotores cuya expresión se veía incrementada en respuesta a la adhesión. El resultado de estos experimentos reveló que el promotor del gen *yeeE* actúa como un promotor sensible a la

adhesión, incrementando la expresión de mCherry que está bajo su control en bacterias adheridas a la célula diana.

Por último, en esta tesis también se ha demostrado la utilidad de las SAs para dirigir la adhesión de nanopartículas no vivas (minicélulas) derivadas de *E. coli*, hacia células tumorales que expresan un marcador de relevancia terapéutica, como es EGFR. Además, las minicélulas generadas en este trabajo carecen de algunas de las estructuras bacterianas con mayor capacidad inmunogénica, como las fimbrias tipo 1, el flagelo y el lípido A hexa-acilado. Estas modificaciones adicionales podrían aumentar la bioseguridad de terapias basadas en minicélulas cargadas con moléculas terapeúticas.

Por tanto en esta tesis se demuestra el potencial de las SAs para controlar la adhesión de *E. coli* y mejorar de este modo su eficacia para colonizar *in vivo* tumores sólidos, en cualquier caso esta tecnología podría ser muy útil en otras aplicaciones biomédicas como el desarrollo de vacunas o la intervención frente a patógenos o incluso en aplicaciones de carácter industrial como el desarrollo de biosensores o consorcios microbianos para su uso en biorreactores. Además, dado el alto grado de conservación de la maquinaria celular empleada para el plegamiento y translocación a la membrana externa de los barriles β como el presente en Intimina, es probable que las SAs sean también funcionales en otras bacterias Gram negativas ampliamente utilizadas en proyectos de bilogía sintética como por ejemplo *Pseudomas putida*.

INTRODUCTION

1 Bacteria in biomedical applications.

1.1 Bacteria and their interaction with humans.

Some bacterial species are frequently found associated with other living forms such as plants or animals. In humans this association is generally considered as detrimental since is responsible of bacterial infections such as tuberculosis, cholera or foodborne illness. However, most of the interactions between bacteria and human cells do not lead to pathogenic situations. Indeed, the human body is colonized by a huge amount of microbes that outnumber human cells 10 to 1. This microbial population, mainly conformed by bacteria, is termed **microbiota** and is extensively distributed through the skin and the mucosal surfaces of the human body, although it is especially abundant in the gut. Benefits of include harvesting of otherwise inaccessible nutrients for the host, competition with pathogens for the colonization of different environments and contribution to the proper development of a fully functional immune system (Martin et al., 2013) (Fig. 1). Moreover, microbiota has also been proposed as an important factor in brain development and behavior (Diaz Heijtz et al., 2011). The impact of microbiota in many physiological processes is understood thanks to the study of axenic (germ-free) animals, which face many health disorders (Smith et al., 2007).

Human microbiota is an inherently dynamic population that changes along life (Gerber, 2014). Indeed, humans are essentially born germ-free but normally acquire a complex intestinal microbiota soon after birth, in a process termed colonization in which bacterial adhesion plays a key role. After colonization and along life, microbiota composition changes in response to several factors such as diet, age, environment, antibiotic treatments etc (Claesson et al., 2012). Sometimes these changes could break the balanced microbial ecosystem leading to a situation termed dysbiosis involved in a great variety of different illness. For instance, opportunistic pathogens could take advantage of a dysbiosis situation to colonize the gut. Additionally, metagenomic studies suggest that diseases like obesity or type 2 diabetes could be influenced by prolonged dysbiosis situations (Qin et al., 2012; Turnbaugh et al., 2009). Nevertheless, the clearest correlation between dysbiosis and disease has been found in inflammatory bowel diseases (IBD), in which the chronic inflammation of the digestive system seems to be related with a decreased number of *Faecalibacterium prausnitzii* bacteria inhabiting the gastrointestinal tract (Sokol et al., 2008).

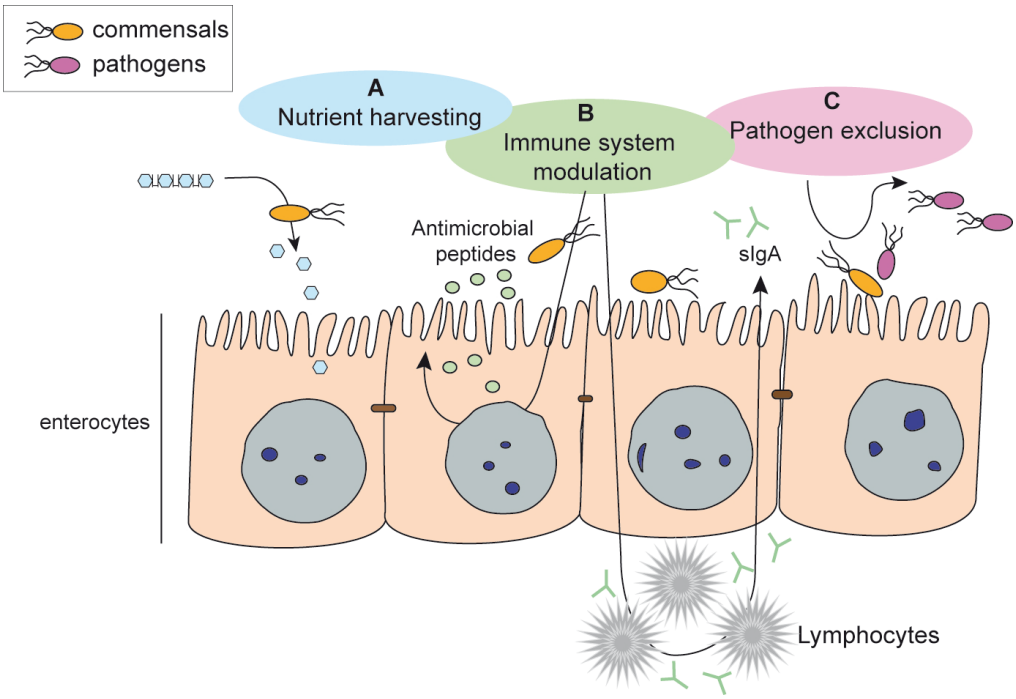

Figure 1. Roles of microbiota in human health. Scheme of the different actions that normal microbiota inhabiting human gastrointestinal tract carry out. Microbiota is able to harvest otherwise inaccessible nutrients for human cells (blue), as well as to induce the secretion of antimicrobial peptides or immunoglobulins (green) that contribute to maintain a balanced microbial population in the gut. Additionally microbiota mediates pathogen exclusion (purple) by competing either for nutrients or for cell receptors.

1.2 The use of bacteria for the benefit of human health.

Beneficial relationships between bacteria and humans do not end with natural microbiota, since our current knowledge allows us to actively use bacteria for our benefit.

1.2.1 Probiotics.

Probiotics are live microorganisms that, when administered in adequate amounts, confer a health benefit on the host (World Health Organization definition). Most probiotic strains that are currently in use belong to *Lactobacillus* and *Bifidobacterium* genera, although some strains of *Escherichia coli* are also being employed (Aureli et al., 2011).

Probiotics are commonly used to fight or to prevent the great variety of illness that could take place because of a dysbiosis state, restoring a balanced bacteria ecosystem either, by modulation of the host immunity, and/or by competing against pathogens. For instance, the administration of probiotic strain *Lactobacillus rhamnosus* GG (LGG) alleviate clinical symptoms of IBD and atopic dermatitis by enhancing the production of the anti-inflammatory cytokine IL-10 (Pessi et al., 2000), while *E. coli* Nissle 1917 (EcN) strain has been used for IBD treatment given its immunomodulatory role (Schultz, 2008), as well as in the prevention of traveller's diarrhea because of its ability to compete for nutrients with enterohaemorrhagic *E.*

coli (EHEC) strains in the gut (Maltby et al., 2013). Thus, probiotics are intended to complement the functions that microbiota carry out at the intestine (Fig. 1).

Recently it has been developed a therapy against recurrent urinary tract infections based on a probiotic *E. coli* strain termed ABU 83972, which was isolated from a patient of asymptomatic bacteriuria (Lindberg et al., 1975). Patients that suffer recurrent urinary tract infections are intentionally infected with *E. coli* ABU 83972, to protect against the infection of other bacteria that could lead to a pathogenic situation in the urinary tract (Sunden et al., 2006).

Fecal bacteriotherapies have also attracted the attention of scientific community. These therapies involve transplantation of fecal bacteria from healthy individual into a recipient and have produced good results combating infections caused by hypervirulent and hyperresistant Clostridium *difficile* strains (van Nood et al., 2013). Additionally, IBD (Anderson et al., 2012) or even neurological diseases as multiple sclerosis (Borody and Khoruts, 2012) are susceptible of being treated with fecal transplantation therapies.

1.2.2 Classic Vaccines.

With the development of vaccines, humans understood how to use bacteria to overcome bacterial infections.

Vaccines are based on the intentionally administration of a microorganism or purified subunit(s) unable to cause disease but that still retains the antigenic potential needed for inducing a protective immune response. Classically, vaccines against bacterial pathogens has been made from a chemically or heat-inactivated bacteria, such as the vaccine against *Bacillus anthracis*, the first vaccine against a bacterial infection conceived by Pasteur in 1881, or from a live bacteria that naturally does not infect humans but it is related with an human pathogen such as BCG vaccine against *Mycobacterium tuberculosis*.

1.2.3 Bacteria as agents to fight cancer.

Bacteria also have been used as agents to destroy solid tumors. At the end of XIX century, physicians W. Busch and W. Coley reported spontaneous tumor remissions associated with erysipelas, upper dermis acute infections caused by *Streptococcus pyogenes*. Prompted by these remissions, Coley started to systematically treat bone and soft tissue sarcoma patients, with live *Streptococcus pyogenes* bacteria first, and with isolated preparations of bacterial toxins later (Coley, 1910). However, the variability in clinical outcomes of Coley's treatment, ranging from complete tumor remission to death, reduced clinical attention to his findings. At that time, the mechanisms by which bacteria preferentially grow in tumor areas were not understood, but currently we have a deeper understanding about why anaerobic bacteria, such as *Salmonella enterica*, *E. coli or Clostridium* target tumors. It has been proposed that the chaotic and leaky newly formed vasculature in tumor areas could enhance bacterial entry into

solid tumors, in a phenomenon termed enhanced permeation and retention effect (Forbes et al., 2003; Maeda, 2013). Additionally, a chemotaxis towards compounds produced by tumors has been demonstrated *in vitro* (Kasinskas and Forbes, 2006). Lastly, the anoxic and immune-deficient microenvironment present in the tumor favors bacterial replication unimpeded by the macrophage and neutrophil clearance mechanisms that normally serve to eliminate them in normal organs (Westphal et al., 2008).

A recent study involving systemic administration of wild type *E. coli* K-12 strain to tumor-bearing mice demonstrated that this strain was not only able to efficiently colonize tumors, but also to significantly alter the tumor microenvironment, leading to an increase in the amount of necrotic tissue, a change in the expression profile of tumor cells, and even a strong reduction of pulmonary metastasic events (Weibel et al., 2008).

1.3 The use of modified bacteria for the benefit of human health.

Since the development of genetic engineering, researchers have pursued the goal of modifying organisms to obtain products of biomedical interest from them, such as the production in *E. coli* of human insulin (Goeddel et al., 1979), followed by the production of interleukins (Taniguchi et al., 1983) and antibodies (Cabilly et al., 1984). Alternatively, scientists have also tried to obtain, instead of a product, novel beneficial functions from the whole microorganism.

1.3.1 Engineered probiotics.

Engineered probiotics provide the possibility for *in situ* delivery on immunomodulatory agents. For instance, *Lactococcus lactis* bacteria have been engineered to *in situ* secrete IL-10, an interleukin that plays a critical role in regulation of the mucosal immune system by preventing excessive inflammatory responses toward normal intestinal bacteria. The engineered strain, tested in a phase I clinical trial, demonstrated a reduction in Crohn's disease (a kind of IBD) activity mediated by an induction of suppressor Th cells (Braat et al., 2006; Huibregtse et al., 2012).

Antibody-derived fragments against TNF-α have been also used as therapeutic molecules delivered *in situ* by *L. lactis*, achieving a reduction in the inflammation rate of mice suffering from induced chronic colitis (Vandenbroucke et al., 2010). In addition to *L. lactis*, *E. coli* has also been used to *in situ* secrete immunomodulatory components, such as alpha-defensin 5, or beta-defensin 2, antimicrobial peptides whose expression is limited in Crohn's disease patients (Seo et al., 2012).

Probiotics can be also armed in order to compete with pathogens, for instance *Lactobacillus jensenii,* a microorganism that is part of the normal human vagina flora, has been engineered to stably express cyanovirin-N, a cyanobacterial protein with antiviral activity against HIV. Notably, the strain tested in rhesus macaques showed that animals challenged with simian HIV showed

a 63% reduction in HIV infection rate (Lagenaur et al., 2011). Engineered strain derived from EcN also has been used to fight against *Vibrio cholera,* by interfering with Quorum Sensing signaling mechanisms of the pathogen (Duan and March, 2010). Lastly, an engineered *E. coli* strain, with a modified LPS structure that mimics the receptor of Shiga toxin, has been demonstrated as 100% effective to protect mice against an otherwise fatal dose of Shiga-toxin (Stx)-producing *E. coli* strains (Paton et al., 2000).

1.3.2 Engineered bacterial vaccines.

With the development of modern molecular biology, the way in which vaccines were generated changed dramatically. Currently, most of the vaccines that are in use are toxoid or conjugated vaccines. Toxoid vaccines involve the administration of genetically detoxified toxins that maintain immunogenic protein structure but have lost enzymatic activity, such as the detoxified pertussis toxin employed in vaccination against whooping cough caused by *Bordetella pertussis* (Pizza et al., 1989).

Conjugated vaccines are intended to create immunity against bacterial components that do not elicit a strong immune response. To do that, bacterial antigens that would not generate an immune response are coupled to a carrier protein known by its ability to stimulate the immune system (i.e. non-active mutant version of diphtheria toxin). An example of this approach is the vaccine against *Haemophilus influenzae* type b (Kelly et al., 2004).

There are other experimental vaccination approaches involving living bacteria as vaccination agents, such as bacteria that secrete antigens from harmful pathogens (Hess et al., 1996; Tzschaschel et al., 1996), bacteria that display on their surface antigens from pathogens (Lee et al., 2006) or bacteria that deliver antigen expression vectors into the cytosol of mammalian cells (DNA vaccines). Lastly, vaccination strategies involving bacteria-derived vehicles (described below) such as, bacterial ghosts (Paukner et al., 2005), minicells (Carleton et al., 2013) and outer membrane vesicles (OMVs) (Ellis and Kuehn, 2010) have been also developed.

1.3.3 Engineered bacteria as agents to fight against cancer.

The development of genetic engineering also allowed researches to improve bacteria as vehicles for anti-cancer therapy.

One approach has been the generation of gene deletion mutants with improved tumor targeting properties. For instance, *Salmonella enterica* serovar Typhimurium is an interesting vector for cancer-therapy since grow under either aerobic or anaerobic conditions, as those that take place within solid tumors and it is able to invade and survive within in epithelial and immune cells (Pawelek et al., 1997). However, its use is associated with undesired side effects given its pathogenic potential. Therefore, mutations on *purI* and *msbB* genes involved in biosynthesis of

purines and LPS respectively, were carried out. The resulting strain, termed VNP-20009, showed an increased specificity for tumor areas, as a result of its purines synthesis auxotrophy and lower toxicity since its pentacylated lipid A of LPS is less immunogenic. VNP-20009 has become the reference strain for tumor targeting with *Salmonella,* and it has been tested in clinical trials with modest results (Toso et al., 2002).

In order to confer new capabilities to bacteria targeting tumors, the expression of heterologous genes has been also widely studied (Fig. 2). For instance, bacterial bioluminescent systems from different light emitting bacteria have been expressed in tumor targeting-bacteria, providing a system to follow bacterial infections in real time by light emission (Min et al., 2008). To improve tumor destruction rates, tumor targeting bacteria have been equipped with genes encoding for bacterial toxins, such as cytolysin A (Jiang et al., 2010) or genes encoding for pro-drug converting enzymes like herpes simplex virus thymidine kinase (TK) (Pawelek et al., 1997) or *E. coli* cytosine deaminase (CD) (King et al., 2002), able to convert a non-toxic compound or prodrug (i.e. ganciclovir, 5-Fluorocytosine) in a toxic compound or drug (i.e. ganciclovir monophosphate, 5-Fluorouracil), resulting in a bacterial-directed enzyme prodrug therapy (BDEPT) (Lehouritis et al., 2013) localized in tumor areas.

Additionally, tumor-targeting bacteria have been engineered to induce apoptosis in tumor cells, by secreting tumor necrosis factor-related apoptosis-inducing ligand (TRAIL) (Ganai et al., 2009) and Fas ligand (Loeffler et al., 2008), or to induce an immune response against tumor cells by secreting cytokines such as LIGHT, a human TNF-family cytokine known to promote tumor rejection (Loeffler et al., 2007). Genetic transfer to tumor cells of genes encoding for cytotoxic agents (Fu et al., 2008) anti-angiogenic factors (Lee et al., 2004) or cytokines (Yuhua et al., 2001) has been also addressed with tumor-targeting bacteria. Additionally, genetic transfer mediated by bacteria has also been employed to silence the expression of genes important for tumor development, by a mechanism known as RNA interference (Hannon, 2002). One of the approaches involves the transfer to host cells of plasmids encoding for short hairpin RNAs (shRNAs). *Salmonella* has been employed as a vector to transfer plasmids encoding shRNAs toward tumor cells to silence the expression of the anti-apoptotic host gene *bcl2* (Yang et al., 2008), while *E. coli* has been used to silence the expression of host gene encoding for catenin β-1, whose overexpression is involved in several types of cancer (Xiang et al., 2006).

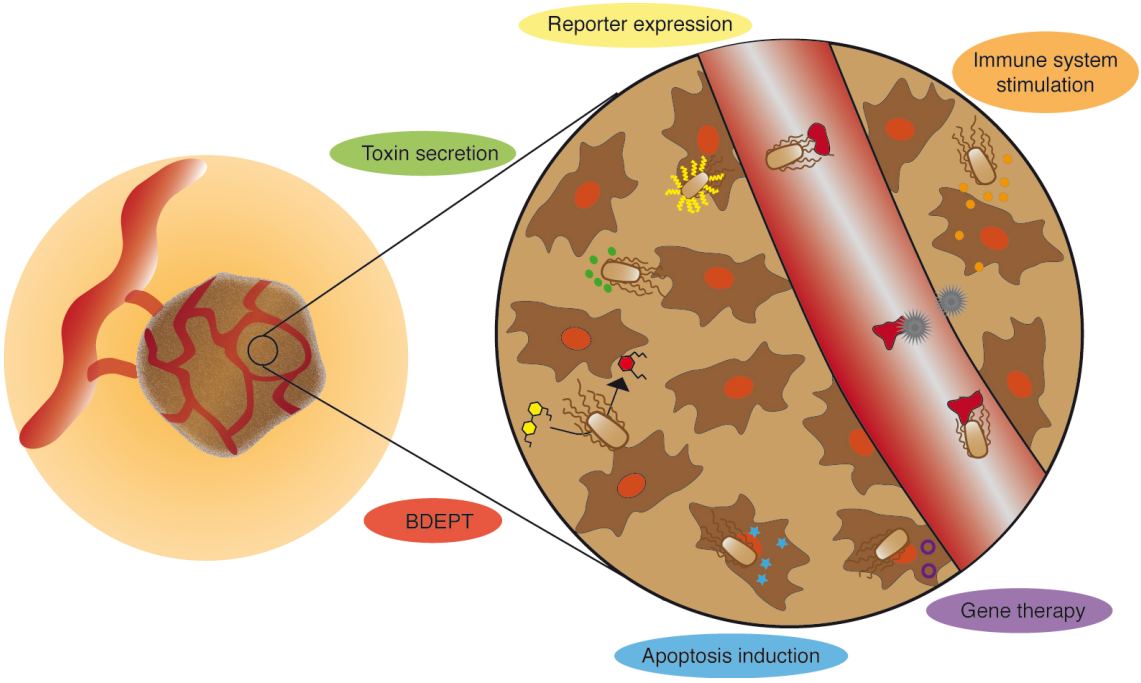

Figure 2. Engineered bacteria in cancer therapies. Scheme showing some approaches to improve bacteria as agents in cancer therapies. Bacterial accumulation inside tumors is mediated by the leaky vasculature of blood vessels found in tumors (red marks in the blood vessel) The scheme includes expression of reporter genes to follow infection in real time, generally by light emission (yellow wavy lines), localized secretion of bacterial toxins (green dots), Bacterial-directed enzyme prodrug therapy (BDEPT) that allows site-specific conversion of prodrugs (yellow molecule) into drugs (red molecule), localized secretion of cytokines (orange dots) to stimulate immune cells (grey cells), intracellular secretion of pro-apoptotic molecules (blue stars) and release of expression vectors (purple circles) coding for different genes or shRNAs.

1.3.4 Engineered bacteria-derived nanoparticles to fight cancer.

During the last decade, cancer therapies involving chemically-synthesized nanoparticles, have attracted the attention of scientists (Malam et al., 2009). These nanosized vehicles are able to deeper penetrate in tissues and mediate a controlled drug delivery. Nanocarries obtained from biological sources, incluiding bacteria have also been tested for the targeted release of therapeutic agents. For instance, minicells (also called nanocells) are bacteria-derived anucleate nanoparticles (400 nm), produced as a result of mutations in cell division genes (Adler et al., 1967), such as for instance *minCD* genes. The products of *minCD* together with *minE*, whose deletion results lethal for *E. coli*, form the MinCDE system that inhibits the formation of division septum away from midcell (Lutkenhaus, 2007). Minicells produced by *Salmonella typhimurium* Δ*minCD* strain, have been purified and subsequently loaded *in vitro* with chemotherapeutics (MacDiarmid et al., 2007b), cell cycle inhibitors (MacDiarmid et al., 2007a) and sh-RNAs encoding plasmids (MacDiarmid et al., 2009). To ensure the specific delivery of these compounds to tumor cells, drug-loaded minicells were incubated with bispecific monoclonal antibody (Mazor et al.) dimers, in which one mAb recognize a component

on the minicell surface (e.g. LPS) and the other a cell surface receptor for the targeted tumor cell (e.g. EGFR).

OMVs are nanosized (20-250 nm) bilayered proteoliposomes that are continuously released from the surface of many Gram-negative bacteria, influencing multiple biological processes such as secretion, nutrient acquisition or biofilm development (Kulp and Kuehn, 2010). Recently, OMVs have been engineered to target tumor cells and specifically deliver small interfering RNA (siRNA) against kinesine spindle protein, a microtubule-associated protein whose inhibition causes cell cycle arrest (Gujrati et al., 2014). Selective delivery of siRNA was achieved by the display on the surface of *E. coli* bacteria and their derived OMVs of a fusion protein, composed of the C-terminal domain of ClyA protein and an engineered version of *Staphylococcus aureus* protein A (i.e. affibody) that binds HER2, a human cell transmembrane receptor of the EGFR family with an important role in cell proliferation (Gutierrez and Schiff, 2011).

2 Designed bacteria and synthetic biology.

2.1 Synthetic biology, genetic parts and modules.

During the last years the idea of using a rational design to generate completely new microorganisms for specific applications, rather than modifying pre-existing ones, has gained pace promoted by the rise of synthetic biology. Synthetic biology is an emergent area of research that aims to design and produce biological components or systems that do not already exist in the natural world, or to redesign the previously existing natural biological systems (http://syntheticbiology.org).

These ideas are supported by recent reports on the creation, by chemical synthesis, of whole bacterial chromosome (Gibson et al., 2008), and the successful transfer of this synthetic chromosome to a receptive cytoplasm (Gibson et al., 2010). Notably, similar technology allowed the creation of a synthetic chromosome from *Saccharomyces cerevisiae* (Annaluru et al., 2014). Paradoxically, success in synthetizing synthetic chromosomes has highlight our inability to *de novo* design a genome, meaning that although writing a new genome is the long-term objective of synthetic biology, our current limited knowledge, just allow us to copy and edit an existing genome (Porcar et al., 2011).

However, what synthetic biology is currently doing is to create genetic parts and modules that could be ideally assembled in a *de novo* synthesized genome in the future. An example of this way of thinking the Registry of Standard Biological Parts (http://parts.igem.org/Catalog), a standardized collection of biological parts such as promoters, ribosome binding sites (RBS), transcriptional terminators etc. designed to have a modular architecture, allowing easy

combination of the biological parts. Moreover, ideally these biological parts should be selected from repertoires that would cover all the functionality landscape, to in that way allow a fine-tuning of gene expression. To this end, libraries of promoters (Blount et al., 2012), RBS sequences (Egbert and Klavins, 2012) and transcriptional terminators (Chen et al., 2013) of variable strengths have been constructed. Combination of genetic parts leads to the generation of genetic modules or devices with predictable behaviors.

2.2 Synthetic biology for biomedical applications.

One of the aims of synthetic biology is the rational design of microorganisms for biomedical applications (Hasty, 2012) (Fig. 3). This requires the availability of genetic modules with predictable phenotype that could be integrated into complex cellular assemblies, without perturbing or being perturbed by other cellular functions (i.e. orthogonal behavior in synthetic biology jargon). These modules should also be stably inherited through cell generations (Porcar et al., 2011). Some useful modules have already been designed. For instance, it is possible to reprogram *E. coli* chemotaxis toward areas in which a pathogen such as *Pseudomonas aeruginosa* is present and induce the secretion of microcine S and DNaseI, for pathogen killing and biofilm degradation, respectively (Hwang et al., 2013).
Also it has been designed a module allowing bacteria to sense their location inside a vacuole and induce a lysin (Huh et al., 2013), which could be useful for the selective delivery of therapeutic compounds inside targeted cells. An additional genetic module regulates the expression of desired bacterial genes, in response to environmental conditions found inside solid tumors (i.e. hypoxia) (Arrach et al., 2008). In this regard, a genetic module able to program *E. coli* adhesion to different targets could be extremely useful to improve current bacterial therapies (e.g. probiotics, vaccines, tumor targeting bacteria etc).

These and other modules must be integrated in a genetic context that provides the essential functions needed to keep a cell alive (i.e. chassis in synthetic biology jargon). Since we are not yet able to synthesize *de novo* a genome, currently available bacterial chassis are obtained by genome reduction (Csorgo et al., 2012; Martinez-Garcia and de Lorenzo, 2011).

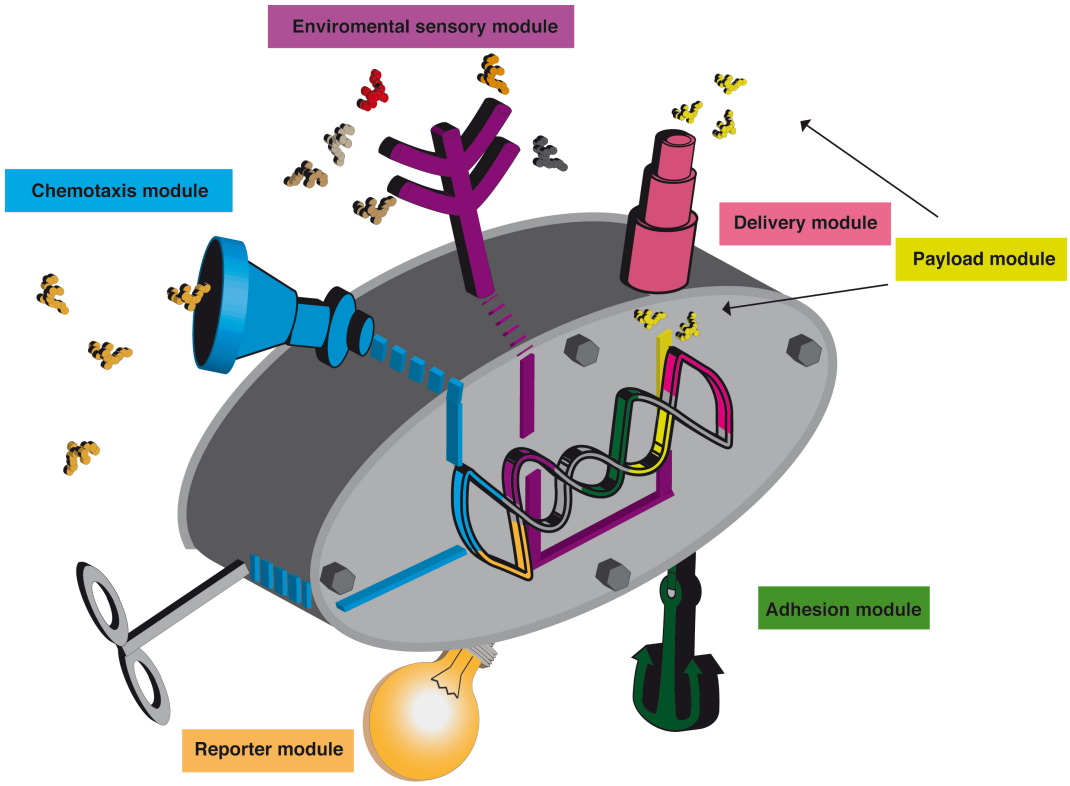

Figure 3. Synthetic bacteria for biomedical applications. Scheme of a nanomachine based on bacterial chassis (grey) carrying some of the genetic modules that would be interesting for bacterial therapies. A chemotaxis module (light blue) could control bacterial migration in response to chemoatractant signals (orange molecules). Selective attachment of bacteria could be mediated by the adhesion module (green) and monitored through the reporter module (orange). A sensory module (purple) could detect environmental signals and response by activating the transcription of the payload module (yellow). Product of the payload module (yellow molecules) could be secreted outside bacteria through the delivery module (pink) to exert a therapeutic effect.

3 *E. coli* adhesion.

To engineer a genetic module to program *E. coli* adhesion, it is important to understand how bacteria adhere to surfaces and host tissues and which bacterial structures have evolved to mediate bacterial adhesion.

3.1 *E. coli* lifestyle transition.

Although usually motile, most bacteria in nature are also able to attach to and live in close association with surfaces (biotic or abiotic). *E. coli* is a motile unicellular microorganism that frequently inhabits the GIT of several vertebrates, being associated with host tissues rather than in a motile unicellular lifestyle within the host body. Both, pathogenic and beneficial associations are mainly determined by the ability of bacteria to adhere to host cells, in order to withstand natural fluxes and perturbations. The molecules that mediate bacterial adhesion to

host cells or abiotic surfaces are proteinaceous appendages that stick out from bacterial membrane termed adhesins (see below). In general bacterial adhesion is a two-step process. First, proteinaceous adhesins mediates an initial attachment, recognizing molecular structures found on the biotic or abiotic surface and later, the production of polysaccharides by bacteria, generates a matrix around them that facilitates a tighten attachment of bacteria to the surface. The community formed by adhered bacteria embedded in that matrix mainly conformed by polysaccharides is termed biofilm (Beloin et al., 2008). Biofilms have a tremendous impact in several medical and industrial areas, since they are extremely resistant to disinfectants (Bridier et al., 2011) or antibiotics (Hoiby et al., 2010).

Transition between planktonic (motile) to sessile (adhered) lifestyle is associated with both, transcriptional and non-transcriptional changes in bacteria, although the molecular mechanisms underlying the sensing and development of this transition are not fully understood (Kirkpatrick and Viollier, 2012).

3.1.1 Non-transcriptional changes upon bacterial adhesion.

In first term adhesion requires a reduced activity of flagellar propellers, to avoid the disruption of proteinaceous adhesins and cell receptors interaction. This immediate adaptation to the sessile lifestyle is mediated by post-translational mechanisms, rather than a transcriptional or translational regulation, whose effects would take longer time to being effective.

The cyclic di-nucleotide c-di-GMP is a soluble molecule that acts as second-messenger in bacteria being involved in many signaling processes in bacteria, among them the transition between motile to sessile life styles (Hengge, 2009). Steady-state levels of c-di-GMP are maintained by a balanced activity of diguanylate cyclases (DCGs) that synthesize c-di-GMP, and phospodiesterases (PDEs) that degrade it. Although the nature of the signals that regulate DCGs and PDEs activities is not fully characterized, it is known that many PDEs and DCGs contain one or more transmembrane helices, allowing the placement of sensory domains of these proteins in the periplasm, where they can perceive oxygen and redox conditions, among others (Jenal and Malone, 2006). The genome of *E. coli* encodes for 19 predicted DCGs and 13 PDEs (Romling et al., 2005). Deletion of a single PDE termed YhjH leads to an increase of c-di-GMP levels that impairs bacterial motility, although this phenotype can be supressed by an additional mutation in the gene encoding for the c-di-GMP binding protein YcgR (Ryjenkov et al., 2006). These findings prompted to hypothesize that YcgR could be involved in the transition between motile and sessile lifestyles by interfering with flagellar apparatus in a c-di-GMP dependent-manner (Wolfe and Visick, 2008).

In fact, different groups have demonstrated the interaction of YcgR with several components of the flagellar apparatus (i.e. FliG, FliM, MotA) (Boehm et al., 2010; Fang and Gomelsky, 2010; Paul et al., 2010), and remarkably, some studies suggest that YcgR may be positioned to

associate with the flagellar switch complex prior to c-di-GMP binding, allowing a fast c-di-GMP dependent regulation of flagellar motility (Fang and Gomelsky, 2010; Paul et al., 2010).

3.1.2 Transcriptional changes upon bacterial adhesion.

Several studies have tried to unravel the transcriptional changes associated with biofilm development. For *E. coli* bacteria several comprehensive DNA microarray studies have been performed. The change in transcriptional pattern has been analyzed for (a) *E. coli* K-12 reference strain MG1655 upon 32 h growth on a glass slide (Schembri et al., 2003); (b) *E. coli* K-12 substrain TG1 upon 5 to 8 days biofilm development in microfermenters (Beloin et al., 2003); (c) *E. coli* K-12 substrain JM109 upon 7 h growth on glass wool (Ren et al., 2004); (d) *E. coli* ABU 83972 and VR50 strains after 42 h growth on petri dishes filled wit human urine (Hancock and Klemm, 2007); and (e) *E. coli* K-12 substrain BW25113 after shorter periods of biofilm formation on glass (from 4 to 24 hours) (Domka et al., 2007). Unfortunately, all these transcriptome analyses showed modest overlapping in their results, suggesting that even for the same bacteria (i.e. *E. coli*), each experimental condition leads to a different biofilm, resulting in a different transcriptional profile.

Strikingly, although adhesion is the first step for biofilm development, fewer studies have focused on the transcriptional changes that bacteria suffer immediately upon adhesion. Early studies using differential display PCR showed individual genes whose expression was upregulated in adhered bacteria. For instance, the expression of *kpsD* gene, involved in K capsular antigen biosynthesis, was found upregulated in the uropathogenic *E. coli* strain NU149 adhered by Type 1 fimbriae to mannose-coated Sepharose beads for 90 minutes (Schwan et al., 2005), whereas the expression of *barA*, which encodes a sensor histidine protein kinase essential for iron starvation response, was upregulated in the uropathogenic *E. coli* strain DS17 adhered to human red blood cells by PapG adhesin for 30 minutes (Zhang and Normark, 1996). CpxRA signal transduction system was upregulated in *E. coli* K-12 substrain MC4100, after 1 hour adhesion to glass beads (Otto and Silhavy, 2002). More recently, a comprehensive transcriptome analysis, based on DNA microarray technology, measured the transcriptional changes of hyperfimbriated *E. coli* CSH50 strain upon adhesion to mannose-coated agarose beads for 1 hour (Bhomkar et al., 2010). Genes related with removal of reactive oxygen species (e.g. *grxA*, *marA*) assimilatory sulfate reduction (e.g. *cysD*, *cysJ*), and some with unknown function (e.g. *yeeE*, *ygaD*) were among the most upregulated genes upon adhesion, whereas genes encoding for flagellar components (e.g. *fliM*, *flgB*) and tricarboxilic acid (TCA) cycle enzymes (i.e. *sdhC*) were downregulated in response to adhesion.

3.2 *E. coli* main adhesins.

The molecular composition of bacterial cell surface determines the ability of bacteria to interact with the environment, but in Gram-negative bacteria such as *E. coli,* surface display of proteins involves translocation across both, inner (IM) and outer membranes (OM). In *E. coli,* translocation of adhesins to OM occurs by different protein secretion systems (Gerlach and Hensel, 2007). This variety of systems to translocate adhesins, together with the remarkable array of adhesins encoded in *E. coli* genome, highlight the importance of being associated with abiotic and host surfaces for *E. coli*.

Adhesins can be subdivided by their assembly mechanism and structure into two major classes: fimbrial adhesins, and non-fimbrial adhesins.

3.2.1 Fimbrial adhesins.

Fimbrial adhesins constitute a group of filamentous fibers anchored in the OM that are composed of hundreds to thousands subunits. Type 1 fimbriae, P fimbriae and Curli are the fimbrial adhesins that have been clasically studied, associated to uropathogenic *E. coli* (UPEC) strains. However, Mat fimbriae, also termed *E. coli* common pilus, is the most common fimbrial structure among both, commensal and pathogenic strains (Rendon et al., 2007). In addition, genome analysis of *E. coli* K-12 and some pathogenic *E. coli* strains showed the presence of multiple operons encoding for putative fimbriae (Blattner, 1997; Perna et al., 2001; Welch et al., 2002), suggesting the existence of an armory of fimbrial adhesins with different roles and specificities in *E. coli* (Korea et al., 2011).

Except for Curli, the general structure of fimbrial adhesins and the secretion pathway employed is quite conserved. Operons encoding for fimbrial adhesins strains contain all the genes needed for the adhesin formation and also for its translocation across the OM through the chaperone/usher pathway, also termed type VII secretion system (Desvaux et al., 2009). In this pathway, pilus subunits associate with a dedicated periplasmic chaperone immediately after crossing the IM through the Sec translocon. The periplasmic chaperone binds to pilus subunits to prevent their aggregation in the periplasm, and transport them to the OM usher, a fimbrial assembly platform and translocon. Surface exposed pilus subunits, which vary in number and relative abundance between different fimbrial adhesins, are translocated to the outer space by the usher in an ordered way, which involves donor strand complementation between the incoming subunits, in order to complete the characteristic Ig-like fold of pilus components (Sauer et al., 2002). This ordered assembly allows the placement the pilus adhesin at the tip of the filament.

On the other hand, Curli fimbriae are secreted to the OM through the nucleation/precipitation pathway, which has also been defined as Type VIII Secretion System (T8SS) (Desvaux et al., 2009).

Given their variety, it is obvious that fimbrial adhesins play different roles in different *E. coli* strains. Type 1 fimbriae expression through the *fim* operon is widely distributed among different *E. coli* strains, and mediates the binding to mannose residues present on the surface of host cells through the FimH adhesin subunit. Surprisingly, whereas commensal and laboratory strains display FimH variants that bind with high affinity trimannose residues, UPEC strains present FimH molecules that exhibit higher affinity for monomannose residues, more prevalent in cells of the urinary tract, suggesting and environmental adaptation mechanism (Hommais et al., 2003). P fimbriae, encoded by the *pap* operon, are mainly expressed by UPEC strains and bind through the PapG adhesin subunit to the α-D-galactopyranosyl-(1-4)-β-D-galactopyranoside moiety of glycolipids of upper urinary tract cells and erythrocytes (Leffler). As for FimH, there are PapG variants that recognize related versions of their host cell receptors, meaning that expression of different PapG variants drives tissue and host specificity (Pizarro-Cerda and Cossart, 2006). Curli fibers lack a clear ligand-binding specificity, since they have been proposed to mediate bacterial attachment to a wide variety of proteins such as fibronectin, laminin, plasminogen and class I major histocompatibility complex (Olsen et al., 1998). Curli fibers also have a role in biofilm formation on abiotic surfaces, promoting both, bacterium-surface and bacterium-bacterium interactions (Uhlich et al., 2006). Curli expression only takes place at room temperature, however some UPEC strains also express Curli fimbriae at 37ºC suggesting a role in pathogenicity (Bian et al., 2000).

Mat fimbriae were originally reported as fimbrial structures expressed by meningitis associated pathogroups grown at low temperatures (Pouttu et al., 2001). In spite of this, recent studies have demonstrated the ubiquitous expression of Mat fimbriae in both, commensal and pathogenic groups, in a temperature independent fashion, at least for EHEC strains (Rendon et al., 2007). Expression of Mat fimbriae is involved in early biofilm development (Lehti et al., 2010) and host cell recognition (Garnett et al., 2012; Rendon et al., 2007; Saldana et al., 2009) although the exact nature of the moieties recognized by Mat fimbriae on the surface of mammalian cells has not been determined yet. Despite that *mat* operon structure in *E. coli* K-12 seems to be functional, expression of Mat fimbriae has never been detected in this strain. However, given the conservation of *mat* genes across *E. coli* species, it is likely that Mat fimbriae belong to the group of cryptic *E. coli* adhesins (Korea et al., 2010) that could be expressed under very specific conditions encountered, for instance, in *in vivo* situations (van Diemen et al., 2005).

3.2.2 Non-fimbrial adhesins.

Contrary to fimbrial adhesins, in which different subunits conform the shaft and the adhesive domains, non-fimbrial adhesins contain these domains in a single polypeptide. As outer membrane proteins (Pulido et al.), non-fimbrial adhesins should be translocated across the OM, following the Type V secretion system (T5SS) also termed autotransporter pathway (Henderson et al., 2004). In this secretion system, the polypeptide with a N-terminal signal peptide crosses the IM through the Sec translocon. Once in the periplasm, a domain of the polypeptide, with a β-barrel structure, is inserted in the OM with the mediation of the β-barrel assembly machinery (BAM) complex Bam complex, allowing the translocation of the remaining polypeptide, termed passenger domain, toward the bacterial surface. Many non-fimbrial adhesins, such as Antigen 43, are members of the classical autotransporter (AT) family, which contains the β-barrel domain at the C-terminal region of the polypeptide, and has N-terminal passenger domains on the bacterial surface folded as long rods of parallel β-helix structure. Antigen 43, encoded by *flu* gene, is a non-fimbrial adhesin conserved in most *E. coli* strains that is involved in biofilm formation and bacterial self-aggregation. However, given the strong sequence similarity between Antigen 43 and other AT adhesins (e.g. AIDA-I) recognizing glicoproteins on the surface of mammalian cells, a role in host-cell recognition for Antigen 43 cannot be rule out (van der Woude and Henderson, 2008).

3.2.2.1 Intimins. Structure, secretion and properties.

Intimins are non-fimbrial adhesins, encoded by *eae* gene, found in bacterial pathogens such as enteropathogenic and enterohaemorrhagic *E. coli* (EPEC and EHEC) strains and *Citrobacter* spp., which cause a characteristic intimate adhesion to enterocytes and the effacement of brush border microvilli (i.e. the attaching and effacing lesion). Intimins are highly homologous to Invasins from *Yersinia* spp., constituting together a subfamily of the T5SS with an opposite topology to classical ATs, having N-terminal β-barrel domains and C-terminal surface-exposed passengers (Leo et al., 2012). Structure of Intimin from EPEC and EHEC strains is defined by an OM anchoring domain composed of a 12-stranded β-barrel, and four surface-exposed globular domains showing either, immunoglobulin (Ig)-like fold (e.g. D0 D1 and D2 domains) or lectin-like fold (e.g. D3 domain) (Fairman et al., 2012). Translocation of Intimin to the OM involves its translocation to the periplasm, DsbA-dependent formation of a disulfide bond in the D3 lectin-like domain, and interaction with SurA, and in a lesser extent with with Skp and DegP chaperones, to assist its transport to the BAM complex for OM insertion (Fig. 4) (Bodelon et al., 2009). Intimin is an extremely stable OMP, resistant to strong denaturants such as SDS and urea. Moreover, Intimin was found to be highly resistant to the action of extracellularly added proteases (Bodelon et al., 2009).

Intimin takes part of an original “velcro-like” bacterial adhesion system in which bacteria provide both, the ligand (i.e. Intimin) and the receptor for the adhesion (El Hamidi et al.). The translocated intimin receptor (El Hamidi et al.) is an effector molecule of the Type III secretion system present in EPEC and EHEC strains that allows the direct injection of proteins into the cytoplasm of mammalian cells, through a bacterial OM needle-like structure termed the injectisome (Coburn et al., 2007). Once translocated inside the host cell, Tir is inserted into the host cell membrane leaving an extracellular domain called TirM accessible for the interaction with Intimin D3 domain (Kenny et al., 1997).

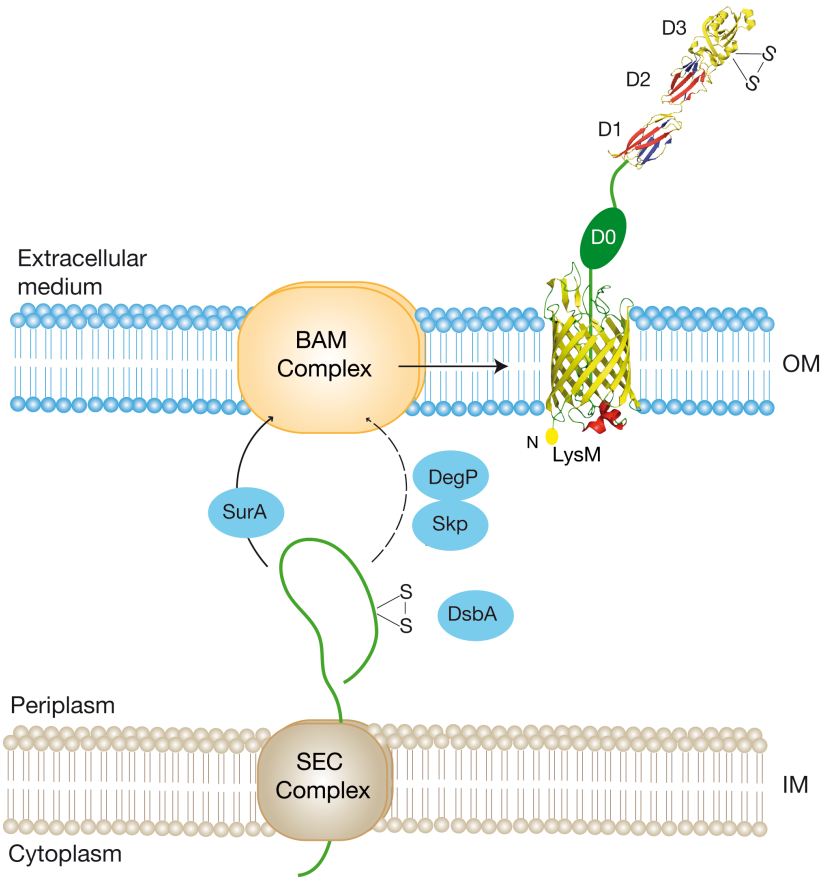

Figure 4. Intimin secretion. Schematic view of Intimin structure, folding and translocation to the OM in *E. coli.* Intimin polypeptide crosses the IM through the Sec complex to reach the periplasm where DsbA protein catalizes the formation of a disulfide bond in the D3 lectin-like domain of Intimin. In addition, SurA chaperone and, in a lesser extent, DegP and Skp chaperones are involved in periplasmic transport and folding of the N-terminal domain of Intimin, which is subsequently inserted in the OM in a process mediated by Bam complex, leading to the translocation of D0 D1 D2 and D3 domains of Intimin to the extracellular side of OM.

Interestingly, many fimbrial and non-fimbrial adhesins contain Ig-like domains in their structure. Although Ig-domains are widespread in nature, they are especially recognized for their role in proteins of the immune system of vertebrates (i.e. antibodies). It is not clear if the existence of Ig-like folding structures, in molecules so phylogenetically distant as bacterial adhesins and vertebrate antibodies, constitutes a case of evolution from a common ancestor or alternatively,

a mechanism of convergent evolution towards an energetically favorable folding (Bodelon et al., 2012). In either case, it is surprising how bacteria (i.e. adhesins) and vertebrates (i.e. antibodies) have maintained or evolved the same protein folding to face a common problem: specific ligand recognition.

4 Immunoglobulins and their expression and selection in *E. coli.*

Antibodies (Abs), also known as immunoglobulins (Ig), are large polypeptides produced by the immune system of vertebrates that are able to specifically recognize foreign molecular structures (i.e. antigens) that are not part of the host (Fanning et al., 1996; Schroeder and Cavacini, 2010).

The extreme ligand specificity showed by antibodies together with the possibility of targeting virtually any molecule with them, has turned antibodies into valued molecules for medical and biotechnological purposes.

4.1 Structure of antibodies and heavy-chain-only antibodies.

Conventional Abs are large heterotetetrameric protein complexes with Y shape consisting in two 2 large polypeptidic chains termed heavy (H) chains and two smaller polipeptides known as light (L) chains. Both chains are organized in autonomously folding functional units termed Ig domains, which are composed of around 120 aminoacids folded as two sandwiched β-pleated sheets joined by one disulfide bond between conserved cysteine residues (canonical disulfide bond). Pairing of the N-terminal Ig domains of L and H chains constitute the antigen-binding site, meaning that each Ab has two antigen-binding sites. These Ig-domains responsible of antigen binding have a more variable primary sequence and are termed as variable (V) domains, as opposed to the other Ig domains of the H and L chains, which are referred as constant (C) domains. Each V domain contains three hypervariable regions or complementary determining regions (CDRs) that define antigen specificity of antibodies (Fig. 5).

Interestingly, members of the family Camelidae (i.e. dromedaries, camels, llamas, alpacas, vicuñas and guanacos), in addition to conventional Abs with H and L chains, also produce Ab molecules that naturally lack L chains, named as heavy-chain-only Abs (HCAbs) (Fig. 5) (Hamers-Casterman et al., 1993). As a result of this L chain absence, the antigen-binding site of HCAbs is formed by a single domain termed VHH (VH of HCAbs). In addition, HCAbs also lack the constant domain CH1, providing a possible explanation to the absence of associated light chains, since this domain mediates association between heavy and light chains.

4.2 Recombinant antibodies and their use in therapy.

Currently over 40 different antibodies have received the approval from the Food and Drug Administration (FDA) (http://www.antibodysociety.org/news/approved_mabs.php). Approved antibodies are designed for the treatment of several diseases such as cancer, autoimmune disorders or rare diseases (Dimitrov and Marks, 2009). Most recent Abs being approved and entering in clinical trials are completely based on human sequences. These human monoclonal antibodies (named with suffix –umab) are obtained either from transgenic mice that produce human antibodies (Green et al., 1994; Lee et al., 2014; Macdonald et al., 2014; Murphy et al., 2014), or from libraries of human V domains (i.e. antibody fragments, see below) that are screened by phage display (McCafferty et al., 1990), ribosome display (He and Khan, 2005), yeast display (Chao et al., 2006) or bacterial display (Li et al., 2013) against the desired antigen. Selected V-domains of both heavy and light chains are cloned in a genetic scaffold encoding constant domains of human antibodies leading to the generation of fully human antibody molecules with antigen binding sites selected from libraries.

Despite the widespread use of full-length Ab molecules (e.g. IgG) for therapy, small antibody fragments that retain full antigen binding capacity have some advantages compared to full-length antibodies. Their simplified structure allows their expression in microorganisms like bacteria (Fernandez, 2004) or yeast (Feldhaus and Siegel, 2004) that have been essential for the screening of antibody fragments libraries. Additionally, small antibody fragments could be valuable molecules by it self, since the smaller size of fragments allows a better penetration into certain tissues such as tumors (Yokota et al., 1992). On the other hand, small Ab-fragments are rapidly degraded in humans and have short circulating half-lifes (Nelson, 2010).
Fab molecules are the oldest class of monoclonal antibody fragments developed (Better et al., 1988), composed of two polypeptides (VL-CL and VH-CH1) joined by a disulfide bond (Fig. 5). Next smaller Ab fragments were developed based on a single polypeptide chain (single chain Fv or scFv) containing the VH and VL domains joined with a short linker peptide (Fig. 5) (Bird and Walker, 1991). Although the stability of scFvs is lower than that of Fabs, they are commonly used since expression of a single polypeptide represents a clear advantage for correct folding.
Lastly, the discovery of HCAbs led to the expression of single domain VHH sequences that have high similarity with human sequences of the VH3 family, which make them suitable for human therapy. VHH fragments, also known as nanobodies, are the smallest recombinant Ab fragments generated to date (ca. 12-14 kDa) (Fig. 5). Despite their small size, antigen affinity of VHHs is similar to that of conventional antibodies, with equilibrium dissociation constants in the range of nano- or even picomolar concentrations (Muyldermans, 2013). In addition, VHH

molecules have been demonstrated as extremely resistant to chemical or thermal denaturation (van der Linden et al., 1999). Lastly, probably because of their naturally evolved single chain and monodomain structure, VHH molecules show higher solubility than other Ab fragments such as scFvs (Veiga et al., 2004).

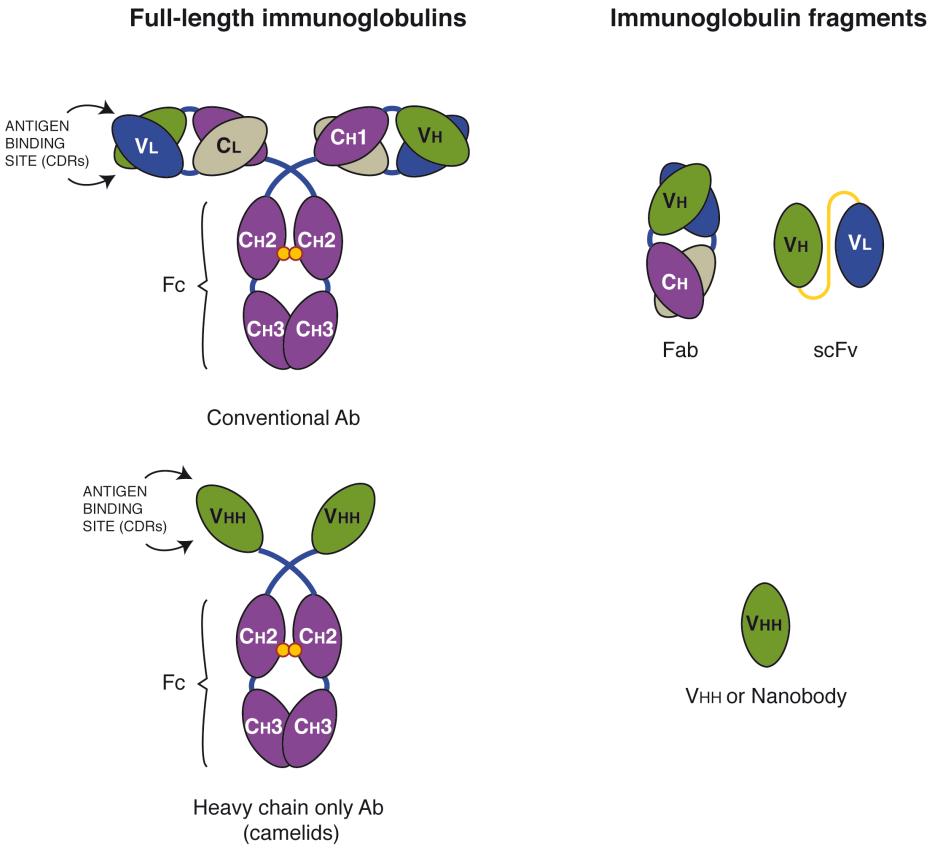

Figure 5. Antibodies and their fragments. Schematic representation of conventional and heavy-chain-only antibodies and their fragments. Conventional Abs (e.g. IgG) are composed of two heavy (H) chains and two light (L) chains, and the antigen-biding site is determined by the joining of the variable (V) domain of both, H and L chains. Fab fragments are devoid of the constant region (Fc), whereas scFvs are composed only by the VH and VL joined by a short linker peptide (shown in yellow). HCAbs lack L chains, as well as the CH1 domain, and their antigen-binding site is determined by a single domain, termed VHH or Nanobody.

4.3 Cell surface display of Igs in *E. coli.*

E. coli has been used to produce libraries of either, Ab fragments (Fernandez, 2004) or full-length Abs (Mazor et al., 2007) and to select desired clones from these libraries, using phage display (Smith, 1985) and anchored-periplasmic expression (APEx) systems (Harvey et al., 2004), respectively. The expression strategies for these systems involves the secretion of Ab molecules to the periplasm, since the reducing conditions found in the cytoplasm of wild-type *E. coli* strains impede the formation of disulfide bonds required for the proper folding of Ab molecules (Jurado et al., 2006; Jurado et al., 2002). In addition, it has been demonstrated that periplasmic chaperones (e.g. FkpA, Skp) and disulfide bond forming and isomerization

enzymes (e.g. DsbA, DsbC) assist correct folding of aglycosilated Abs in the periplasm of *E. coli* (Bodelon et al., 2012).

In order to facilitate the selection of desired clones from libraries, direct display of Ab molecules on the bacterial surface has been also attempted. However, the presence of the OM in *E. coli* has hindered the development of effective cell surface display methods for Ab selection, since in order to be displayed on the surface, polypeptides produced in the cytoplasm should traverse the IM, the periplasm, and be inserted into the OM. In addition display of heterologous proteins on the surface of *E. coli* often affects cell physiology, resulting in growth arrest, cell lysis and poor display performance. Thus, OM proteins native to the organism have served as convenient targeting and anchoring portions and are generally used for display, though heterologous anchor proteins have also been evaluated. For instance, scFvs have been displayed on the surface of *E. coli* using a tripartite fusion protein comprising de secretion signal of Lpp protein a fragment of OmpA protein and the scFv fragment (Francisco et al., 1993). Unfortunately, the expression of heterologous proteins on the surface of *E. coli* mediated by lipoprotein fusions severely disturbs the integrity of OM causing significant leakiness and toxicity (Georgiou et al., 1996). Furthermore, since Lpp-OmpA fusions are based on a truncated fragment of the native 8-stranded β-barrel structure of OmpA, they probably lack the characteristic stability of native β-barrels found in most OM proteins (Fairman et al., 2011). Our group previously reported that that scFv and VHH clones could be displayed on the surface of *E. coli* fused to different autotransporter proteins, such as the IgA protease from *Neisseria gonorrhoeae* (Veiga et al., 2004), or the EhaA adhesin from EHEC (Marin et al., 2010). This autotransporter display technology reduce bacterial toxicity found in lipoproteins display system, although a significant amount of the heterologous protein is found in culture media, since autotransporters are prone to proteolysis as part of their secretion mechanism (Leyton et al., 2012). More recently, our group also reported an effective *E. coli* display system for VHHs based on the β-domain of Intimin from EHEC, which allowed the screening of VHH libraries for the selection of high-affinity clones (Salema et al., 2013). Intimin-VHH fusions were also shown to be resistant to the action of proteases and denaturing agents, turning this display system into an attractive technology to modify the adhesion properties of *E. coli.*

OBJECTIVES

- To investigate whether fusion proteins composed of the outer membrane anchoring domain of Intimin and the adhesive domain based on VHH single domain antibodies could act as synthetic adhesins, driving the specific adhesion of *E. coli* bacteria to target antigenic surfaces.

- To engineer constitutive and stable expression of the adhesion module based on synthetic adhesins from the chromosome of an *E. coli* chassis strain lacking a conserved set of natural adhesins.

- To demonstrate that engineered *E. coli* strains constitutively expressing synthetic adhesins specifically attach to target tumor cells and to characterize the adhesion process.

- To demonstrate the functionality of synthetic adhesins *in vivo* and their ability to improve the efficiency of solid tumor colonization by engineered *E. coli* bacteria.

- To investigate short-term transcriptional response of engineered *E. coli* strains upon specific adhesion to tumor target cells mediated by synthetic adhesins.

- To generate non-live bacterial-derived nanoparticles devoid of chromosomal DNA maintaining the expression of synthetic adhesins against antigens present on the surface of tumor cells.

- Investigar si la proteínas de fusión generadas mediante la combinación del dominio de anclaje a membrana externa de Intimina y de los dominios de adhesión basados en anticuerpos monodominio VHH, podrían actuar como adhesinas sintéticas que dirijan la adhesión específica de bacterias *E. coli* hacia superficies antigénicas diana.

- Diseñar un módulo de adhesión basado en adhesinas sintéticas que se exprese de manera estable y constitutiva desde el cromosoma de una cepa "chasis" de *E. coli* carente de un conjunto de adhesinas naturales conservadas.

- Demostrar que las cepas modificadas de *E. coli* que expresan de modo constitutivo adhesinas sintéticas se unen específicamente a células tumorales diana, y caracterizar dicho proceso de adhesión.

- Demostrar la funcionalidad de las adhesinas sintéticas en experimentos *in vivo* y su capacidad para mejorar la eficiencia de *E. coli* para colonizar tumores sólidos.

- Investigar la respuesta transcripcional de las cepas modificadas de *E. coli* inmediatamente después de su adhesión mediada por adhesinas sintéticas a células tumorales diana.

- Generar nanopartículas derivadas de bacterias, carentes de ADN cromosómico y por tanto no vivas, que mantengan la expresión de adhesinas sintéticas frente a antígenos presentes en la superficie de células tumorales.

MATERIALS AND METHODS

1. Bacterial strains and growth conditions.

The *E. coli* strains used in the experiments described in this work are listed in Table M1. Bacteria were grown in Luria-Bertani (LB) liquid medium and agar-plates (1.5% w/v), at 37°C, unless otherwise indicated. When needed for plasmid or strain selection, antibiotics were added to the media at the following concentrations: chloramphenicol (Cm) at 30 µg/ml, kanamycin (Km) at 50 µg/ml and ampicillin (Ap) at 150 µg/ml, except for minicells-producer strains with Ap resistance gene in their chromosome that were selected with Ap at 75 µg/ml. *E. coli* DH10B-T1^R strain was used as host for cloning and propagation of plasmids with a pBR origin of replication (e.g. pAK-Not, pNV-derivatives). For cloning and propagation of suicide pGE-plasmid derivatives, containing the conditional pi-dependent R6K origin of replication (Stalker et al., 1982), the *E. coli* strains BW25141 or CC118-λpir were used. For inducible expression of the SAs from plasmid vectors with *plac* promoter (i.e. pNVfib, pNVgfp), EcM1 bacteria bearing the corresponding plasmid, were grown in LB-Cm at 30°C and 0.05 mM isopropyl-thio-β-D-galactoside (IPTG) was added at an optical density 600 nm (OD_{600}) of 0.5. The cultures were further grown for 2 h at 30°C with agitation (160 rpm). Bacteria with constitutive expression of the synthetic adhesins and the *lux* operon from the chromosome were always grown statically at 37°C in LB, except for analysis of their growth curve in which cultures were grown at 37°C with agitation (160 rpm), and except for minicells-producer bacterial strains that were also grown at 37°C with agitation (160 rpm). Bioluminescence of bacterial colonies grown on LB plates were monitored in a Chemi-doc XRS+ (Bio-Rad).

2. *E. coli* genome modification and strain construction.

The *E. coli* strains generated in this work are listed in Table M1. Site-specific deletions and insertions in the chromosome of *E. coli* were done with the marker-less strategy of genome edition based on expression of I-SceI endonuclease (Posfai et al., 1999; Posfai et al., 2006). Briefly, the *E. coli* strain to be modified was initially transformed with plasmid pACBSR (Cm^R) (Herring et al., 2003), expressing I-SceI and λ Red proteins under the control of P_{BAD} promoter (inducible with L-arabinose), and subsequently electroporated with the corresponding pGE-based suicide vector (Km^R). Cointegrants were selected on LB-Cm-Km plates incubated at 37°C. Individual colonies were isolated and grown for 6 h in LB-Cm liquid medium containing L-arabinose 0.4% (w/v) with agitation (160 rpm). After this period, a ~1 µl sample of these cultures was streaked on LB-Cm plates using an inoculating loop and incubated overnight. Individual colonies were replicated in LB-Cm and LB-Cm-Km plates to screen for Km-sensitive colonies that have performed resolution of the cointegrant vector after I-SceI induction. Individual Km-sensitive colonies were screened by PCR with specific oligonucleotides to identify those with the desired modification in their chromosome (i.e. deletion, insertion, substitution). Plasmid pACBSR was cured from the final strains by growth in liquid LB and

streaking on LB-plates. Individual colonies were replicated in LB and LB-Cm plates to screen for Cm-sensitive colonies. Minicells producer-strains were obtained through substitution of *minCD* genes by an Ap resistance gene cassette (*bla* gene) flanked by Flippase Recognition Target (FRT) sites. To excise *bla* gene, minicells producer strains were transformed with plasmid pCP20 (Cm^R) (Cherepanov and Wackernagel, 1995), a thermosensitive plasmid that expresses Flp recombinase under thermal induction. Individual colonies carrying pCP20 were grown for 6 h in LB liquid medium at 42º C with agitation (160 rpm). After thermal induction of Flp recombinase, individual Ap-sensitive colonies were screened by PCR to further confirm genome modification.

Construction details of individual *E. coli* strains are described below.

Table M1. *E. coli* strains used in this study

Name	Genotype	Reference
DH10B-T1^R	(F- λ-) *mcrA* Δ*mrr-hsdRMS-mcrBC* φ80*lacZDM15* Δ*lacX74 recA1 endA1 araD139* Δ*(ara, leu)7697 galU galK rpsL (Str^R) nupG tonA*	Novagen
BW25141	(F- λ-) Δ*(araD-araB)567*, Δ*lacZ4787*(::rrnB-3), Δ*(phoB-phoR)580*, *galU95*, Δ*uidA3*::*pir*, *recA1*, *endA9*(del-ins)::*FRT*, *rph-1*, Δ*(rhaD-rhaB)568*, *hsdR51*	(Datsenko and Wanner, 2000)
CC118 λ*pir*	Δ(*ara-leu*) *araD* Δ*lacX74 galE galK phoA20 thi- rpsE rpoB argE(Am) recA1,* λ*pir*	(Herrero et al., 1990)
MG1655	K-12 (F- λ-)	(Blattner, 1997)
EcM1	MG1655Δ*fim*A-H	(Salema et al., 2013)
EcM1 Δ*fli*	MG1655Δ*fim*A-H Δ*fliCD*	(Majander et al., 2005)
EcM1SAgfp	EcM1Δ*flu::P$_{N25}$-SAgfp*	This work
EcM1SAtir	EcM1Δ*flu::P$_{N25}$-SAtir*	This work
EcM1*lux* Δ*flu*	EcM1Δ*flu* Δ*matB::P$_2$-luxCDABE*	This work
EcM1*lux*SAgfp	EcM1Δ*flu::P$_{N25}$-SAgfp* Δ*matB::P$_2$-luxCDABE*	This work
EcM1*lux*SAtir	EcM1Δ*flu::P$_{N25}$-SAtir* Δ*matB::P$_2$-luxCDABE*	This work
EcM1*lux*SAega	EcM1Δ*flu::P$_{N25}$-SAega* Δ*matB::P$_2$-luxCDABE*	This work
EcM1 Δ*fli*SAgfp	EcM1Δ*fli* Δ*flu::P$_{N25}$-SAgfp*	This work
EcM1*lux*SAgfp-Δ*ycgR*	EcM1Δ*flu::P$_{N25}$-SAgfp* Δ*matB::P$_2$-luxCDABE* Δ*ycgR*	This work
EcM1*lux*SAega-P*cysP*Cherry	EcM1Δ*flu::P$_{N25}$-SAega* Δ*matB::P$_2$-luxCDABE P$_{cysP}$-mCherry*	This work
EcM1*lux*SAega-P*cysD*Cherry	EcM1Δ*flu::P$_{N25}$-SAega* Δ*matB::P$_2$-luxCDABE P$_{cysD}$-mCherry*	This work
EcM1*lux*SAega-P*yeeE*Cherry	EcM1Δ*flu::P$_{N25}$-SAega* Δ*matB::P$_2$-luxCDABE P$_{yeeE}$-mCherry*	This work
EcM1*lux*SAega-P*ydjN*Cherry	EcM1Δ*flu::P$_{N25}$-SAega* Δ*matB::P$_2$-luxCDABE P$_{ydjN}$-mCherry*	This work
EcM1*lux*SAega-P*ldhA*Cherry	EcM1Δ*flu::P$_{N25}$-SAega* Δ*matB::P$_2$-luxCDABE P$_{ldhA}$-mCherry*	This work
EcM1*lux*SAega-P*fruB*Cherry	EcM1Δ*flu::P$_{N25}$-SAega* Δ*matB::P$_2$-luxCDABE P$_{fruB}$-mCherry*	This work
EcM1Δ*fli* Δ*msbB*	MG1655Δ*fim*A-H Δ*fliCD* Δ*msbB*	This work
EcMini	EcM1Δ*fli* Δ*msbB* Δ*minCD*	This work
EcMini-WT	MG1655 Δ*minCD*	This work
EcMini-SAgfp	EcM1Δ*fli* Δ*msbB* Δ*minCD* Δ*flu::P$_{N25}$-SAgfp*	This work
EcMini-SAega	EcM1Δ*fli* Δ*msbB* Δ*minCD* Δ*flu::P$_{N25}$-SAega*	This work

EcM1SAgfp: The EcM1 strain carrying pACBSR (Cm^R) was transformed with pGE*flu*-SAgfp (Km^R) and cointegrants were selected on LB-Km-Cm plates. Cointegrants were resolved by I-SceI expression and individual Km sensitive colonies were checked by PCR with primer pairs: VHH-Sfi2 and VHH-Not for VHH detection; Yoe1 and NeaeR1 for checking upstream integration site; Neae4 / YeeR2 for checking downstream integration site.

EcM1SAtir: The EcM1 strain carrying pACBSR (Cm^R) was transformed with pGE*flu*-SAtir (Km^R) and cointegrants were selected on LB-Km-Cm plates. Cointegrants were resolved by I-SceI expression and individual Km sensitive colonies were checked by PCR with primer pairs: VHH-Sfi2 and VHH-Not for VHH detection; Yoe1 and NeaeR1 for checking upstream integration site; Neae4 / YeeR2 for checking downstream integration site.

EcM1*lux* Δ*flu*: The EcM1 strain carrying pACBSR (Cm^R) was transformed with pGE*flu* (Km^R), and cointegrants were selected on LB-Km-Cm plates. Cointegrants were resolved by I-SceI expression and individual Km sensitive colonies were checked by PCR with primers Yoe1 and YeeR2 to confirm the *flu* gene deletion. Subsequently, EcM1Δ*flu* strain bearing pACBSR was transformed with pGE*mat-lux* (Km^R). Cointegrants were resolved by I-SceI expression and individual Km sensitive colonies were tested for light emission. To ensure site specific integration of the *lux* operon, the bioluminescent colonies were checked by PCR primer pairs: ykgL-For and LuxC-Rev for upstream integration site and LuxE-For and yagX-Rev for downstream integration site.

EcM1*lux*SAgfp: The EcM1SAgfp strain carrying pACBSR (Cm^R) was transformed with pGE*mat-lux* suicide plasmid (Km^R). Cointegrants and individual bioluminescent colonies were selected and screened as described above for strain EcM1*lux*Δ*flu*.

EcM1*lux*SAtir: The EcM1SAtir strain carrying pACBSR (Cm^R) was transformed with pGE*mat-lux* suicide plasmid (Km^R). Cointegrants and individual bioluminescent colonies were selected and screened as described above for strain EcM1*lux*Δ*flu*.

EcM1*lux*SAega: The EcM1*lux*SAgfp strain carrying pACBSR (Cm^R) was transformed with pGE*flu*-SAega (Km^R). Cointegrants were resolved by I-SceI expression and individual Km sensitive colonies were checked by PCR with primer pairs: VHH-Sfi2 and Ega CDR3 to confirm VHH exchange; Yoe1 and NeaeR1 for checking upstream integration site; Neae4 / YeeR2 for checking downstream integration site.

EcM1Δ*fli*SAgfp: The EcM1Δ*fli* strain carrying pACBSR (Cm^R) was transformed with pGE*flu*-SAgfp (Km^R) and cointegrants were selected on LB-Km-Cm plates. Cointegrants were resolved by I-SceI expression and individual Km sensitive colonies were checked by PCR with primer pairs: VHH-Sfi2 and VHH-Not for VHH detection; Yoe1 and NeaeR1 for checking upstream integration site; Neae4 / YeeR2 for checking downstream integration site.

EcM1*lux*SAgfp-Δ*ycgR*: The EcM1*lux*SAgfp strain carrying pACBSR (Cm^R) was transformed with pGE*ycgR* suicide plasmid (Km^R). Cointegrants were resolved by I-SceI expression and individual Km sensitive colonies were checked by PCR with primer pairs XhoI HR1 ycgR / SphI HR2 ycgR to confirm *ycgR* gene deletion.

EcM1*lux*SAega-P*cysP*Cherry: The EcM1*lux*SAega strain was transformed with pGEP*cysP*CherryT0 suicide plasmid (Km^R). Cointegrants were selected on Kanamycin plates and analyzed by PCR with primer pairs: cysP ups check / SpeI Cherry for checking upstream integration site; and NotI-RBS-Cherry / cysP down check for checking downstream integration site.

EcM1*lux*SAega-P*cysD*Cherry: The EcM1*lux*SAega strain was transformed with pGEP*cysD*CherryT0 suicide plasmid (Km^R). Cointegrants were selected on Kanamycin plates and analyzed by PCR with primer pairs: cysD ups check / SpeI Cherry for checking upstream integration site; and NotI-RBS-Cherry / cysD down check for checking downstream integration site.

EcM1*lux*SAega-P*yeeE*Cherry: The EcM1*lux*SAega strain was transformed with pGEP*yeeE*CherryT0 suicide plasmid (Km^R). Cointegrants were selected on Kanamycin plates and analyzed by PCR with primer pairs: yeeE ups check / SpeI Cherry for checking upstream integration site; and NotI-RBS-Cherry / yeeE down check for checking downstream integration site.

EcM1*lux*SAega-P*ydjN*Cherry: The EcM1*lux*SAega strain was transformed with pGEP*ydjN*CherryT0 suicide plasmid (Km^R). Cointegrants were selected on Kanamycin plates and analyzed by PCR with primer pairs: ydjN ups check / SpeI Cherry for checking upstream integration site; and NotI-RBS-Cherry / ydjN down check for checking downstream integration site.

EcM1*lux*SAega-P*ldhA*Cherry: The EcM1*lux*SAega strain was transformed with pGEP*ldhA*CherryT0 suicide plasmid (Km^R). Cointegrants were selected on Kanamycin plates and analyzed by PCR with primer pairs: ldhA ups check / SpeI Cherry for checking upstream integration site; and NotI-RBS-Cherry / ldhA down check for checking downstream integration site.

EcM1*lux*SAega-P*fruB*Cherry: The EcM1*lux*SAega strain was transformed with pGEP*fruB*CherryT0 suicide plasmid (Km^R). Cointegrants were selected on Kanamycin plates and analyzed by PCR with primer pairs: fruB ups check / SpeI Cherry for checking upstream integration site; and NotI-RBS-Cherry / fruB down check for checking downstream integration site.

EcM1Δ*fli* Δ*msbB*: The EcM1Δ*fli* strain carrying pACBSR (Cm^R) was transformed with pGE*msbB* suicide plasmid (Km^R). Cointegrants were resolved by I-SceI expression and individual Km sensitive colonies were checked by PCR with primer pairs XbaI HR1 msbB / SphI HR2 msbB to confirm *msbB* gene deletion.

EcMini: The EcM1Δ*fli* Δ*msbB* strain carrying pACBSR (Cm^R) was transformed with pGE*minCD*-AmpFRT suicide plasmid (Km^R). Cointegrants were resolved by I-SceI expression and individual Km sensitive colonies were checked by PCR with primer pairs XbaI minE / SphI minC to confirm *minCD* gene deletion. Subsequently pCP20 (Cm^R) was transformed and the strain carrying this plasmid was grown at 42ºC for six hours to induce FLP recombinase expression, which mediates excision of FRT flanked Ampicillin resistance gene. Bacterial growth at 42ºC also leads to pCP20 plasmid curing. Amp sensitive colonies were checked by PCR with primer pairs XbaI minE / SphI minC to confirm AmpR gene cassette excision.

EcMini-WT: The *E. coli* K-12 MG1655 strain carrying pACBSR (Cm^R) was transformed with pGE*minCD*-AmpFRT suicide plasmid (Km^R). Cointegrants were resolved by I-SceI expression and individual Km sensitive colonies were checked by PCR with primer pairs XbaI minE / SphI minC to confirm *minCD* gene deletion. Subsequently pCP20 (Cm^R) was transformed and the strain carrying this plasmid was grown at 42ºC for six hours to induce FLP recombinase expression, which mediates excision of FRT flanked Ampicillin resistance gene. Bacterial growth at 42ºC also leads to pCP20 plasmid curing. Amp sensitive colonies were checked by PCR with primer pairs XbaI minE / SphI minC to confirm AmpR gene cassette excision.

EcMini-SAgfp: The EcMini strain carrying pACBSR (Cm^R) was transformed with pGE*flu*-SAgfp (Km^R). Cointegrants were resolved by I-SceI expression and individual Km sensitive colonies were checked by PCR with primer pairs: VHH-Sfi2 and VHH-Not for VHH detection; Yoe1 and NeaeR1 for checking upstream integration site; Neae4 / YeeR2 for checking downstream integration site.

EcMini-SAega: The EcMini strain carrying pACBSR (Cm^R) was transformed with pGE*flu*-SAega (Km^R). Cointegrants were resolved by I-SceI expression and individual Km sensitive colonies were checked by PCR with primer pairs: VHH-Sfi2 and VHH-Not for VHH detection; Yoe1 and NeaeR1 for checking upstream integration site; Neae4 / YeeR2 for checking downstream integration site.

3. Plasmids, DNA constructs, and oligonucleotides.

The plasmids constructed and used in this study are summarized in Table M2. Oligonucleotides were synthesized by Sigma Genosys and are listed in Table M3. PCRs were performed with Taq DNA polymerase for standard amplifications in screenings and with proof-reading DNA

polymerases, Vent DNA polymerase (New England Biolabs) and High-expand fidelity (Roche) for cloning purposes. All plasmid constructs were fully sequenced (Secugen). Details of plasmid constructions are described below.

Table M2. Plasmids used in this study

Name	Relevant properties	Reference
pAK-Not	(Cm^R), $lacI^q$-P*lac* promoter, pBR322 ori	(Salema et al., 2013)
pNeae	pAK-Not-derivative; Neae polypeptide [$Intimin_{EHEC}$ (1-659)-E-His-tag]	(Bodelon et al., 2009)
pNeae2	pAK-Not-derivative; Neae-myc polypeptide [$Intimin_{EHEC}$ (1-659)-E-His-myc-tag]	(Salema et al., 2013)
pNVgfp	pNeae2-derivative; VHH anti-GFP fused to Neae2 [$Intimin_{EHEC}$ (1-659)-E-Vgfp-myc-tag]	(Salema et al., 2013)
pNVfib	pNeae2-derivative; VHH anti-human Fibrinogen fused to Neae2 [$Intimin_{EHEC}$ (1-659)-E-Vfib-myc-tag]	This work
pNVtir	pNeae2-derivative; VHH anti-TirM fused to Neae2 [$Intimin_{EHEC}$ (1-659)-E-Vfib-myc-tag]	(Salema et al., 2013)
pNVega	pNeae2-derivative; VHH anti-human EGFR fused to Neae2 [$Intimin_{EHEC}$ (1-659)-E-Vfib-myc-tag]	This work
pDisplay	(Amp^R, $G418^R$) P_{CMV}-IgK signal peptide-HA-polylinker-myc tag-PDGFR transmembrane domain	Life technologies
pDisplay-GFP-tm	pDisplay derivative; GFP-tm fusion (display of GFP)	(Han et al., 2004)
pDisplay-TirM-tm	pDisplay derivative; TirM-tm fusion (display of $TirM_{EHEC}$ and mWasabi)	This work
pGE	(Km^R), R6K-ori, polylinker flanked by two I-SceI restriction sites	This work
pGE*flu*	pGE derivative; with homology regions flanking the *flu* gene of *E. coli* K-12	This work
pGE*flu*-SAgfp	pGE*flu* derivative; P_{N25}-SAgfp (constitutive expression of SA binding GFP)	This work
pGE*flu*-SAtir	pGE*flu* derivative; P_{N25}-SAtir (constitutive expression of SA binding TirM)	This work
pGE*flu*-SAega	pGE*flu* derivative; P_{N25}-SAega (constitutive expression of SA binding hEGFR)	This work
pGE*mat-lux*	pGE derivative; P_2-*luxCDABE* with homology regions flanking the *matB* gene of *E. coli* K-12	This work
pACBSR	(Cm^R), p15A-ori, P_{BAD} promoter, I-SceI endonuclease, λ Red	(Herring et al., 2003)
pCP20	(Amp^R, Cm^R) rep101ts, Flippase expression under thermal induction	(Cherepanov and Wackernagel, 1995)
pGE*ycgr*	pGE derivative; with homology regions flanking the *ycgR* gene of *E. coli* K-12	This work
pGEP*cysP*CherryT0	pGE derivative; *E. coli* K-12 *cysP* promoter, mCherry, T0 transcriptional terminator	This work
pGEP*cysD*CherryT0	pGE derivative; *E. coli* K-12 *cysD* promoter, mCherry, T0 transcriptional terminator	This work
pGEP*yeeE*CherryT0	pGE derivative; *E. coli* K-12 *yeeE* promoter, mCherry, T0 transcriptional terminator	This work
pGEP*ydjN*CherryT0	pGE derivative; *E. coli* K-12 *ydjN* promoter, mCherry, T0 transcriptional terminator	This work
pGEP*ldhA*CherryT0	pGE derivative; *E. coli* K-12 *ldhA* promoter, mCherry, T0 transcriptional terminator	This work
pGEP*fruB*CherryT0	pGE derivative; *E. coli* K-12 *fruB* promoter, mCherry, T0 transcriptional terminator	This work
pGE*msbB*	pGE derivative; with homology regions flanking the *msbB* of *E. coli* K-12	This work
pGE*minCD*-AmpFRT	pGE derivative; with homology regions flanking the *minCD* genes of *E. coli* K-12 and the *bla* gene (Amp^R) flanked by two FRT sites inserted between homology regions.	This work

Table M3. Oligonucleotides used in this study (1/3)

Name	Sequence (5'- 3')	Use
Sfi TirM For	GTCCTCGCAACTGCGGCCCAGCCGGCCCAGGCGCTTGCATTGACGCCGG	pDisplay-TirM-tm construction
TirM Xma Rev	TCCCCCCGGGCGAACCACCACCCGATGAAACTTTCAGCTCCTCCTG	pDisplay-TirM-tm construction
PN25-Sac-Xba 1	CTCATAAAAAATTTATTTGCTTTCAGGAAAATTTTTCTGTATAATAGATTCATAAATTTGAGAGAGGAGTTT	PN25 promoter generation
PN25-Sac-Xba 2	CTAGAAACTCCTCTCTCAAATTTATGAATCTATTATACAGAAAAATTTTCCTGAAAGCAAATAAATTTTTTATGAGAGCT	PN25 promoter generation
Xho yeeP	CCGCTCGAGATGACCGTGCCCTGTCTGTGGATG	*flu* 5' Homology Region
Sac yeeP	CCGGAGCTCTCAGAAGAAAATCCAGTTCCATACCGC	*flu* 5' Homology Region
Ang43 Spe	GACTAGTTTCCACTGCAGGCAGCGGGATGACGTTCTC	*flu* 3' Homology Region
Ang43 Sph	ACATGCATGCCCAGCCAGCGAATATGGAACAACCGGGTTATG	*flu* 3' Homology Region
Yoe1	CGGTTCACAGGCAATTGGCGGTATTGTTAAC	5' check SAs integration in *flu*
NeaeR1	TGTTGTGCCGCATAATTTAATGCCTTGTCATC	5' check SAs integration in *flu*
Neae4	CGTAATGGCAATAGCTCTAACAATGTA	3' check SAs integration in *flu*
YeeR2	ACATCAGTGACGGTGAAATATCGTACTGTAACG	3' check SAs integration in *flu*
MatA XhoI	CCGCTCGAGCTGAACTGATTGTGGATATCGACAG	*mat* 5' Homology Region
MatA SacI	CCGGAGCTCTGCATTTCTTCCCGAGTTGAATTGAGG	*mat* 5' Homology Region
MatBC SpeI	GACTAGTGCATCTGGAGCGGCGACGTTAGCGTAC	*mat* 3' Homology Region
MatBC SphI	ACATGCATGCCACAGCGCTGCGGTTGGCATTATCG	*mat* 3' Homology Region
YkgL For	ACTCAGTCTCCTCCCTTTGCG	5' check *lux* integration in *mat*
LuxC Rev	TGCCAACAGATGTACAGATTTACC	5' check *lux* integration in *mat*
LuxE For	TATATCATAACCGGAGGCGGCTGG	3' check *lux* integration in *mat*
YagX Rev	ACTTATGTCAGCAGCGCTGGC	3' check *lux* integration in *mat*
VHH Sfi2	GTCCTCGCAACTGCGGCCCAGCCGGCCATGGCTCAGGTGCAGCTGGTGGA	VHHs amplification
VHH Not	GGACTAGTGCGGCCGCTGAGGAGACGGTGACCTGGGT	VHHs amplification
R6K1	TCCCCCCGGGTAGGGATAACAGGGTAATCCATGTCAGCCGTTAAGTGTTCCTGTGTC	pGE vector construction
R6K2	TTGGCGCGCCGATCTGAAGATCAGCAGTTCAACC	pGE vector construction
Km1	TTGGCGCGCCGACGTCTTGTGTCTCAAAATCTCTG	pGE vector construction
Km2	TCCCCCCGGGATTACCCTGTTATCCCTATTATTAGAAAAATTCATCCAGCATCAG	pGE vector construction
MCS1	CCGGTCTCGAGACGCGTGAGCTCCATATGTCTAGAGCTAGCAAGCTTACTAGTCCTAGGGCATGCA	pGE vector construction
MCS2	CCGGTGCATGCCCTAGGACTAGTAAGCTTGCTAGCTCTAGACATATGGAGCTCACGCGTCTCGAGA	pGE vector construction
XhoI HR1 ycgR	GACGTCTCGAGATTATCGCTATCGAATCGGGTGG	*ycgR* 5' Homology Region
XbaI HR1 ycgR	CATTCTAGATTTACATCGCGTCCAGTGCCTGC	*ycgR* 5' Homology Region
XbaI HR2 ycgR	TACTCTAGAGCGGAAAAACTCCTGACTGAC	*ycgR* 3' Homology Region

Table M3. Oligonucleotides used in this study (2/3)

Name	Sequence (5'- 3')	Use
SphI HR2 ycgR	TTAGCATGCTTATTCTCTTCGCAGGAGGCG	*ycgR* 3' Homology Region
Ega CDR3 Rev	AGTCATAGTCCAAGGGCCTTTGG	Check cloning in pGE*flu*-SAega
XbaI HR1 msbB	CATCTAGACGACAATGTGGAAGAAGCTATTGCC	*msbB* 5' Homology Region
SpeI HR1 msbB	CAACTAGTAAAAGCCTCTCGCGAGGAGAGG	*msbB* 5' Homology Region
SpeI HR2 msbB	AGACTAGTGCTTTTCCAGTTTCGGATAAGG	*msbB* 3' Homology Region
SphI HR2 msbB	ACGCATGCAGAGGTGTTGATTTCGCCATGCC	*msbB* 3' Homology Region
NotI-RBS-Cherry	ACTGCGGCCGCAAGAAGGAGATATACATATGGTGAGCAAGGGCGAGGAGG	*mCherry* gene amplification
SpeI Cherry	TCTACTAGTTTACTTGTACAGCTCGTCCATGC	*mCherry* gene amplification
XhoI cysP Prom	AGCACTCGAGAGTCGAACCCGGAAGATCCAGAGTCG	P*cysP* amplification
NotI cysP Prom	AGGTGCGGCCGCTGCGCACCCTTATAAATTTAATG	P*cysP* amplification
cysP ups check	CTTAACGAAAGCGGCGATTGTTGG	5' check *mCherry* integration in *cysP*
cysP down check	TTGCCCATTGTTGCTCAAACGG	3' check *mCherry* integration in *cysP*
XhoI cysD Prom	ACAGTCTCGAGAGTGAGTCCTTAAATACCATGC	P*cysD* amplification
NotI cysD Prom	TCATGGCGGCCGCAACCGTTCCTTTGCAATACCG	P*cysD* amplification
cysD ups check	GGCAGATAACATTTCTGCAGGAGTTCC	5' check *mCherry* integration in *cysD*
cysD down check	TTTATGCACCAGCAGTTCGCAGCC	3' check *mCherry* integration in *cysD*
XhoI yeeE Prom	AGCTCTCGAGCCTGCTGGCAATCAACTTCG	P*yeeE* amplification
NotI yeeE Prom	TCATGGCGGCCGCAAATTAATTAACCAGATGAATG	P*yeeE* amplification
yeeE ups check	GCTTCTTCGGTTATGTACACCC	5' check *mCherry* integration in *yeeE*
yeeE down check	GATATACCCACCTATAACAGTACC	3' check *mCherry* integration in *yeeE*
XhoI ydjN Prom	AGGACTCGAGCCCACAGTCTGCTGGCGGTATTTGC	P*ydjN* amplification
NotI ydjN Prom	AGCAGCGGCCGCCCCCGTTCTCCTGATCTTATTATTTC	P*ydjN* amplification
ydjN ups check	CAAAAATGCCGAGCTGACGCC	5' check *mCherry* integration in *ydjN*
ydjN down check	TGATTTTGCCTAACTGAGATGC	3' check *mCherry* integration in *ydjN*
XhoI ldhA Prom	AGGACTCGAGCAAGCAGAATCAAGTTCTACCG	P*ldhA* amplification
NotI ldhA Prom	ACCTGCGGCCGCAAGACTTTCTCCAGTGATGTTGAATC	P*ldhA* amplification
ldhA ups check	TGGATATCAGAGGTTAATGCG	5' check *mCherry* integration in *ldhA*
ldhA down check	AAGGTCGACGTTATTGAAACCG	3' check *mCherry* integration in *ldhA*
XhoI fruB Prom	ACGCCTCGAGCATCGGTAAGAAAAATACTGAGTGTCG	P*fruB* amplification
NotI fruB Prom	AGCTGCGGCCGCAGTTCTCCTCTCTTGCTGAATTGAAACG	P*fruB* amplification
fruB ups check	TTACCAGAATCCCAATGACAGC	5' check *mCherry* integration in *fruB*

Table M3. Oligonucleotides used in this study (3/3)

Name	Sequence (5'- 3')	Use
fruB down check	AACGTTGAGGTTTGCTGTTCG	3' check *mCherry* integration in *fruB*
SpeI terminator	AAACCCTGGCGACTAGTCTTGG	T0 terminator amplification
SphI terminator	ATACGCATGCCAAGGTTCTGGACCAGTTGCG	T0 terminator amplification
XbaI-minE	GCTCTAGAAGATAAATGCGCTTTTACAGCGGGC	*minCD* 5' Homology Region
HindIII-minD	CCCAAGCTTGCGCATCAAACTCGTCGGCGTGATCC	*minCD* 5' Homology Region
SpeI-minC	GACTAGTTGTGGAGCATAAATACGCTGACCG	*minCD* 3' Homology Region
Sph-minC	ACATGCATGCCTATAACATGCCTTATAGTCTTCG	*minCD* 3' Homology Region
HindIII-FRT-bla	CTAAAGCTTGAAGTTCCTATACTTTCTAGAGAATAGGAACTTCGGAATAGGAACTTCATGAGTAAACTTGGTCTGACAG	pGE*minCD*-Amp-FRT construction
SpeI-FRT-bla	ATACTAGTGAAGTTCCTATTCCGAAGTTCCTATTCTCTAGAAAGTATAGGAACTTCTCGGGGAAATGTGCGCGGAACC	pGE*minCD*-Amp-FRT construction

pNVfib: A DNA fragment encoding a VHH binding human fibrinogen (Campuzano et al., 2014) was cloned between *Sfi*I and *Not*I sites of pNeae2.

pNVega: a DNA fragment encoding a VHH binding human EGFR (Roovers et al., 2007) was cloned between *SfiI* and *NotI* sites of pNeae2.

pDisplay-TirM-tm: the DNA sequence corresponding to amino acid residues 252 to 360 of the translocated intimin receptor of EHEC was amplified by PCR from pET28a-TirM_{EHEC} (Salema et al., 2013) template with oligonucleotide primers Sfi-TirM-For and TirM-Xma-Rev. The amplified fragment was digested with *Sfi*I and *Xma*I and cloned into the same sites of pDisplay vector. Subsequently, a DNA fragment encoding mWasabi (GeneBank Accession Number EU024648) was synthesized (GeneArt, Life Technologies) with flanking *Sma*I and *Sac*II restriction sites and cloned into pDisplay.

pGE: This 1436 bp Km^R-suicide plasmid contains two I-SceI sites flanking a multiple cloning site (MCS) with the following restriction sites: *Xma*I, *Xho*I, *Bsa*I, *Sac*I, *Nde*I, *Xba*I, *Hind*III, *Spe*I, *Avr*II, *Sph*I and *Xma*I. This plasmid was constructed ligating three DNA fragments, one encompassing the R6K origin of replication, a Km resistance cassette and the MCS. A DNA fragment of 424 bp corresponding to R6K origin of replication was PCR amplified from plasmid pEMG (Martinez-Garcia and de Lorenzo, 2011) with R6K1 and R6K2 primers. This PCR product has *Xma*I and I-*Sce*I sites at its 5'-end and an *Asc*I site at its 3'-end. The Km resistance cassette was amplified by PCR from pEMG with Km1 and Km2 primers. This PCR product of 958 bp has an *Asc*I site at its 5'-end and I-*Sce*I and *Xma*I sites at its 3'-end. The MCS was obtained annealing oligonucleotides MCS1 and MCS2 generating a DNA fragment of 74 bp with XmaI cohesive ends. PCR fragments of R6K and Km were digested with *Xma*I and *Asc*I, and ligated to the MCS.

pGE*flu*: This suicide plasmid is a pGE-derivative with two homology regions (HR) of ca. 500 bp flanking the *flu* gene that were amplified by PCR from the chromosomal DNA of *E. coli* K-12 MG1655. The 5'-HR was amplified with oligos XhoI-yeeP and SacI-yeeP and cloned between *Xho*I-*Sac*I sites of pGE. The 3'-HR was amplified with oligonucleotides Ang43-Spe and and Ang43-Sph and cloned into *Spe*I and *Sph*I restriction sites of pGE vector backbone.

pGE*flu*-SAgfp: The sequence encoding NVgfp fusion was obtained by digesting pNVgfp (Salema et al., 2013) with *Xba*I and *Hind*III and cloned into same sites of pGE*flu*. Promoter P_{N25} sequence, obtained by hybridizing oligonucleotides PN25-Sac-Xba1 and PN25-Sac-Xba2, was cloned upstream NVgfp between *Sac*I and *Xba*I sites.

pGE*flu*-SAtir: The sequence encoding the VHH anti-TirM and C-terminal myc-tag was obtained by digestion of pNVtir (Salema et al., 2013) with *Nco*I and *Hind*III and cloned into the same sites of pGE*flu*-SAgfp replacing the VHH anti-GFP and myc-tag of SAgfp.

pGE*mat-lux*: This suicide plasmid is a pGE-derivative contains the *luxCDABE* operon with P_2 constitutive promoter and two homology regions (HR) of ca. 500 bp flanking the *matB* gene of *E. coli* K-12 MG1655. The 5'-HR was amplified by PCR using primers matA-XhoI and matA-SacI and cloned between *Xho*I and *Sac*I sites of pGE. The 3'-HR was amplified by PCR using primers matBC-SpeI and matBC-SphI and cloned into *Spe*I and *Sph*I sites of pGE. The *luxCDABE* operon was obtained by *Hind*III and *Spe*I digestion of pSEVA226 (Silva-Rocha et al., 2013) and cloned into the same sites of pGE vector backbone. The P_2 promoter sequence was cloned between *Sac*I and *Hind*III sites of pGE. The constitutive P_2 promoter is a synthetic tandem promoter based on P_{A1} and Ptac promoters (Brunner and Bujard, 1987) with the following sequence (5'-TTATCAAAAAGAGTATTGGCTTAAAGTCTAACCTATAGGATACTT ACAGCCATCGAGAGGGACACGGCGAATCTAGAGTCGACCTGCAGGCATGCAAGCTCTTC TGAAATGAGCTGTTGACAATTAATCATGGGCTCGTATAATAGATTCAT-3')

pGE*ycgR*: This suicide plasmid is a pGE-derivative with two homology regions (HR) of ca. 500 bp flanking the *ycgR* gene that were amplified by PCR from the chromosomal DNA of *E. coli* K-12 MG1655. The 5'-HR was amplified with oligos XhoI HR1 ycgR and XbaI HR1 ycgR. The 3'-HR was amplified with oligos XbaI HR2 ycgR and SphI HR2 ycgR. pGE vector was digested with *XhoI* and *Sph I* restriction enzymes, the 5' HR was digested with *XhoI* and *XbaI* and the 3' HR was digested with *XbaI* and *SphI* restriction enzymes. The pGE*ycgR* plasmid was constructed ligating these 3 DNA fragments at the same time.

pGE*flu*-SAega: The sequence encoding the VHH anti-ega and C-terminal myc-tag was obtained by digestion of pNVega with *Nco*I and *Hind*III and cloned into the same sites of pGE*flu*-SAgfp replacing the VHH anti-GFP and myc-tag of SAgfp.

pGEP*cysP*CherryT0: This suicide plasmid is a pGE-derivative contains the *mCherry* gene with P*cysP* promoter (i.e. 500 pb upstream the start codon of *cysP* gene) and the lambda T0 derived transcriptional terminator sequence. mCherry gene was amplified from pP35mCherry plasmid (a gift from Jean-Marc Ghigo and Christophe Beloin) with oligos NotI-RBS-Cherry and SpeI Cherry. P*cysP* promoter was amplified by PCR from the chromosomal DNA of *E. coli* K-12 MG1655 with oligos XhoI cysP Prom and NotI cysP Prom. T0 transcriptional terminator was amplified from pSEVA226 (Silva-Rocha et al., 2013) with oligos SpeI terminator and SphI terminator. The 3 fragments were digested and cloned into their respective sites present in pGE*yeeJ*PtetGFP plasmid, leading to the substitution of GFP coding gene by mCherry coding

gene, Ptet promoter and *yeeJ* 5' HR by P*cysP* promoter sequence, and *yeeJ* 3' HR by T0 transcriptional terminator.

pGEP*cysD*CherryT0: The P*cysD* promoter sequence (i.e. 500 pb upstream the start codon of *cysD* gene) was amplified by PCR from the chromosomal DNA of *E. coli* K-12 MG1655 with oligos XhoI cysD Prom and NotI cysD Prom, and cloned into *XhoI* and *NotI* sites of pGEP*cysP*CherryT0, replacing P*cysP* promoter by P*cysD* promoter.

pGEPyeeECherryT0: The P*yeeE* promoter sequence (i.e. 500 pb upstream the start codon of *yeeE* gene) was amplified by PCR from the chromosomal DNA of *E. coli* K-12 MG1655 with oligos XhoI yeeE Prom and NotI yeeE Prom, and cloned into *XhoI* and *NotI* sites of pGEP*cysP*CherryT0, replacing P*cysP* promoter by P*yeeE* promoter.

pGEPydjNCherryT0: The P*ydjN* promoter sequence (i.e. 500 pb upstream the start codon of *ydjN* gene) was amplified by PCR from the chromosomal DNA of *E. coli* K-12 MG1655 with oligos XhoI ydjN Prom and NotI ydjN Prom, and cloned into *XhoI* and *NotI* sites of pGEP*cysP*CherryT0, replacing P*cysP* promoter by P*ydjN* promoter.

pGEP*ldhA*CherryT0: The P*ldhA* promoter sequence (i.e. 500 pb upstream the start codon of *ldhA* gene) was amplified by PCR from the chromosomal DNA of *E. coli* K-12 MG1655 with oligos XhoI ldhA Prom and NotI ldhA Prom, and cloned into *XhoI* and *NotI* sites of pGEP*cysP*CherryT0, replacing P*cysP* promoter by P*ldhA* promoter.

pGEP*fruB*CherryT0: The P*fruB* promoter sequence (i.e. 500 pb upstream the start codon of *fruB* gene) was amplified by PCR from the chromosomal DNA of *E. coli* K-12 MG1655 with oligos XhoI fruB Prom and NotI fruB Prom, and cloned into *XhoI* and *NotI* sites of pGEP*cysP*CherryT0, replacing P*cysP* promoter by P*fruB* promoter.

pGE*msbB*: This suicide plasmid is a pGE-derivative with two homology regions (HR) of ca. 500 bp flanking the *msbB* gene that were amplified by PCR from the chromosomal DNA of *E. coli* K-12 MG1655. The 5'-HR was amplified with oligos XbaI HR1 msbB and SpeI HR1 msbB. The 3'-HR was amplified with oligos SpeI HR2 msbB and SphI HR2 msbB. The pGE vector was digested with *XbaI* and *SphI* restriction enzymes, the 5' HR was digested with *XbaI* and *SpeI* and the 3' HR was digested with *SpeI* and *SphI* restriction enzymes. The pGE*ycgR* plasmid was constructed ligating these 3 DNA fragments at the same time.

pGEminCD-AmpFRT: This suicide plasmid is a pGE-derivative with two homology regions (HR) of ca. 500 bp flanking the 3' end of *minC* gene and the 5' end of *minD* gene. In addition between the two HRs, an Ampicillin resistance gene cassette flanked by two Flippase Recognized target (FRT) sites, was cloned. HRs were amplified by PCR from the chromosomal

DNA of *E. coli* K-12 MG1655 using oligos XbaI-minE and HindIII-minD for 5' HR and SpeI-minC and SphI-minC for 3' HR. The 5' HR was digested with *XbaI* and *HindIII*, whereas the 3' HR was digested with *SpeI* and *SphI* and both fragments were cloned into their respective sites in pGE vector. The Ampicillin resistance gene was amplified by PCR from pUC18 plasmid (Vieira and Messing, 1982) with oligos HindIII-FRT-bla and SpeI-FRT-bla that included FRT sites at both ends of the fragment. The PCR product was digested with *HindIII* and *SpeI* enzymes and cloned into the same sites of pGE vector backbone.

4. *In vitro* cell culture and plasmid transfection.

The human epithelial tumor cell line HeLa (ATCC, CCL-2) was grown as monolayer in Dulbecco's modified Eagle's medium (DMEM), supplemented with 10% fetal bovine serum (FBS) and 2 mM glutamine (complete DMEM), at 37°C with 5% CO_2. For transfection, HeLa cells were seeded in 24-well tissue culture plates (BD Falcon) (~10^5 cells/well), grown for 20 h at 37°C with 5% CO_2, and transfected with 0.6 µg/well of plasmids pDisplay-GFP-tm or pDisplay-TirM-tm following the calcium phosphate method (Jordan et al., 1996). After 22 h incubation at 37°C with 5% CO_2, the medium was removed, wells were washed three times with phosphate-buffered saline (PBS) and filled with complete DMEM medium containing G418 (0.5 mg/ml, Invitrogen, Life Technologies). After 24 h incubation, cells were passed to T75 flask (BD Falcon) with the same medium and further grown. G418-resistant HeLa cells expressing GFP or mWasabi fusion proteins were selected from these cultures by fluorescence activated cell sorting (FACS) using Epics-Altra Cell Sorter (Beckman Coulter). HeLa-GFP-tm and HeLa-TirM-tm positive cells populations were expanded on complete DMEM medium.

5. Flow cytometry analyses.

Bacteria (equivalent to a final OD_{600} of 1.0) were harvested from cultures by centrifugation (4000 xg, 3 min), washed with PBS and resuspended in 1 ml of PBS containing 10% (v/v) goat serum (Sigma). An aliquot sample of 200 µl was incubated for 1 h on ice with anti-myc mAb clone 9B11 (1:200; Cell Signaling Technology). Next, bacteria were washed in PBS, resuspended in 500 µl of PBS containing 10% (v/v) goat serum, and stained for 40 min in the dark with Alexa 488-conjugated anti-mouse IgGs (1:500; Molecular Probes, Life Technologies). Bacteria were finally washed and resuspended in a final volume of 1 ml of PBS, and analyzed in a flow cytometer (Gallios, Beckman Coulter).

6. Protein extract preparation, SDS-PAGE, and Western blots.

Whole-cell protein extracts were prepared in urea-SDS sample buffer as described previously (Bodelon et al., 2009). SDS-polyacrylamide gel electrophoresis (PAGE) and immunoblotting conditions to polyvinylidene difluoride membrane (PVDF, Immobilon-P; Millipore) have been

reported (Bodelon et al., 2009; Salema et al., 2013). For immunodetection, the PVDF-membranes were incubated with anti-myc mAb clone 9B11 (1:2000; Cell Signaling Technology) to detect myc-tagged SAs and anti-mouse IgG-peroxidase (POD) conjugate (1:5000; Sigma) as secondary antibody. GroEL was detected with anti-GroEL MAb-POD conjugate (1:5000; Sigma). Membranes were developed by chemiluminescence using a mixture in 100 mM Tris-HCl (pH 8.0) containing 1.25 mM luminol (Sigma), 0.22 mM cumaric acid (Sigma), and 0.0075% (v/v) H_2O_2 (Sigma), and exposed to an X-ray film (Curix, Agfa).

7. Adhesion assays to antigens immobilized on a plastic surface.

Purified GFP (Upstate, Millipore) or human fibrinogen (Enzyme Research Laboratories) as indicated, were diluted in PBS to 10 µg/ml and 100 µl were adsorbed onto ELISA plates (Maxisorb, Nunc) overnight at 4°C. Antigen-coated plates were washed with PBS and blocked for 1 h at room temperature with PBS containing 3% (w/v) skimmed milk. Next, a bacterial suspension (100 µl) of the indicated strain was added at an OD_{600} of 3.0 in PBS and incubated for an additional hour. The plates were then washed with PBS three times, and the presence of bound bacteria was visualized by light microscopy and macroscopically detected by staining with crystal violet solution (Sigma).

8. Bacterial adhesion assays to *in vitro* cultured HeLa or NIH 3T3 derived cells and immunofluorescence microscopy.

Bacteria from the indicated *E. coli* strain were harvested by centrifugation (4000 xg, 3 min) from static liquid LB cultures grown overnight at 37 ^{o}C. An OD_{600} of 1.0 from these cultures grown statically was determined to contain ~$3x10^8$ CFU/ml by plating in LB-agar. Bacteria were washed in PBS and resuspended at $3x10^7$ CFU/ml in PBS or DMEM. For an infection at MOI 300:1, a 1 ml sample of this bacterial suspension was added to a single well of a 24-well tissue culture plate having the indicated HeLa or NIH 3T3 derived cell line (~10^5 cells/well). HeLa or NIH 3T3 derived cells were grown on sterile coverslips (13 mm diameter, VWR international) placed at the bottom of the well. After 1 h infection at 37 ^{o}C, the wells were aspirated and washed five times with 1 ml PBS at room temperature. The coverslips were fixed for 20 min at room temperature with 0. 5 ml of a paraformaldehyde 4% (w/v) solution in PBS and washed three times with 1 ml of PBS. Coverslips were blocked and stained for 1 h at room temperature in a wet chamber with 50 µl of PBS-10% goat serum solution, having a rabbit polyclonal serum anti-*E. coli* O and K antigenic serotypes (1:1000; Biodesign) for HeLa cells immunofluorescences, or having rabbit polyclonal serum anti-*E. coli* O and K antigenic serotypes (1:1000; Biodesign) and mouse mAb anti-EGFR (1:500; Calbiochem) for NIH 3T3 derived cell lines immunofluorescences . The coverslips were washed by immersion 15 times in a large volume of PBS (100 ml), placed again the wet chamber and incubated for 40 min at

room temperature with 50 µl of PBS-10% goat serum solution, having a goat anti-rabbit IgG-Alexa 594 conjugated secondary antibody (1:500; Molecular Probes, Life Technologies) and DAPI (1:500; Sigma) for HeLa cells immunofluorescences, and having goat anti-rabbit IgG-Alexa 594 conjugated secondary antibody (1:500; Molecular Probes, Life Technologies), goat anti-mouse IgG-Alexa 488 (1:500; Molecular Probes, Life Technologies) and DAPI (1:500; Sigma) for NIH 3T3 derived cells immunofluorescences. Next, the coverslips were washed with PBS as above, the excess of liquid was removed touching a kimwipe with the edge of the coverslip, and mounted with 2 µl of Prolong (Invitrogen) on glass slides. The samples were examined by epifluorescence microscopy (Zeiss Axio imager microscope) or by confocal microscopy (Leica TCS SP5 multispectral confocal system). For time-lapse live cell video microscospy, HeLa-GFP-tm cell, grown on 24-well tissue culture plates, were infected with $1x10^7$ CFU of EcM1*lux*SAgfp in a final volume ~0.3 ml/well (MOI 100:1) and monitored using an Olympus IX71 microscope equipped with an Olympus cell^R motorized TIRF system.

9. Bacterial adhesion assays to *in vitro* cultured NIH 3T3 derived cells to screen adhesion-dependent promoters.

The indicated bacterial strains expressing SAs against hEGFR and the mCherry protein under the control of different promoters were harvested by centrifugation (4000 xg, 3 min) from static liquid LB cultures grown overnight at 37 ^oC. An OD_{600} of 1.0 from these cultures grown statically was determined to contain ~$3x10^8$ CFU/ml by plating in LB-agar. Bacteria were washed in PBS and resuspended at $4x10^7$ CFU/ml in DMEM. For the infections at MOI 100:1, a 250 µl sample of this bacterial suspension was added to a single well of a 24-well tissue culture plate having 3T3#2.2 or Her14 cells (~10^5 cells/well) growing over sterile coverslips (13 mm diameter, VWR international), placed at the bottom of the well. After 15 minutes of infection at 37 ^oC, the wells of tissue culture plates containing Her14 cells were aspirated and washed three times with 1 ml of pre-heated DMEM to remove unbound bacteria. After that, plates were placed again at the incubator for two additional hours to allow mCherry protein translation, maturation and accumulation. Lastly, coverslips were fixed for 20 min at room temperature with 0. 5 ml of a paraformaldehyde 4% (w/v) solution in PBS and washed three times with 1 ml of PBS before mount them with 2 µl of Prolong (Invitrogen) on glass slides. On the other hand, tissue culture plates containing 3T3#2.2 cells were infected with the indicated bacterial strains for 2 hours, but after 1 hour of infection 0,5 ml of pre-heated fresh DMEM was added to each well in order to maintain a bacterial density similar to the one of Her14 infected cells. After 2 hours of infection, the medium in which the infection took place (0,75 ml) containing the non-adhered bacteria was collected and centrifuged (4000g, 3 min). Bacterial pellet was fixed for 20 min at room temperature with 0. 5 ml of a paraformaldehyde 4% (w/v) solution in PBS and washed three times with 1 ml of PBS. After fixation, 100 µl of the bacterial suspension were placed over Poly-

L-Lysine (SantaCruz Biotechnology) coated coverslips and incubated for 20 minutes. Lastly, the excess of liquid was removed touching a kimwipe with the edge of the coverslip before mount them with 2 µl of Prolong (Invitrogen) on glass slides. All samples were examined by epifluorescence microscopy (Zeiss Axio imager microscope)

10. Minicells adhesion assays to in vitro cultured NIH 3T3 derived cells and immunofluorescence microscopy.

Minicells with the desired SA specificity were harvested by centrifugation (4000g, 20 min), from minicells purifications stored at 4 ºC in OptiPrep™ solution at 4% (w/v) in water, and resuspended at $4x10^8$ minicells/ml in DMEM. For a minicell-mammalian cell co-incubation at MOI 1000:1, a 250 µl sample of this minicell suspension was added to a single well of a 24-well tissue culture plate having the indicated or NIH 3T3 derived cell line (~10^5 cells/well) that were grown on sterile coverslips (13 mm diameter, VWR international) placed at the bottom of the well. After four hours of coincubation at 37 ºC, the coverslips were washed by immersion 15 times in a large volume of PBS (100 ml) to remove unbound minicells. Subsequently, the coverslips were treated as in NIH 3T3 derived cell lines immunofluorescences carried out in bacterial adhesion assays and examined by confocal microscopy (Leica TCS SP5 multispectral confocal system)

11. Double staining protocol to distinguish intra- and extracellular bacteria.

Bacteria from the indicated *E. coli* strain were harvested by centrifugation (4000 xg, 3 min) from static liquid LB cultures grown overnight at 37 ºC. An OD_{600} of 1.0 from these cultures grown statically was determined to contain ~$3x10^8$ CFU/ml by plating in LB-agar. Bacteria were washed in PBS and resuspended at $4x10^7$ CFU/ml in DMEM. For the infections at MOI 100:1, a 250 µl sample of this bacterial suspension was added to a single well of a 24-well tissue culture plate having HeLa-GFP-tm or Her14 cells (~10^5 cells/well) growing over sterile coverslips (13 mm diameter, VWR international), placed at the bottom of the well. After 15 minutes of infection at 37 ºC, the wells were aspirated and washed five times with 1 ml PBS at room temperature. Coverslips were blocked and stained for 30 minutes at 4 ºC in a wet chamber with 50 µl of PBS-10% goat serum solution, having a rabbit polyclonal serum anti-*E. coli* O and K antigenic serotypes (1:500; Biodesign) for HeLa-GFP-tm cells immunofluorescences, or having rabbit polyclonal serum anti-*E. coli* O and K antigenic serotypes (1:500; Biodesign) and mouse mAb anti-EGFR (1:250; Calbiochem) for Her14 cells immunofluorescences. After this staining, coverslips were washed by immersion 15 times in a large volume of PBS (100 ml) and fixed for 20 min at room temperature with 0. 5 ml of a paraformaldehyde 4% (w/v) solution in PBS, which was washed three times with 1 ml of PBS. Subsequently, coverslips were placed again the wet chamber and incubated for 40 min at room

temperature with 50 µl of PBS-10% goat serum solution, having a goat anti-rabbit IgG-Alexa 546 conjugated secondary antibody (1:500; Molecular Probes, Life Technologies) for HeLa-GFP-tm cells immunofluorescences, and having goat anti-rabbit IgG-Alexa 594 conjugated secondary antibody (1:500; Molecular Probes, Life Technologies), and goat anti-mouse IgG-Alexa 647 (1:500; Molecular Probes, Life Technologies) for Her14 cells immunofluorescences. After extracellular bacteria staining, cells were permeabilized for 10 min at room temperature with 0. 5 ml of a Triton X-100 0,2% (v/v) solution in PBS, which was washed four times with 1 ml of PBS. After cell permeablization, both extra- and intracellular bacteria were stained following the same procedure that the one used before permeablization, but using as secondary antibodies anti-rabbit IgG-Alexa 647 conjugated antibody (1:500; Molecular Probes, Life Technologies) for HeLa-GFP-tm cells immunofluorescences, and anti-rabbit IgG-Alexa 488 conjugated antibody (1:500; Molecular Probes, Life Technologies) for Her14 cells immunofluorescences. After stainining, samples were mounted with 2 µl of Prolong (Invitrogen) on glass slides, and examined by confocal microscopy (Leica TCS SP5 multispectral confocal system)

12. Infection of tumor-bearing mice and recovery of bacteria from tissues.

All animal experiments were done in accordance with protocols approved by the CNB Ethics Committee for Animal Experimentation (ref 11034) and by the Hospital Universitario Puerta de Hierro Animal Care and Use Committee, in compliance with Spanish and European Union legislation. Five-week-old athymic female Hsd:Athymic Nude-*Foxn1*^{nu} were obtained from Harlan (Harlan Ibérica). Tumor-bearing mice were generated by subcutaneous injection of ~1x10^6 HeLa-GFP-tm or HeLa cells, as indicated, in 100 µl PBS containing 20% (v/v) Matrigel (BD Biosciences), into the abdominal right flank of 6-week-old Nude mice. Tumor volumes were estimated with calipers according to the formula: width^2×length×0.52. When tumors reached a volume between 200-400 mm^3, the mice were randomly divided into experimental groups. Bacteria were grown and harvested as described above for the *in vitro* adhesion assays, and resuspended in sterile PBS at 1x10^8 CFU/ml. For each independent experiment the number of CFU in this bacterial suspension was determined, showing an experimental error below 10%. This bacterial stock was directly used for systemic inoculation of mice receiving a dose of 1x10^7 CFU by injection of 100 µl into the lateral tail vein using a 0.5 ml syringe with a 29G needle (Becton Dickinson). Alternatively, for mice receiving a dose of 1x10^5 CFU, the original bacterial stock was diluted in PBS to 1x10^6 CFU/ml and 100 µl were injected per mouse as above. These bacterial doses did not cause any apparent disease symptoms in the animals, which showed normal phenotype throughout the entire experiment (i.e. mobility, weight, feeding behavior). For determination of bacterial CFU per gram (CFU/g) of tumors, livers and spleens, animals were euthanized and tumors and organs were excised, placed individually into (pre-

weighed) sterile tubes containing 5 ml of PBS and weighed. Samples were then transferred to sterile sampling bags (VWR) and Triton X-100 (Sigma) was added to a final concentration of 0.2% (v/v). Samples were homogenized by soft mechanical squeezing. Next, a 100-µl sample of the homogenates was serially diluted in LB, plated in LB-agar and incubated overnight at 37 ^{o}C to determine CFU. Bacterial titers were expressed as CFU/g of tissue. For statistical analysis a minimal bacterial titer of 50 CFU/g, corresponding to the detection limit of the assay, was considered in those cases in which no bacteria were detected by plating.

13. Bioluminescence imaging.

Bacterial light emission from LB plates or from tissue culture plates was captured using a ChemiDoc XRS system (Bio-Rad). For live imaging of bioluminescent bacteria in tumor-bearing mice, animals were anesthetized with 4% Isoflurane (Forene, Abbott) and maintained under 1% Isoflurane in a thermostated chamber with a high-resolution charge-coupled-device (CCD) cooled digital camera ORCA-2BT (Hamamatsu Photonics). Imaging analysis was done with the Hokawo software (Hamamatsu Photonics).

14. RNA extraction from adhered or non-adhered bacteria.

Bacteria from the indicated *E. coli* strain were harvested by centrifugation (4000 xg, 3 min) from static liquid LB cultures grown overnight at 37 ^{o}C. An OD_{600} of 1.0 from these cultures grown statically was determined to contain ~$3x10^8$ CFU/ml by plating in LB-agar. Bacteria were washed in PBS and resuspended at 10^8 CFU/ml in DMEM. For an infection at MOI 100:1, a 9 ml sample of this bacterial suspension was added to a 150 cm^2 cell culture dish (BD Falcon) containing approximately $9x10^6$ cells of the indicated HeLa or NIH 3T3 derived cell line. For RNA extraction a DEPC (Sigma)- treated water solution containing 1% (v/v) Acid Phenol (Sigma), 19% (v/v) Ethanol and 0,2% (w/v) SDS (Sigma), termed lysis buffer was prepared. After 15 minutes of infection at 37 ºC, infection media of cell culture dishes containing HeLa or 3T3#2.2 cells (non-adhered bacteria) was collected and mixed with an equal volume of pre-cooled 2X lysis buffer. On the other hand, after 15 minutes of infection at 37 ºC, cell culture dishes containing Hela-GFP-tm or Her14cells (adhered bacteria) were washed 3 times with pre-heated DMEM to remove unbound bacteria, and treated with pre-cooled 1X lysis buffer containing DNAse I RNAse free (Roche). Both, adhered and non-adhered bacteria were incubated with 1X or 2X lysis buffer for 30 minutes at 4 ºC. Subsequently lysis buffers containing bacteria were centrifuged for 1 hour at 7200g and bacterial pellets were washed 2 additional times with pre-cooled 1X lysis buffer to ensure mammalian cell lysis. After that, bacterial pellets were resuspended in a TE solution (Tris-HCl pH 8; EDTA 1mM) containing Lysozyme (Sigma) at 2 mg/ml, and incubated for 5 minutes at room temperature to break bacterial cell wall. Bacterial RNA was isolated using Trizol (Life Technologies) following

manufacturer's recommendations, adding two additional Chloroform washing steps to avoid any phenol contamination. The resulting aqueous phase from Trizol-mediated RNA isolation was precipitated with Isopropanol (Merck) and 20 µg of glycogen (Roche) for 1h at 4ºC. Lastly, bacterial RNA was treated with turbo DNA free kit (Life Technologies) for complete digestion of DNA and cleaned-up with RNAeasy kit (Quiagen) to remove DNAse. Quality and concentration of isolated bacterial RNA was determined using Bioanalyzer 2100 (Agilent), obtaining RNA Integrity Numbers (RIN) ranging from 8.6 to 9.8.

15. Transcriptomic profiling by RNAseq.

RNA preparations were treated with the rRNA capture hybridization approach from the MicrobExpress kit (Ambion) according to manufacturer's instructions. Non directional cDNA libraries were prepared from enriched fragmented mRNA using the TruSeq RNA sample preparation V2 kit set A (Illumina). Fragments of cDNA (ca. 150 bp), ligated with Illumina adapters and amplified per PCR, were purified from each library. Quality was confirmed on a Bioanalyzer (Agilent) and quantification done using a Qubit® dsDNA HS Assay Kit (Invitrogen). Sequencing of 49 bases was performed in single-end mode, using an Illumina HiSeq2000 instrument (Illumina). Samples were multiplexed on two lines on the flowcell (eight per line). Sequences shorter than 25 nucleotides, of poor quality, and those corresponding to adapters were discarded for further analysis. Bowtie software (Langmead et al., 2009) was employed to align the reads to the *E. coli* genome.

Statistical analysis were carried out with R software and the DESeq package (Anders and Huber, 2010). For each strain the count data were normalized according to DESeq procedure with the default parameter. A p-value reflecting the significance of the biological effect (i.e. adhesion to target cells) was then computed and adjusted according to the Benjamini and Hochsberg (BH) procedure for each gene (Benjamini). Genes with an adjusted p-value below 0,05 were considered differentially expressed.

16. Trancriptomic profiling by DNA microarrays.

RNA preparations were transformed to cDNA and fluorescently labeled with either Cy3 or Cy5 using the SuperScript Indirect cDNA Labeling System (Invitrogen). The labeled cDNAs corresponding to the adhered and non-adhered conditions from EcM1luxSAega strain were mixed and used to hybridize a oligonucleotide-based *E. coli* genome-wide DNA microarray (Agilent Microarray Design ID 020097). Four hybridizations, corresponding to four independent experiments (biological replicas), were used. The results for each replica (median intensity for each spot) were normalized and statistically analyzed as described using the LIMMA software package (Smyth, 2004), which deduces the differential expression values of the genes in the microarray using linear models and moderated *t*-statistics using the empirical Bayes approach.

The probability values obtained (*p*-values) were adjusted for multiple testing to control the false discovery rate (Benjamini). Genes with an adjusted p-value below 0,05 were considered differentially expressed.

17. Isolation and analysis of LPS.

Samples of LPS from the indicated stains were extracted using an ammonium hydroxide-isobutyric acid method and subjected to negative-ion matrix-assisted laser desorption ionization-time of flight (MALDI-TOF) mass spectrometry analysis, as previously described (El Hamidi et al., 2005; Perez-Gutierrez et al., 2010) Briefly, lyophilized crude cells (10 mg) were resuspended in 400 µl isobutyric acid-1 M ammonium hydroxide (5:3, v/v) and were incubated in a screw-cap test tube at 100°C for 2 h with occasional subjection to a vortex. Samples were cooled in ice water and centrifuged at 2000g for 15 min. The supernatant was transferred into a new tube, diluted with an equal volume of water, and lyophilized. The sample was then washed twice with 400 µl methanol and centrifuged at 2000g for 15 min. The insoluble lipid A was solubilized in 100 to 200 µl chloroform-methanol-water mixture (3:1.5:0.25, v/v/v). Analyses were performed with a Bruker Autoflex II MALDI-TOF mass spectrometer (Bruker Daltonics, Inc.) in negative reflective mode with delayed extraction. Each spectrum was an average of 300 shots. The ion-accelerating voltage was set at 20 kV. Dihydroxybenzoic acid (Sigma) was used as a matrix. A sample of a few microliters of a lipid A suspension (1 mg/ml) was desalted with a few grains of ion-exchange resin (Dowex 50W-X8; H^+) in an Eppendorf tube. A 1-µl aliquot of the suspension (50 to 100 µl) was deposited onto the target and covered with the same amount of the matrix suspended at 10 mg/ml in a 0.1 M solution of citric acid. A peptide calibration standard (Bruker Daltonics) was used to calibrate the MALDI-TOF mass spectrometer.

18. Minicells purification.

A 10-ml LB pre-inocolum of the minicell producer strain was grown during 8 hours at 37 ºC with agitation (160rpm), after that, pre-inocolum was transferred to a flask containing one liter of fresh LB that was grown overnight at 37 ºC with agitation (160rpm). A culture of one liter of *minCD*- mutant bacteria was subjected to initial differential centrifugation at 550g for 40 minutes at 4 ºC to decrease the bulk of the bacterial burden. The resulting bacterial cell/minicell supernatant was centrifuged at 4000g for 20 min at 4 ºC to harvest the bacteria/minicell content, which was resuspended in Optiprep solution at 4% (w/v) (see below) and subjected to two sequential density gradient centrifugation steps using a isotonic biologically compatible medium (OptiPrep™, Axis-Shield PLC, Scotland), which is a sterile 60% (w/v) solution of iodixanol in water. Gradients were performed with OptiPrep solutions ranging from 20% to 6% (w/v). After both density gradient centrifugations minicells were found in a low-density band, whereas bacteria were found in the pellet. The enriched minicell fraction still contained some residual

bacterial cells that were eliminated after incubating the suspension in LB liquid media for 30 min at 37 ºC and shaking to reactivate any residual bacterial cell and then for 90 minutes in LB liquid media containing gentamycin (100 µg/ml) at 37 ºC with agitation to kill any live bacterial cell. Lastly, the antibiotic treated minicell enriched fraction, was centrifuged at 4000g for 20 min at 4 ºC and resuspended in 4% (w/v) OptiPrep solution and subjected to an additional density gradient centrifugation step to eliminate any dead bacterial cell.

19. Minicells quantification. A method based on minicell protein content determination was developed to quantify minicells. A volume equivalent to $6x10^8$ CFU was collected from an overnight culture of EcM1*lux*SAega grown statically at 37 ºC, centrifuged at 4000g for 3 minutes, resuspended in 200 µl of PBS, sonicated (LabSonic B, Braun) for 40 seconds to release protein content and serially diluted using 2 as the dilution factor. Protein content in all dilutions was determined with bicinchoninic acid (BCA) protein assay kit (ThermoScientific) providing an equation that correlates CFU and protein content. A 100-µl fraction of the purified minicells solution was treated in the same way to obtain a BCA-based protein content estimation in minicells. The equation that correlates protein content and CFU enable to determine the number of minicells from the data of protein content estimated for them, including a correction factor of five given the size difference between bacteria (2 µm) and minicells (0,4 µm). A yield of approximately 10^{10} minicells was routinely obtained from a 1 liter culture of *minCD*-mutant bacteria. Acuraccy of this quantification method was confirmed by determining the number of minicells in a standard purification with Nanosight's NS300 device (Nanosight Ltd.), an alternative method that allows visualization, counting and tracking of nanoparticles in liquid media.

20. Transmission electron microscopy.

Aliquots of five µl from the indicated purified minicells were applied to collodion-coated copper grids and incubated for two minutes at room temperature. After that, grids were washed three times with MilliQ water to remove excess of sample and the excess of MilliQ water was removed touching a kimwipe with the edge of the grid. For negative staining, samples were incubated with Phosphotungstic Acid (PTA) 2% (w/v) solution in MilliQ water for three minutes. Excess of PTA solution was removed touching a kimwipe with the edge of the grid. Images were taken with JEOL 1200EX-II electron microscope operated at 100 kV and recorded at a nominal magnification of 50000X.

21. Statistics.

Statistical analyses comparing the ratio of colonized tumors between experimental groups were conducted with Fisher's exact test to determine two-tailed P values using Prism 5.0 (GraphPad software Inc). Data were considered significantly different when $P < 0.05$.

22. Histology.

For *ex vivo* histological analyses, resected tumors were fixed with 4% (w/v) paraformladehyde in PBS for 16 h at 4 ^{o}C and embedded in paraffin. Serial 6 mm sections were cut at the tumor center with a microtome (Leica RM2155) and placed onto glass slides. The samples were deparaffinized with xylene and ethanol solutions, re-hydrated in PBS, and incubated with 1 M citrate buffer (pH 6.0) and PBS-Tween (PBS, 0.1 % Tween 20) to unmask antigens. Tissue sections were blocked with 10% goat serum in PBS-Tween, and incubated with anti-*E. coli* polyclonal serum (1:100) 1 h at room temperature in the same buffer. Next, samples were washed with PBS-Tween and incubated with goat anti-rabbit IgG-Alexa 594 conjugated secondary antibody (1:500) in PBS-Tween with 10% goat serum for 1 h at room temperature. Samples were mounted in Vectashield media (Vector Labs) and images were obtained with a fluorescence microscope (Leica DMI6000B fluorescence system with Orca R^2 digital camera from Hamamatsu).

RESULTS

Chapter 1: Construction of Synthetic Adhesins, expression and validation for driving *E. coli* adhesion to antigenic surfaces.

1.1 Synthetic adhesins structure and expression from inducible plasmids.

We hypothesized that synthetic adhesins (SAs) for *E. coli* could be based on two distinct structural and functional domains, one having the specific adhesion function, and a second for anchoring and displaying the protein on the surface of the bacterium. Excellent candidates for the adhesion module were sdAbs from camelids (VHHs or nanobodies) given their superior binding, small size, high solubility and stability properties (see Introduction section 4.2) Previous work of our group assessed the possibility of display VHHs on the surface of *E. coli* with different β-domains from members of the T5SS, a large family of proteins with "self-translocation-capacity" (Marin et al., 2010; Veiga et al., 2004) (see Introduction section 4.3). Recently, it was found that the the β-domains of EhaA autotransporter and Intimin from EHEC mediate the effective display of VHHs on the surface of *E. coli,* allowing the selection of high-affinity clones from immune libraries (Salema et al., 2013). However, the antigen-binding activity of VHHs was higher when displayed with Intimin β-domain than with EhaA β-domain (Salema et al., 2013). In addition, preliminary experiments displaying model VHHs with EhaA β-domain on *E. coli* showed weak bacterial adhesion to plastic surfaces coated with the antigen recognized by the VHH (data not shown). These initial observations, together with the high resistance of Intimin β-domain to the action of denaturing agents (e.g. SDS, urea) and proteases (Bodelon et al., 2009), prompted us to investigate whether VHHs displayed with this OM-anchoring and transport domain could drive the effective adhesion of *E. coli* to target antigenic surfaces.

The β-domain of Intimin used for the display of VHHs corresponds to the first 659 amino acids of EHEC Intimin (also referred to as Neae fragment) (Bodelon et al., 2009). This region comprises the N-terminal signal peptide (SP), the periplasmic LysM domain for peptidoglycan binding, a 12-stranded β-barrel domain for OM insertion, and the first surface-exposed Ig-like domain (named D0), which does not interact with Tir (Bodelon et al., 2009; Fairman et al., 2012).

The Neae polypeptide (ca. 69 kDa) can be fused to a VHH domain (ca. 13kDa) of the desired specificity flanked by short epitopes (E- and myc-tags) for immunodetection, generating a fusion protein termed NVHH or SA with a total mass of ca. 84 kDa. Thus, using as template a natural adhesin of *E. coli* such as Intimin (Fig. 6A) we were able to create SAs of defined specificity (Fig. 6B).

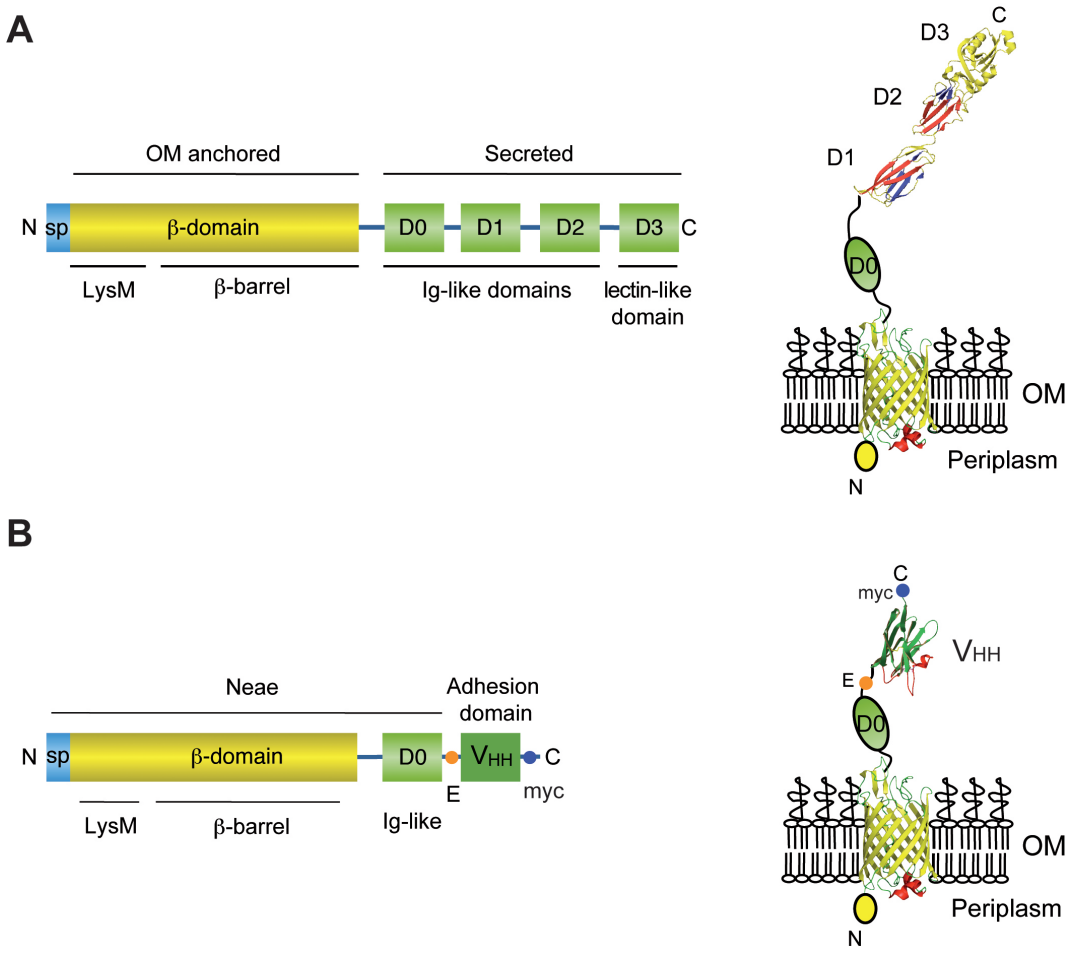

Figure 6. Intimin and synthetic adhesins structure. (A) Scheme of the primary structure of Intimin (left) showing the signal peptide (SP), the OM anchored region comprising LysM and the β-domain, and the secreted region comprising the Ig-like domains (D0, D1 and D2) and the lectin like domain (D3). Structural model of intimin (right) on the bacterial outer membrane (OM) showing the LysM domain in the periplasm (yellow sphere), the β-barrel embedded in the OM and the D0, D1, D2 and D3 domains exposed to the the extracellular milieu. **(B)** Scheme of the primary structure of SAs (left) showing the N-terminal domain of Intimin (Neae), comprising the signal peptide (SP), LysM, β-domain and D0 Ig-like domain, fused to a variable Ig domain from heavy-chain-only antibodies (VHH). The E-tag and myc-tag epitopes flanking the VHH domain are also indicated. Structural model of a SA fusion protein (right) in the bacterial outer membrane (OM) showing the LysM domain in the periplasm (yellow sphere), the β-barrel of Intimin embedded in the OM, and the D0 and VHH Ig-domains exposed to the extracellular milieu.

We constructed two different NVHH fusions binding GFP (NVgfp) and human fibrinogen (NVfib) and expressed them in in *E. coli* K-12 strain EcM1 (MG1655 Δ*fimA-H*; Table M1). This strain has a deletion of the operon encoding encoding Type 1 fimbriae, a major adhesin found in most *E. coli* strains (Connell et al., 1996; Munera et al., 2008) (see Introduction section 3.2.1). Cultures of EcM1 bacteria bearing plasmids encoding NVgfp, NVfib, and the control polypeptide, lacking the myc-tag, Neae (Table M2), were induced with IPTG and the display of the corresponding NVHH fusion on the surface of *E. coli* was confirmed by immunofluorescence and by flow cytometry with anti-myc mAb (Fig. 7).

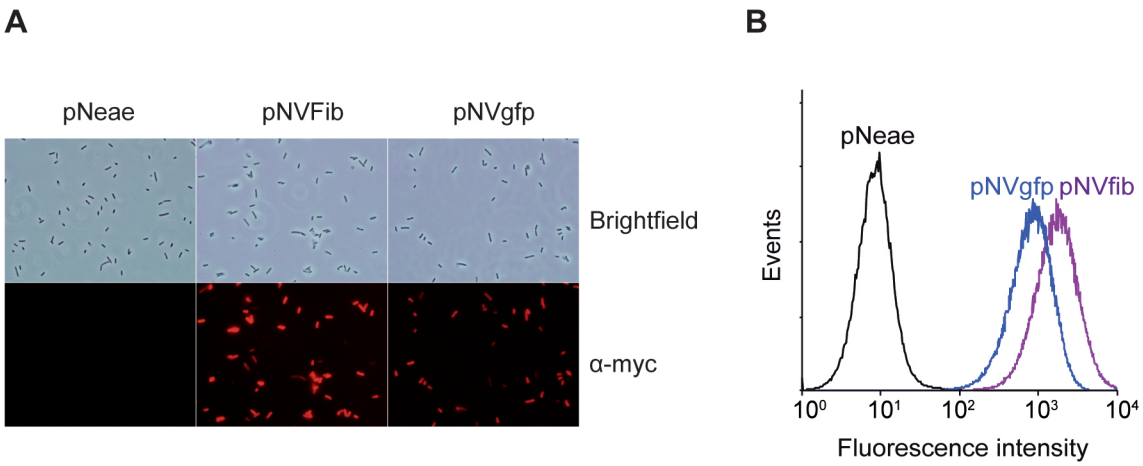

Figure 7. Synthetic Adhesins display on the surface of *E. coli*. (**A**) Fluorescence and light microscopy images of IPTG-induced cultures of EcM1 bacteria expressing Neae polypeptide control (pNeae), lacking myc-tag, or synthetic adhesins against human Fibrinogen (pNVfib) or GFP (pNVgfp) stained with anti-myc mAb and secondary anti-mouse IgG-Alexa 594 (**B**) Same cultures than in A were analyzed by flow cytometry. Histograms show the fluorescence intensity of bacteria stained with anti-myc mAb and secondary anti-mouse IgG-Alexa 488.

1.2 Adhesion of *E. coli* expressing SAs to antigen-coated plastic surfaces.

To investigate whether NVHH fusions could modify the adhesion properties of *E. coli*, we first examined the specific adhesion of bacteria to abiotic surfaces coated with the antigen recognized by the VHH. To this end, IPTG-induced EcM1 bacteria transformed with pNeae, pNVgfp or pNVfib were incubated with GFP- or Fibrinogen (Fib)-coated plastic surfaces, washed with PBS and either, stained with crystal violet (Fig. 8A) or subjected to light microscopy (Fig. 8B). This experiment revealed that, whereas control bacteria expressing Neae control polypeptide did not bind to GFP- or Fib-coated wells, bacteria expressing NVgfp or NVfib bound specifically to their respective antigens. These results demonstrated that NVHH fusions could act as actual SAs, driving the adhesion of *E. coli* bacteria to a target surface.

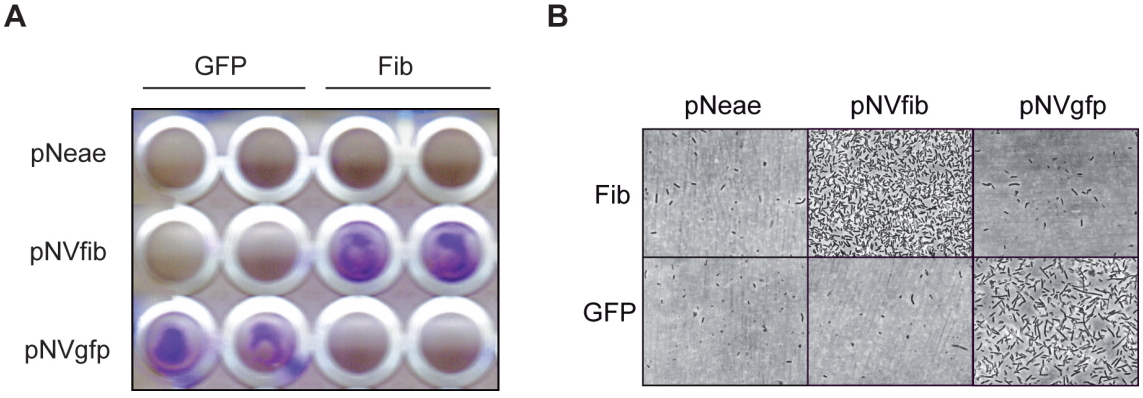

Figure 8. Specific adhesion of *E. coli* expressing SAs to antigens immobilized on plastic surfaces. Induced *E. coli* EcM1 bacteria expressing the Neae polypeptide control (pNeae), or SAs binding GFP (pNVgfp) or human fibrinogen (pNVfib), were incubated with plastic surfaces coated with GFP or human fibrinogen (Fib), as indicated. After 1 hour unbound bacteria were removed by rinsing the wells with PBS and bacterial adhesion was assessed by crystal violet staining (**A**) and light microscopy (**B**).

1.3 Marker-less integration of gene cassettes encoding SAs and bioluminescent *lux* reporter in the chromosome of *E. coli.*

To further investigate *E. coli* adhesion mediated by SAs, we developed constitutive gene expression cassettes that can be integrated as a single copy in the chromosome of *E. coli*. This strategy would allow constant expression of SAs in the absence of any exogenous inducer or antibiotic for plasmid maintenance. For site-specific integration in the chromosome of *E. coli,* we adapted the marker-less gene deletion system employed for *E. coli* genome reduction (Posfai et al., 2006), which enables sequential manipulation of multiple gene loci leaving no antibiotic resistance or vector sequences (Posfai et al., 1999). This technology is based on the insertion of a suicide plasmid bearing homology regions (HRs) of the targeted gene and a restriction site for I-SceI endonuclease. Subsequent expression of I-SceI generates double-strand breaks that are repaired by homologous recombination, resulting in the specific modification of the targeted gene (e.g. gene insertion/deletion). For this genome edition, a suicide vector named pGE (Table 1) was constructed, as well as its derivatives pGE*flu*-SAgfp and pGE*flu*-SAtir for site-specific integration of SAs having VHHs against GFP and TirM, respectively. TirM is the extracellular domain (amino acids 252-360) of the translocated intimin receptor of EHEC (Frankel et al., 2001). In these plasmids the expression of the SAs is driven by the constitutive promoter P_{N25}. The expression cassette (P_{N25} and SA) is flanked by HRs of the *flu* gene in *E. coli* K-12 strain MG1655. The *flu* gene encodes Antigen 43, an adhesin conserved in most *E. coli* strains that is involved in biofilm formation and bacterial self-aggregation (van der Woude and Henderson, 2008) (see Introduction section 3.2.2). Thus, these suicide plasmids allowed the replacement of the *flu* gene in *E. coli* EcM1 by P_{N25}-SAs cassettes generating strains EcM1SAgfp and EcM1SAtir (Fig. 9).

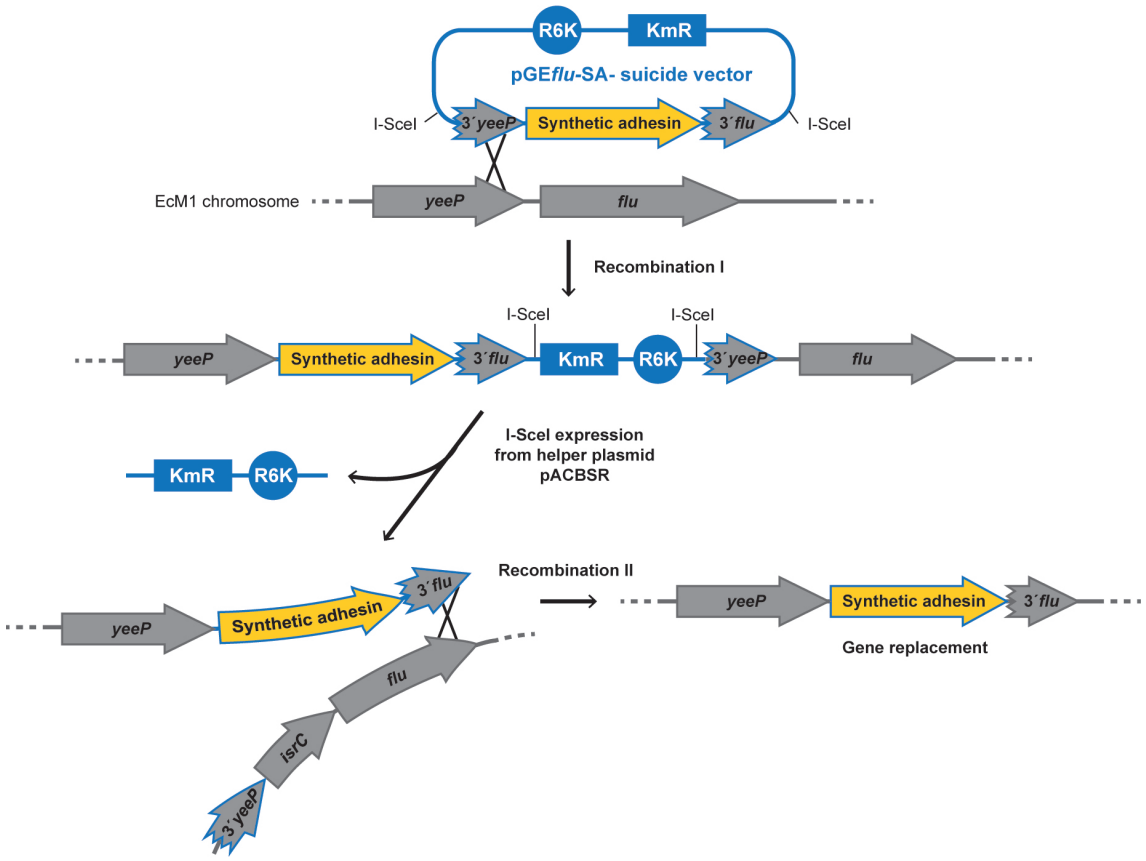

Figure 9. Site-specific integration of synthetic adhesin gene in the chromosome of *E. coli*. Scheme showing the integration of a SA gene in the *flu* locus of *E. coli* K-12 chromosome. Integration is done using a pGE*flu*-SA suicide plasmid containing the π-dependent R6K origin of replication, a kanamycin resistance gene (Km^R) and a synthetic adhesin gene cassette of the desired specificity under the control of the P_{N25} constitutive promoter. The SA gene cassette is flanked by HRs, corresponding to the 3'-ends of the *yeeP* and *flu* genes, and two I-SceI restriction sites. Homologous recombination of the suicide plasmid with the chromosome (Recombination I) leads to Km^R-cointegrants that are later resolved by the expression of I-SceI endonuclease from the helper plasmid pACBSR (Table M2). The double strand breaks, generated by cleavage of DNA with I-SceI, are repaired by a second homologous recombination (Recombination II) that could either, revert the cointegrant to the wild type situation (not shown), or lead to the chromosomal integration of the SA-gene cassette replacing the *flu* gene (as depicted).

In addition, a vector termed pGE*flu*, having *flu* HRs and lacking SA gene cassette, was constructed to generate the isogenic control strain EcM1Δ*flu,* with a deletion in the *flu* gene and not expressing SAs. Next, EcM1Δ*flu*, EcM1SAgfp and EcM1SAtir strains were tagged with a bioluminiscent reporter, the *luxCDABE* operon of *Photorhabdus luminiscens* under the control of a strong constitutive promoter, named P_2, which was inserted in the *matBCDEF* operon with the suicide vector pGE*mat-lux*. This operon encodes the meningitis-associated and temperature-regulated Mat fimbriae, also termed *E. coli* common pilus, which are produced by most *E. coli* pathogroups, being involved in early-stage biofilm development and host cell recognition (Rendon et al., 2007) (see Introduction section 3.2.1). The final bioluminescent strains were named EcM1*lux*Δ*flu*, EcM1*lux*SAgfp and EcM1*lux*SAtir.

1.4 Constitutive expression of Synthetic Adhesins.

Cultures of the bioluminescent strains, grown without any inducer or antibiotic, were analyzed by flow cytometry with anti-myc mAb to determine the expression levels of SAs in these strains. Data indicates that both SAs were displayed on the bacterial surface of these strains with homogeneous levels in the population, being SAgfp expressed at higher levels than SAtir (Fig. 10).

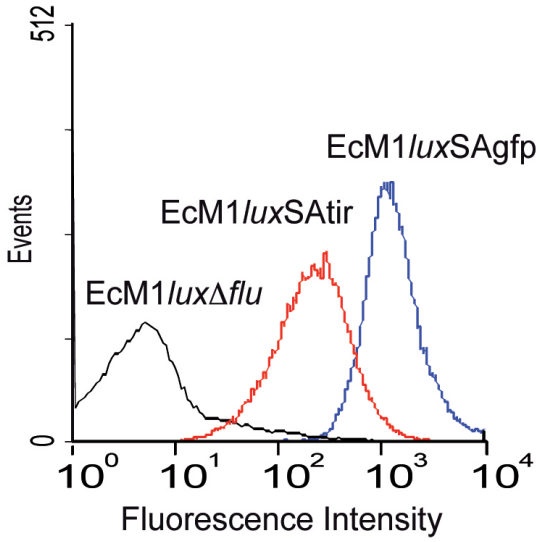

Figure 10. Display levels of SAs in engineered strains. Flow cytometry analysis of *E. coli* EcM1*lux*Δ*flu*, EcM1*lux*SAgfp, or EcM1*lux*SAtir bacteria. Histograms show the fluorescence intensity of bacteria stained with anti-myc mAb and secondary anti-mouse IgG-Alexa 488.

1.5 Viability and growth rate of engineered strains.

To determine whether SAs expression could have an effect on the growth or on the viability of the engineered *E. coli* strains, cultures of the three strains were grown statically in LB media at 37ºC overnight, serially diluted and plated to calculate the number of viable bacteria per unit of optical density at 600nm (OD_{600nm}). The results from these experiments showed nearly identical viability of these strains with around $3x10^8$ CFU/OD_{600nm} (Fig. 11A). In addition, strains expressing SAs showed an identical growth curve than EcM1*lux*Δ*flu* in LB media at 37ºC with agitation (Fig. 11B). These results demonstrated that bacterial growth and viability were not affected by the constitutive expression of SAs.

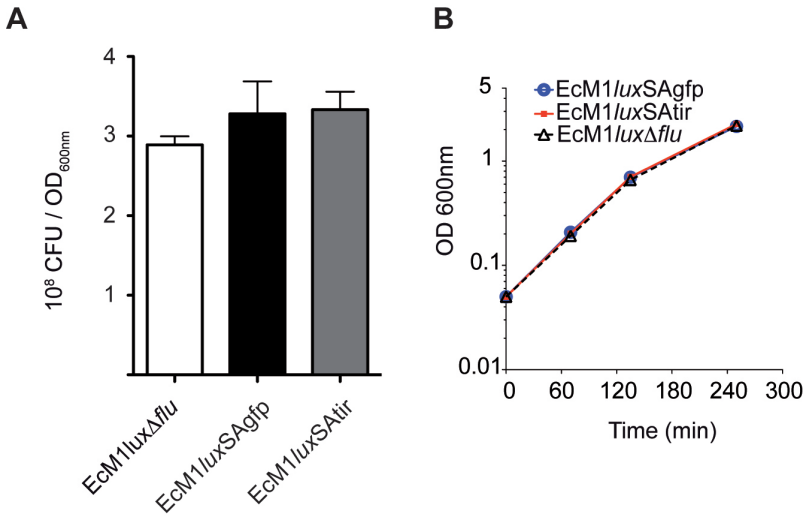

Figure 11. Effect of SAs expression in bacterial viability and growth rate. (A) Number of viable bacterium per OD_{600} of the indicated strains after overnight growth in LB media at 37ºC. Error bars are the standard deviation of bacterial counts from the same culture in three different LB-agar plates. (**B**) Growth curve of the indicated strains at 37ºC in LB media with agitation.

1.6 Stable expression of the introduced gene cassettes.

EcM1*lux*SAgfp and EcM1*lux*SAtir strains were grown at 37ºC for 5 days with a daily dilution (1:2000) in fresh LB medium lacking antibiotics. Every day an aliquot sample of each culture was centrifuged to harvest bacteria. Whole-cell protein extracts from the harvested bacteria were prepared and analyzed by Western blot with anti-myc mAb (to detect the SA) and anti-GroEL mAb, as loading control (Fig. 12A), demonstrating that SAs were stably expressed throughout the length of the experiment (ca. 55 bacterial generations), without the need of any inducer or antibiotic selective pressure. Similarly, samples from each culture were streaked every day on LB-agar plates, incubated at 37ºC for ca. 16 hours and then exposed to a CCD camera to detect bioluminescence of the grown colonies (Fig 12B). This experiment demonstrated that the expression of the lux operon was also stably maintained along the length of the experiment, since all colonies on the plates showed strong bioluminescence signals.

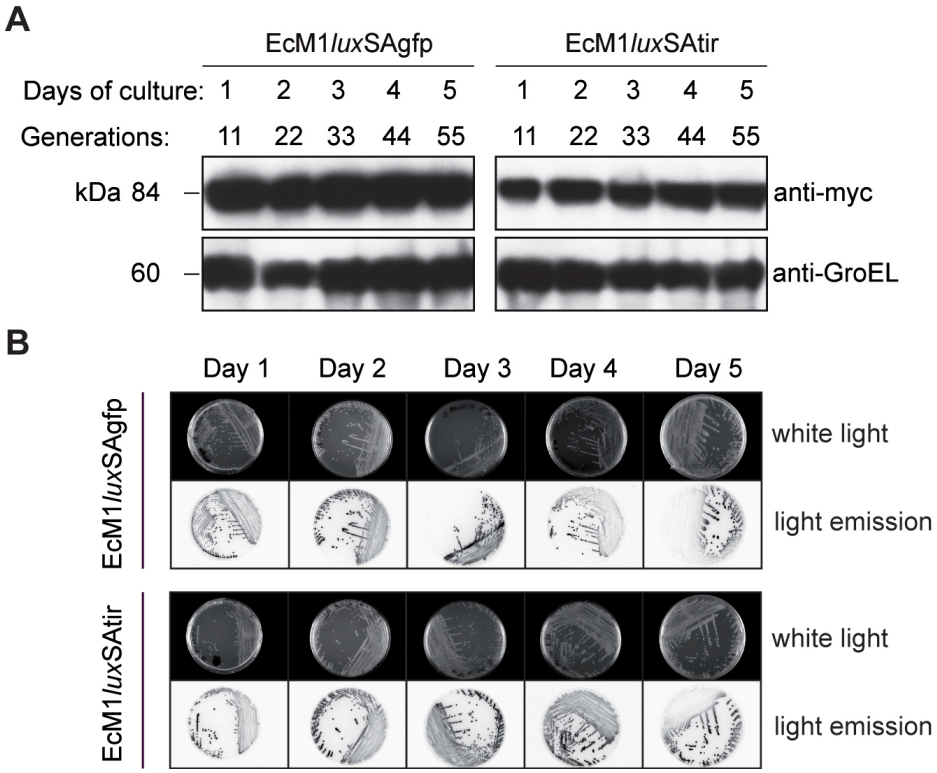

Figure 12. Stable expression of SAs and *lux* gene cassettes. (A) Western blot analysis of the expression of SAs in EcM1*lux*SAgfp and EcM1*lux*SAtir strains grown in LB cultures for the indicated time with a daily dilution (1:2000) with fresh LB medium. SAs were immunodetected with anti-myc mAb. Cytoplasmic GroEL chaperone was used as loading control and was detected with anti-GroEL mAb. **(B)** Stability of the bioluminiscence from EcM1*lux*SAgfp and EcM1*lux*SAtir strains in the cultures employed in panel A. A sample of these cultures from each day was streaked on LB agar plates and white light and light emission images from the plates were acquired.

Taken together these results demonstrated that SAs can drive the adhesion of *E. coli* bacteria to target surfaces and that they can be constitutively expressed, together with the *lux* bioluminescent reporter, from the chromosome of *E. coli*, resulting in a stable and well tolerated expression.

Chapter 2: The use of SAs to drive the adhesion of engineered strains toward mammalian cells expressing cell surface antigens and to characterize the adhesion process.

2.1 Generating stable HeLa cell lines with model antigens on their surface.

Next we investigated the ability of the engineered EcM1/*lux*SAgfp and EcM1/*lux*SAtir strains to adhere to *in vitro* cultured mammalian cells expressing on their surface the target antigen recognized by the SAs. To this end, HeLa cells were stably transfected with plasmids pDisplay-GFP-tm and pDisplay-TirM-tm. These constructions allowed the display of antigens GFP and TirM, respectively, on the extracellular side of plasma membrane by means of a N-terminal signal peptide and a C-terminal transmembrane (Whitman et al.) domain derived from the platelet derived growth factor receptor (PDGFR) (Fig. 8). In addition, pDisplay-TirM-tm construction contains the monomeric mWasabi fluorescent protein (Ai et al., 2008) fused to TirM. The mWasabi green fluorescent protein was evolved from *Clavularia* cyan fluorescent protein, and its primary sequence differs from that of GFP, avoiding the recognition of mWasabi by the VHH anti-GFP of SAgfp (Rothbauer et al., 2008).

Thus the expression of GFP-tm and TirM-tm fusion proteins on the surface of HeLa cells could be monitored by their green fluorescent emission.

Upon stable transfection, green fluorescent HeLa cells were enriched by fluorescence activated cell sorting (FACS) and expanded *in vitro*. The expanded cell populations, named HeLa-GFP-tm and HeLa-TirM-tm, contained cells with variable levels of antigens on their surface, including some cells with undetectable levels of the antigen, specially in the case of HeLa-TirM-tm cell line (Fig. 13).

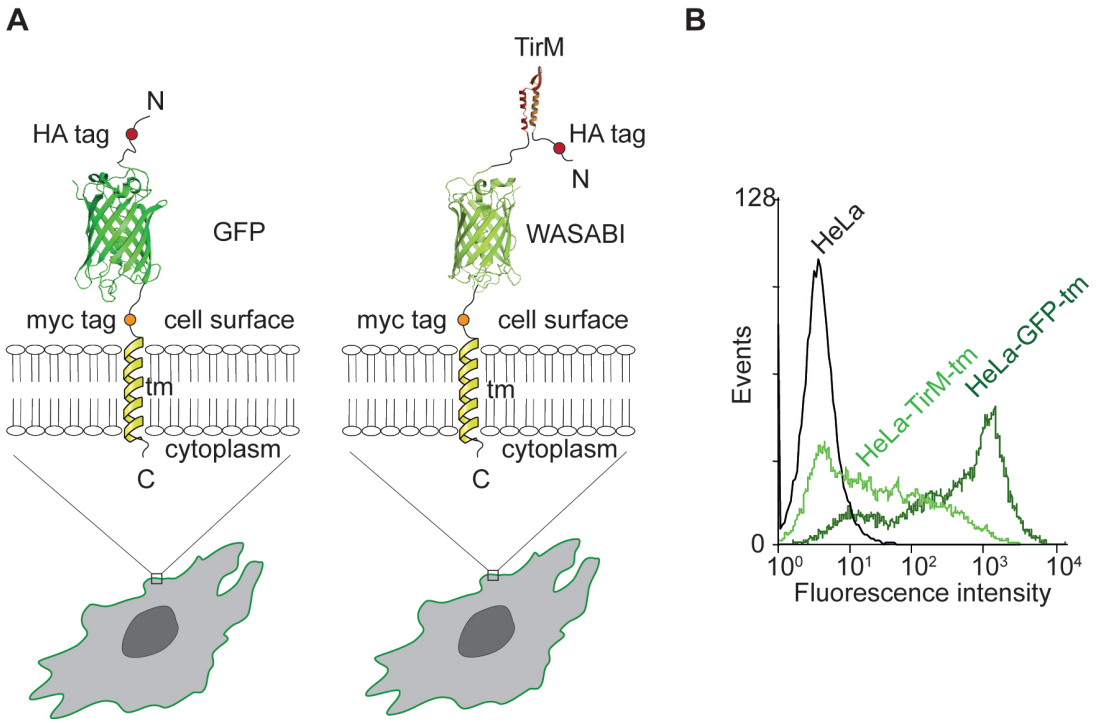

Figure 13. HeLa-GFP-tm and HeLa-TirM-tm cells. (**A**) Schematic model showing GFP-tm and TirM-tm protein fusions in the plasma membrane of stably transfected HeLa-GFP-tm and HeLa-TirM-tm cells, respectively. The transmembrane domain (Whitman et al.) from the platelet derived growth factor receptor (PDGFR) anchors the fusion proteins in the plasma membrane, displaying on the cell surface GFP or mWasabi-TirM protein domains. (**B**) Flow cytometry analysis of HeLa-GFP-tm and HeLa-TirM-tm cells showing fluorescence levels corresponding to the expression of protein fusions GFP-tm and TirM-tm by these cell populations. Untransfected HeLa cells were used as a negative control.

2.2 *In vitro* adhesion assays.

HeLa-GFP-tm and HeLa-TirM-tm cell lines were employed to demonstrate the ability of the engineered bacterial strains to adhere to mammalian cells with target antigens on their surface. Both cell lines were infected with EcM1*lux*SAgfp or EcM1*lux*SAtir bacteria (MOI 300:1). After one hour of infection, unbound bacteria were removed washing with PBS, and samples were fixed and stained with anti-*E. coli* polyclonal antibodies. Inspection of the samples by light and fluorescence microscopy revealed high numbers of EcM1*lux*SAgfp or EcM1*lux*SAtir bacteria (red fluorescence) specifically adhered to HeLa cells expressing different levels of the antigens GFP or TIrM, respectively (green fluorescence) on their surface. In contrast, EcM1*lux*SAgfp and EcM1*lux*SAtir bacteria were not bound to HeLa cells expressing the non-recognized antigen (i.e. TirM for EcM1*lux*SAgfp; GFP for EcM1*lux*SAtir) (Fig. 14).

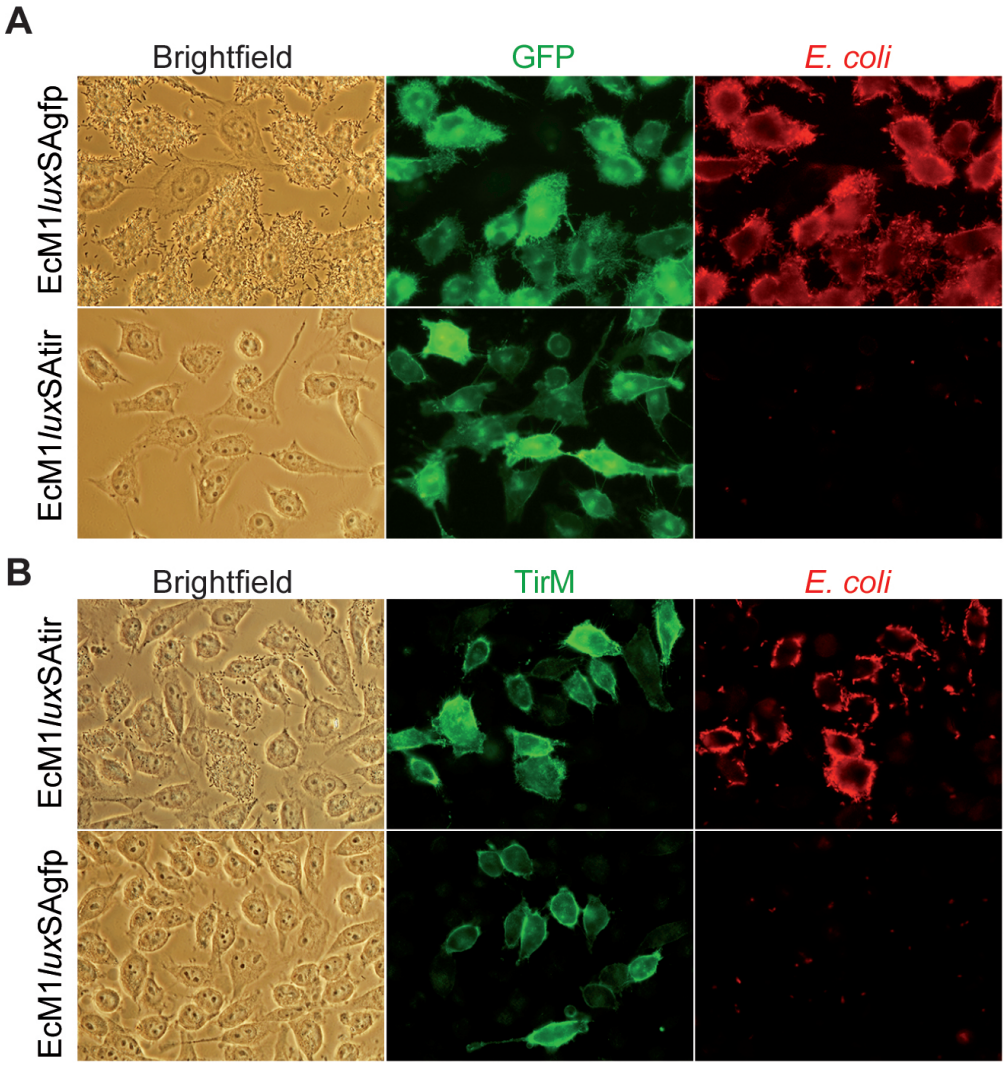

Figure 14. Adhesion of *E. coli* expressing SAs to target mammalian cells. Light and fluorescence microscopy images of HeLa-GFP-tm (**A**) or HeLa-TirM-tm (**B**) cell lines grown in culture and infected (MOI 300:1) with EcM1*lux*SAgfp or EcM1*lux*SAtir as indicated. Expression of the target antigens, GFP and TirM, on the surface of these cells is detected by the green fluorescent emission of the fusion proteins GFP-tm and TirM-tm respectively. Bacteria were stained with anti-*E. coli* polyclonal antiserum and anti-rabbit IgG-Alexa 594.

The adhesion of the engineered strains to HeLa cells expressing GFP or TirM was also assessed by confocal fluorescence microscopy at a higher magnification. This analysis showed that target HeLa cells were largely covered by bound bacteria expressing the corresponding SA (Video 1 and Fig. 15) while antigen-negative cells that can be found in both cell lines (labeled with asterisks in Fig. 15) were free of bound bacteria. These results further demonstrated the exquisite specificity that SAs expression provides in bacterial adhesion.

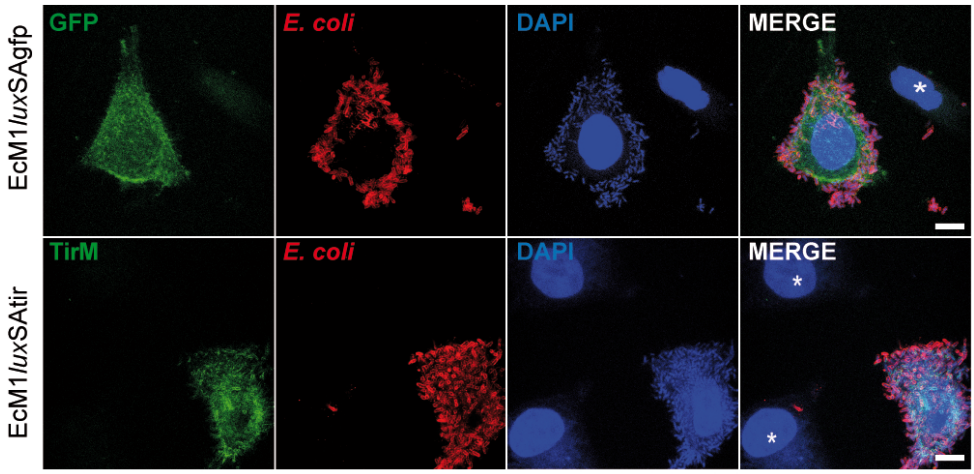

Figure 15. Confocal fluorescence microscopy images of engineered strains targeted adhesion. High magnification confocal microscopy images of HeLa-GFP-tm cells infected with EcM1/*lux*SAgfp (top panels) and HeLa-TirM-tm cells infected with EcM1/*lux*SAtir (bottom panels). Infection and staining were carried out as in Figure 9. In addition cell nuclei and bacterial chromosomes were stained with DAPI (blue). Selected images contain antigen-negative cells (labeled with asterisks on the merge pictures) to show the absence of bacteria bound to them. Scale bars (white lines) showed on the merge pictures represent 10 μm.

2.3 Bioluminescence as reporter of bacterial adhesion.

The possibility of monitoring bacterial adhesion process using the lux operon as bioluminescent reporter was addressed. To this end, Hela, Hela-GFP-tm and HeLa-TirM-tm cells were grown in a multi-well tissue culture plate and infected as above with EcM1/*luxΔflu*, EcM1/*lux*SAgfp and EcM1/*lux*SAtir strains. After one hour of infection the cells were monitored for light emission before and after removing unbound bacteria by rinsing the wells with PBS. After washing, bioluminescent signals were observed only in those wells in which bacteria expressing SAs infected HeLa cells with the recognized antigen on their surface (Fig. 16).

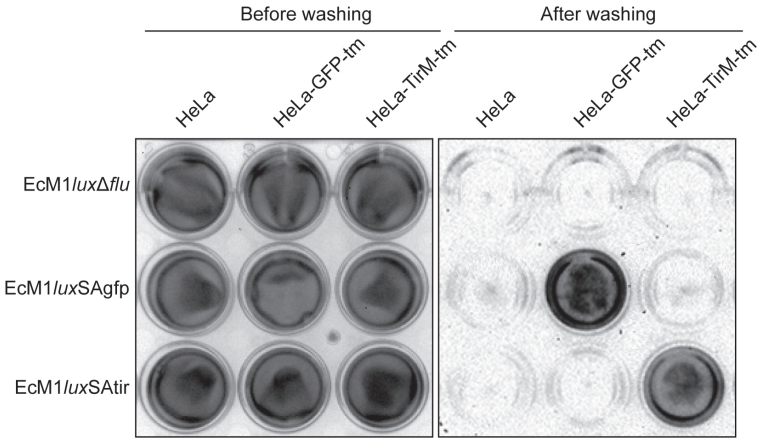

Figure 16. Bioluminescence as reporter of bacterial adhesion to target mammalian cells. HeLa, HeLa-GFP-tm and HeLa-TirM-tm cells were grown in a tissue culture plate and infected (MOI 300:1) with EcM1/*luxΔflu,* EcM1/*lux*SAgfp and EcM1/*lux*SAtir as indicated. After 1 h of infection, the plate was monitored for light emission before (left) and after (right) removing unbound bacteria by rinsing the wells with PBS, revealing positive bioluminescent signals when the engineered bacterial strain with SAs infects its target cell.

2.4 Time-lapse live microscopy analysis of bacterial adhesion mediated by SAs.

To gain further insight into the adhesion process mediated by SAs, we performed time-lapse live microscopy recording the interaction of EcM1*lux*SAgfp bacteria with HeLa-GFP-tm cells. To this end, Hela-GFP-tm cells were infected with EcM1*lux*SAgfp at a MOI of 100:1 to reduce bacteria in the medium that could hinder visualization of mammalian cells. In addition, video was recorded selecting a field in the microscope that allows us to compare the differential behavior of bacteria when they encounter a positive-antigen cell or a negative-antigen cell.

The result of this experiment (Video 2) revealed that antigen-positive HeLa-GFP-tm cells were covered with bacteria in just 5 minutes, whereas almost no bacteria were bound to antigen-negative cells. In fact, once individual bacterium appears in the recorded field, the adhesion event to a GFP-positive cell takes place in a short period of time (<30 sec), after an apparent random collision with the surface of the target cell. After this initial contact with the target cell, bacteria seems to tumble in close proximity to the surface of mammalian cell, eventually establishing a permanent adhesion phenotype and stopping its active motility. In contrast, bacteria that contact with antigen-negative cells tumble close to the cell surface, but finally swim away from the non-target cell.

Taken together, these experiments demonstrated that the engineered *E. coli* strains with constitutive of expression of SAs are able to adhere fast, in high numbers and in a highly specific manner to mammalian cells expressing on their surface the antigens recognized by the SA.

2.5 Influence of the flagellum on bacterial adhesion.

The above experimental observations suggest that, at least *in vitro*, active motility plays an important role during the adhesion of bacteria to target cells. To investigate this process, the SA against GFP was integrated in EcM1Δ*fli* strain (MG1655 Δ*fimA-H* Δ*fliCD*) (Majander et al., 2005). This strain is isogenic to EcM1, with a deletion of *fliC* and *fliD* genes, encoding the components for the filament and the cap of the flagellum, respectively. Using pGE*flu*-SAgfp vector, a strain termed EcM1Δ*fli*SAgfp was generated, which displays the SA against GFP and is unable to swim.

Next, we confirmed the expression of the SA against GFP on the surface of EcM1Δ*fli*SAgfp strain with anti-myc mAb. Flow cytometry analysis demonstrated similar expression levels of SAgfp in both, EcM1Δ*fli*SAgfp, and EcM1*lux*SAgfp strains (Fig. 17).

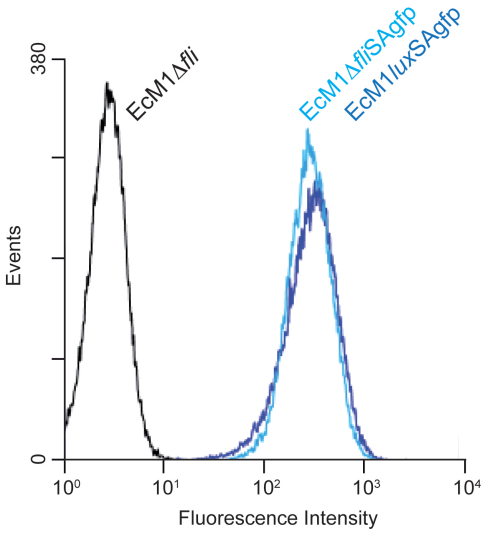

Figure 17. Display levels of SAgfp in EcM1Δ*fli*SAgfp and EcM1*lux*SAgfp strains. Flow cytometry analysis of *E. coli* EcM1Δ*fli*, EcM1Δ*fli*SAgfp or EcM1*lux*SAgfp bacteria. Histograms show the fluorescence intensity of bacteria stained with anti-myc mAb and secondary anti-mouse IgG-Alexa 488.

To evaluate the influence of the bacterial flagellum in the adhesion process mediated by SAs, HeLa-GFP-tm cells were infected (MOI 300:1) with EcM1Δ*fli*SAgfp and the control strain EcM1*lux*SAgfp. After 15 and 60 minutes of infection, cells were washed with PBS to remove unbound bacteria, fixed and incubated with anti-*E. coli* polyclonal antibodies and anti-rabbit IgG-Alexa-594 for fluorescence microscopy analysis. The results showed that at 15 minutes of infection, there were no visible EcM1Δ*fli*SAgfp bacteria adhered to HeLa-GFP-tm cells, while EcM1*lux*SAgfp bacteria can be easily seen attached to the cells (Fig.18). At 60 minutes post-infection, EcM1*lux*SAgfp bacteria were largely covering the surface of HeLa-GFP-tm cells, while the level of adhered EcM1Δ*fli*SAgfp bacteria was significantly lower (Fig. 18).

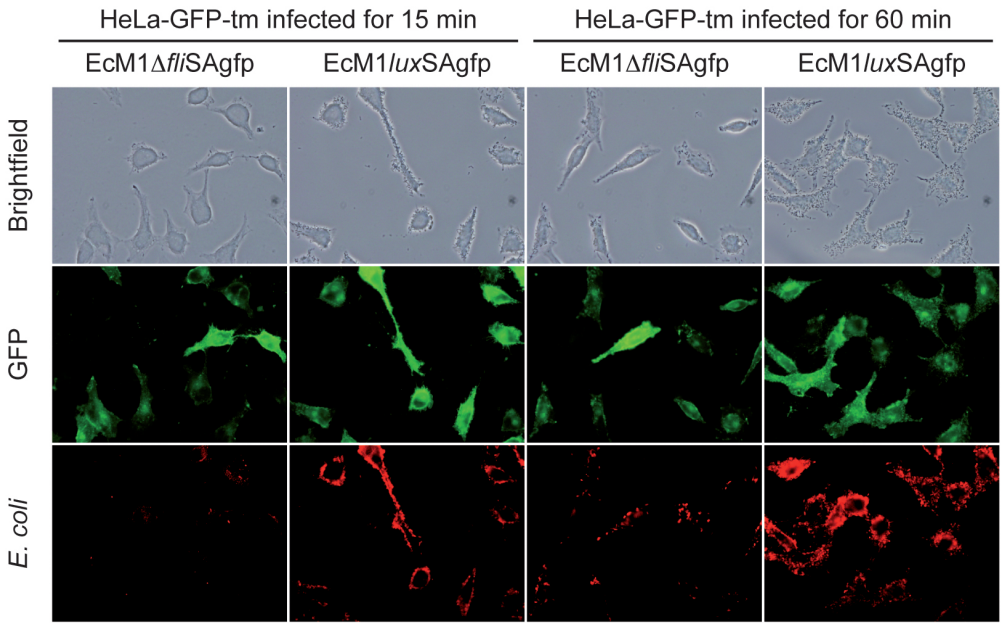

Figure 18. Adhesion of *E. coli* strains with or without flagella and expressing SAs to target mammalian cells. Light and fluorescence microscopy images of HeLa-GFP-tm cells infected with EcM1*lux*SAgfp or EcM1Δ*fli*SAgfp bacteria (MOI 300:1) for 15 or 60 minutes as indicated. Expression of GFP on the surface of HeLa-GFP-tm cells is detected by its green fluorescence emission. Bacteria were stained with anti-*E. coli* polyclonal serum and anti-rabbit IgG-Alexa-594 (red fluorescence).

The number of bacteria adhered to HeLa-GFP-tm cells was quantified for both bacterial strains by plating. To this end, after 15 minutes and 60 minutes of infection, unbound bacteria were removed with PBS and after that, bound bacteria were recovered from infected HeLa-GFP-tm cells in a solution of SDS 0,2% (w/v) in PBS and plated on LB-agar plates. As a control, untransfected HeLa cells were infected with EcM1*lux*SAgfp bacteria as a measure of the infection background (Fig. 19).

The quantification of bound bacteria showed that, at 15 minutes post-infection, the number of EcM1*lux*SAgfp bacteria was ca. 12 times higher than that found for EcM1Δ*fli*SAgfp strain. In fact at that time point, the number of adhered EcM1Δ*fli*SAgfp bacteria was close to the number found in the infection of untransfected HeLa cells by EcM1*lux*SAgfp strain, which represents the adhesion background of the experiment.

After 60 minutes of infection, quantification of bound bacteria for EcM1*lux*SAgfp and EcM1Δ*fli*SAgfp strains showed a similar difference between both strains, compared to the one found after 15 minutes of infection. Interestingly, at this time point the number of bound bacteria for EcM1Δ*fli*SAgfp strain was ca. five times higher than the one found in the control that represents the adhesion background (i.e. EcM1*lux*SAgfp strain infecting untransfected HeLa cells), which indicates that an actual adhesion takes place regardless of the lack of motility. However, the number of bound bacteria for EcM1Δ*fli*SAgfp strain after 60 minutes of infection was still ca. 3 times lower than the one found for EcM1*lux*SAgfp after just 15 minutes of infection. Lastly, the number of bound EcM1*lux*SAgfp bacteria after 60 minutes of infection and all the washing steps was ca. 70% of the initial infective dose (i.e. $3x10^7$ CFU) indicating a great adhesion efficiency for this strain (Fig. 19).

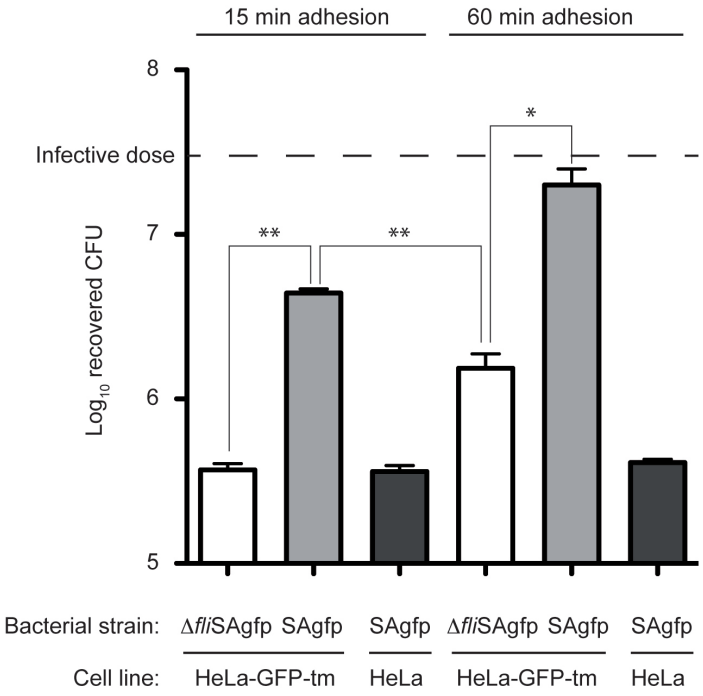

Figure 19. Quantification of adhered bacteria for flagellated and non flagellated *E. coli* engineered strains expressing SAs. The indicated cell lines were infected (MOI 300:1) with EcM1*lux*SAgfp (SAgfp) or EcM1Δ*fli*SAgfp strains (Δ*fli*SAgfp). Each bar represents the number of adhered bacteria (Log_{10} recovered CFU) found for each bacterial strain after the indicated infection times. Black bars represent the background of the experiment, error bars are the standard deviation of bacterial counts obtained on LB-Agar platesfrom three different infection assays, and the dashed line represents the initial bacterial dose employed in the infections ($3x10^7$ CFU). Two tailed P values of t-testare indicated with one asterisk (*) when $P<0.05$ or two asterisks (**) when $P<0.01$.

Taken together, these results demonstrate that, at least *in vitro*, active motility mediated by flagella is important for a fast and effective adhesion to target cells, especially when short infection times are employed.

2.6 Influence of YcgR protein on bacterial adhesion.

Previous data (Video 2) suggested that bacteria could sense adhesion to the target cell and, in response to that, they could stop flagellar rotation. Ycgr protein has been proposed to mediate the transition from motile to sessile bacteria in response to c-di-GMP levels, since upon their association, the complex Ycgr/c-di-GMP is able to interact with some components of the flagellar motor and somehow impair bacterial motility, as a strategy to prepare bacteria for sedentary existence (Boehm et al., 2010; Fang and Gomelsky, 2010; Paul et al., 2010). However, it is not known whether deficiency in YcgR could induce a reduced adhesion phenotype. Hence, to investigate whether YcgR plays a role in the SAs-mediated adhesion, we generated a mutant of EcM1*lux*SAgfp strain with a deletion in *ycgR* gene using a suicide plasmid, termed pGEycgR, with HRs flanking *ycgR*.

The motility of EcM1*lux*SAgfp-Δ*ycgR* and EcM1*lux*SAgfp strains was evaluated in soft LB-agar plates. Cultures of both strains were grown in LB medium at 37ºC and static conditions

overnight, and inoculated in motility plates. In addition, as a negative control for motility, EcM1Δ*fli* strain was also included in the assay. The experiment showed that, as has been previously described (Boehm et al., 2010), *ycgR* gene deletion does not impair motility, since the migration is semi-solid agar plates is similar for EcM1*lux*SAgfp-Δ*ycgR* and EcM1*lux*SAgfp strains (Fig. 20).

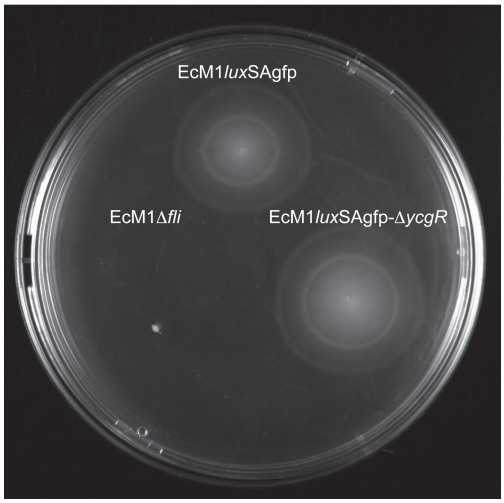

Figure 20. Swimming motility assay. EcM1*lux*SAgfp, EcM1*lux*SAgfp-Δ*ycgR* and EcM1Δ*fli* strains were grown in LB medium overnight, and inoculated as indicated in soft LB-agar plates. The image was taken 8 hours post-inoculation

Next, we investigated whether EcM1*lux*SAgfp-Δ*ycgR* bacteria have impaired adhesion to mammalian cells. To this end, EcM1*lux*SAgfp-Δ*ycgR* bacteria were added to HeLa-GFP-tm cells (MOI 100:1) and the infection was followed by time-lapse live video microscopy (Video 3). This experiment showed that the adhesion behavior of EcM1*lux*SAgfp-Δ*ycgR* bacteria is similar to that one observed for EcM1luxSAgfp (Video 2), since the adhesion to the surface of mammalian cells is equally fast and specific for both strains. After the apparent random collision of EcM1*lux*SAgfp-Δ*ycgR* bacteria with the surface of antigen-positive cells bacteria stop its active motility and establish a permanent adhesion phenotype similar to EcM1*lux*SAgfp bacteria.

This result indicates that the lack of YcgR protein does not affect the ability of EcM1*lux*SAgfp-Δ*ycgR* bacteria to adhere to HeLa-GFP-tm cells. This suggests that the arrest of flagellar rotation upon adhesion is independent of YcgR protein and therefore, additional mechanisms may be controlling this arrest of bacterial motility.

Chapter 3: Improved tissue specificity and tumor colonization by engineered *E. coli* with SAs.

3.1 Tumor model development.

During the last decade, several groups have reported that the intravenous administration of facultative anaerobic bacteria such as *Salmonella* and *E. coli* strains results in the preferential bacterial colonization of solid tumors (Forbes, 2010). Subcutaneously implanted tumors in immunocompetent or athymic nude mice are efficiently colonized (>90%) with a single dose bacterial dose of $5x10^6$ CFU of wild-type *E. coli* K-12 MG1655 administered systemically (Weibel et al., 2008). Three to five days after its intravenous injection, *E. coli* bacteria were recovered in high numbers from the tumor mass (~10^8 CFU/g), whereas organs such as liver or spleen had low bacterial titers (<10^3 CFU/g).

To evaluate the functionality of SAs *in vivo,* we tested whether the engineered bacteria exhibited an improved colonization of solids tumors expressing the antigen recognized by the SA on the surface of tumor cells. To this end, we established an *in vivo* tumor xenograft model based on HeLa-GFP-tm cells in athymic nude mice. These animals received subcutaneously ~10^6 HeLa-GFP-tm cells and developed solid HeLa-GFP-tm tumors of ~200-400 mm^3 in about 10-15 days.

3.2 Systemic administration of 10^7 CFU.

Mice bearing HeLa-GFP-tm tumors were divided into two different experimental groups (n=6) and received intravenously in their lateral tail vein a single dose of $1x10^7$ CFU of EcM1*lux*SAgfp or EcM1*lux*SAtir. Live imaging of animals performed four days post-administration showed bioluminescent signals in the tumors from both experimental groups and bacteria were found in high numbers (~10^8-10^9 CFU/g) in all tumors from each group (6/6), as was determined after tumor excision, homogenization and plating (Fig. 21A). Interestingly, non-target organs such as liver or spleen did not contain bacteria (detection limit $5x10^1$ CFU/g) or had low bacterial titers (<10^3 CFU/g) (Fig. 21B).

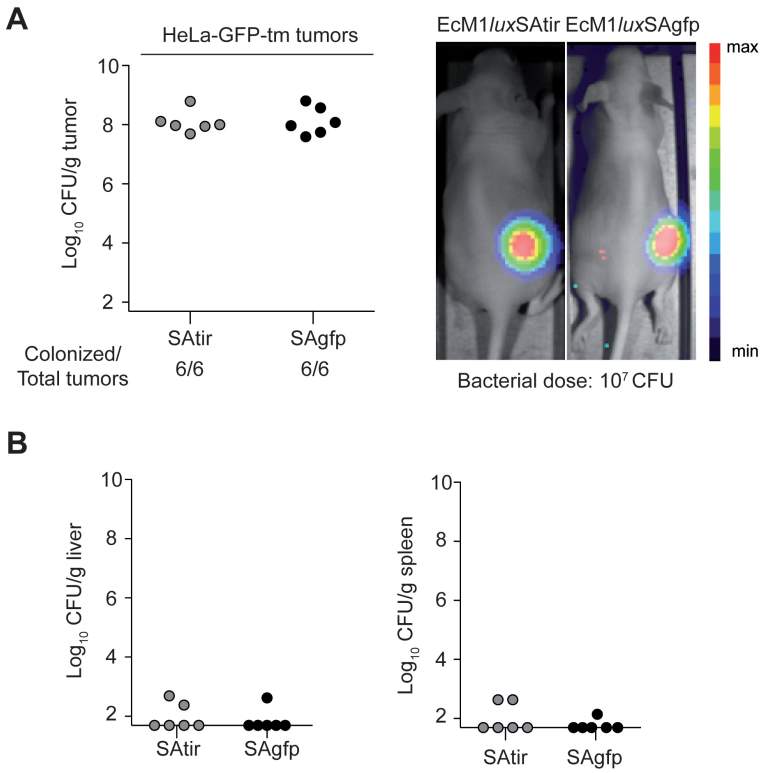

Figure 21. *In vivo* colonization of tumors with high doses of *E. coli* expressing SAs. (**A**) Bacterial colonization of HeLa-GFP-tm solid tumors by EcM1*lux*SAtir (SAtir) and EcM1*lux*SAgfp (SAgfp) strains, as indicated, after their intravenous administration with a dose of $1x10^7$ CFU/mouse. Infected tumor-bearing mice (experimental groups n=6) were euthanized 4-days post-administration and the number of CFU in each tumor was determined. Each circle represents the CFU determined per gram of tumor (Log_{10} CFU/g) for each animal in the different experimental groups. The ratio of colonized tumors in each group is shown at the bottom. On the right, bioluminescence live imaging of HeLa-GFP-tm tumor-bearing mouse infected with $1x10^7$ CFU of EcM1*lux*SAtir (left image) or EcM1*lux*SAgfp (right image). Images are overlays of photographic white-light and bioluminescence signals from a representative tumor-bearing mouse infected with each strain, as indicated on top. The intensities of the bioluminescence signals are represented in pseudocolor according to the scale bar. (**B**) Graphs showing bacterial titers in livers (left) and spleens (right) from those animals with a HeLa-GFP-tm tumor colonized in A by EcM1*lux*SAtir (SAtir) or EcM1*lux*SAgfp (SAgfp) strains. Each circle in the graph represents the CFU determined per gram of tissue (Log_{10} CFU/g).

Importantly, the expression levels of SAs (and the *lux* operon) were identical in the bacterial population administered to mice, and in the tumor-recovered bacterial population, as was demonstrated by flow cytometry (Fig. 22A) and Western blot (Fig. 22B) in the case of SAs expression, and by bioluminescence imaging in the case of *lux* expression (Fig. 22C). These results demonstrated that the expression of these gene cassettes was stably maintained *in vivo* during all the experiment (4 days).

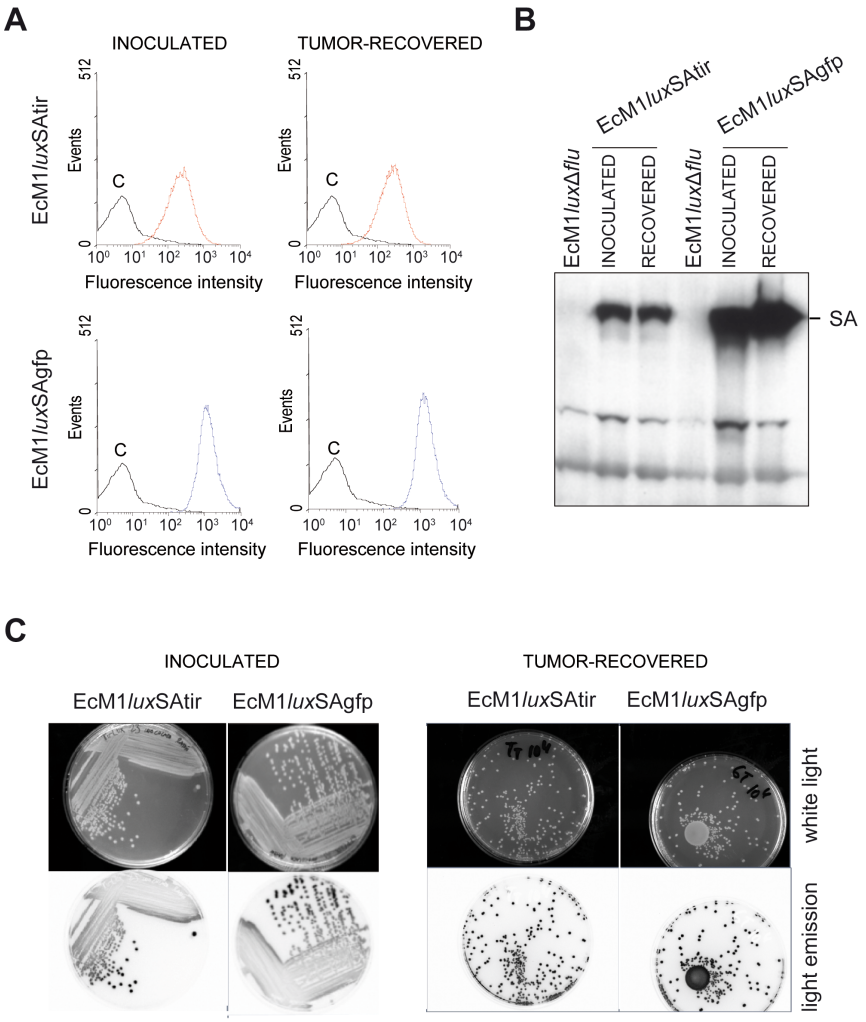

Figure 22. Expression of SAs and bioluminescence in engineered *E. coli* recovered from colonized tumors. (A and **B)** The expression of SAs in inoculated and tumor-recovered EcM1luxSAtir and EcM1luxSAgfp strains, as indicated, was analyzed by flow cytometry (A) and Western blot (B). Bacteria were recovered 4-days post-infection from colonized tumors in Figure 16. For flow cytometry, bacteria were stained with anti-myc mAb and secondary anti-mouse IgG-Alexa 488. Control strain (black line) was EcM1*lux*Δ*flu*. For Western blot, SA protein fusions were detected with anti-myc mAb and anti-mouse IgG-POD conjugate. (**C**) Analysis of bioluminescence of inoculated and tumor-recovered EcM1*lux*SAgfp or EcM1*lux*SAtir bacteria grown in LB agar plates at 37ºC. Images of white light and light emission from the plates were acquired. All individual colonies show strong bioluminescence.

Histological cross-sections of colonized HeLa-GFP-tm tumors stained with anti-*E. coli* antibodies demonstrated the presence of both bacterial strains within HeLa-GFP-tm tumors, and revealed that they were localized preferentially at inner regions of the tumor (Fig. 23). A similar pattern of bacterial distribution was reported for tumors colonized by wild-type *E. coli* K-12 MG1655 strain (Weibel et al., 2008).

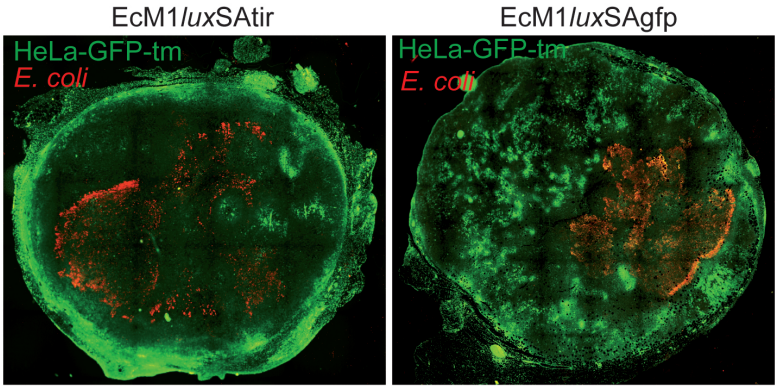

Figure 23. Bacterial distribution in solid HeLa-GFP-tm tumors. Histological cross-sections of colonized HeLa-GFP-tm solid tumors four days post-infection with ~1x10^7 CFU of EcM1*lux*SAtir or EcM1*lux*SAgfp strains per mouse, as indicated. Bacteria were stained with anti-*E. coli* polyclonal antibodies and anti-rabbit IgG-Alexa-594 antibodies (red). The green color corresponds to the fluorescence of GFP in HeLa-GFP-tm cells.

Therefore, the above data indicated that SAs expression was maintained during all the *in vivo* assay, and that the engineered strains retain their capacity to colonize tumors, since the number and distribution of engineered bacteria in solid tumors were similar to those reported for wild type *E. coli* K-12 MG1655 strain (Weibel et al., 2008). However at the bacterial dose employed (1x10^7 CFU) the expression of SAs against the antigen expressed in the tumor, did not confer any improvement in tumor colonization, as both, EcM1*lux*SAgfp and EcM1*lux*SAtir, colonized HeLa-GFP-tm solid tumors.

3.3 Systemic administration of 10^5 CFU.

To investigate whether the expression of SAs could favor tumor colonization when low bacterial doses are employed, first we determined a bacterial dose that is suboptimal of for the colonization of HeLa-GFP-tm tumors by wild-type *E. coli* MG1655. To this end, nine mice bearing HeLa-GFP-tm tumors were infected with 1x10^5 CFU of the wild-type strain. This bacterial dose represents 2% of the dose reported for optimal tumor colonization with wild-type *E. coli* MG1655 (Weibel et al., 2008). Four days after bacterial administration, only one third of the mice (3/9) showed tumor colonization by bacteria (Fig. 24A). Interestingly, the tumors that were colonized had bacterial titers (~10^8 CFU/g) similar to those found when a high bacterial dose (1x10^7 CFU) was employed, suggesting that once *E. coli* succeeded at an early stage of tumor colonization, bacteria proliferate reaching a final titer that is independent of the administered dose. In contrast, livers and spleens of these animals had undetectable levels of bacteria (Fig. 24B).

Next, the ability of EcM1*lux*SAgfp and EcM1*lux*SAtir to colonize HeLa-GFP-tm tumors was compared employing a bacterial dose of 1x10^5 CFU, which was suboptimal for wild-type *E. coli* MG1655. As above, EcM1*lux*SAgfp or EcM1*lux*SAtir bacteria were administered intravenously to two groups of nude mice (n=9) bearing subcutaneous HeLa-GFP-tm tumors (≥ 200 mm^3).

Four days post-inoculation, most of the animals (8/9) that were inoculated with EcM1*lux*SAgfp had their tumors colonized with high bacterial titers (≥10^8 CFU/gr), whereas in the experimental group inoculated with EcM1*lux*SAtir, less that one third of the animals (2/9) had colonized tumors. This differential colonization was also detected by live bioluminescence imaging of the animals (Fig. 24A).

As a control to evaluate targeting specificity, a dose of 1x10^5 CFU of EcM1*lux*SAgfp was administered systemically to a group (n=9) of nude mice bearing tumors derived from un-transfected HeLa cells. Four days after inoculation, HeLa tumors were colonized with low efficiency (2/9) by EcM1*lux*SAgfp, an identical result to that found with by EcM1*lux*SAtir in HeLa-GFP-tm tumors (Figure 24A). In addition, all animals with colonized tumors showed undetectable levels of bacteria in liver and spleen (Figure 24B).

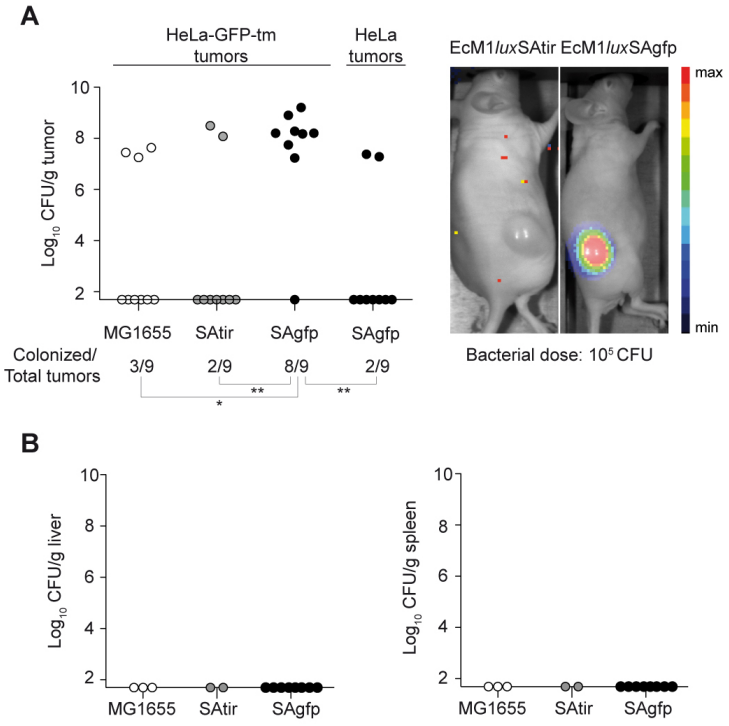

Figure 24. *In vivo* colonization of tumors with low doses of *E. coli* expressing SAs. (**A**) Bacterial colonization of HeLa-GFP-tm or HeLa tumors, as indicated on top, by the following *E. coli* strains: wild type K-12 (MG1655), EcM1*lux*SAtir (SAtir) and EcM1*lux*SAgfp (SAgfp). Each bacterial strain was intravenously administered (1x10^5 CFU/mouse) to tumor-bearing mice (experimental groups n=9) and 4-days post-administration the number of CFU in each tumor was determined. Each circle in the graph represents the CFU determined per gram of tumor (Log_{10} CFU/g) for each animal in the different experimental groups. The ratio of colonized tumors in each group is shown at the bottom along with the statistical analyses between groups connected with lines. Two-tailed P values of Fisher's exact test are indicated with one asterisk (*) when P <0.05 or two asterisks (**) when P =0.015. On the right, bioluminescence live imaging of HeLa-GFP-tm tumor-bearing mouse infected with 1x10^5 CFU of EcM1*lux*SAtir (left image) or EcM1*lux*SAgfp (right image). Images are overlays of photographic white-light and bioluminescence signals from a representative tumor-bearing mouse infected with the strains, as indicated on top. The intensities of the bioluminescence signals are represented in pseudocolor according to the scale bar. (**B**) Graphs showing bacterial titers in livers (left) and spleens (right) from those animals with a HeLa-GFP-tm tumor colonized in A by wild-type K-12 (MG1655), EcM1*lux*SAtir (SAtir), or EcM1*lux*SAgfp (SAgfp) strains. Each circle in the graph represents the CFU determined per gram of tissue (Log_{10} CFU/g).

Taken together, these results demonstrated that engineered *E. coli* with SAs were able to colonize solid tumors expressing a target cell-surface antigen with high efficiency and specificity, allowing the use of doses that are suboptimal for wild type *E. coli* MG1655, or for engineered bacteria with SAs against antigens absent on the surface of tumor cells.

3.4 Lower retention of engineered *E. coli* in non-target tissues.

We investigated whether, in addition to the improved colonization of target tumors shown previously, the engineered strain with SAs and lacking natural adhesins could have a lower retention in non-target organs compared with wild type *E. coli*. To address this question, two groups (n=9) of nude mice without implanted tumors received a high dose ($1x10^7$ CFU) of wild type *E. coli* MG1655 or EcM1*lux*SAgfp strains, and 4, 24 or 48 hours post-inoculation, three mice of each group were euthanized to determine bacterial titers in livers and spleens (Fig. 25).

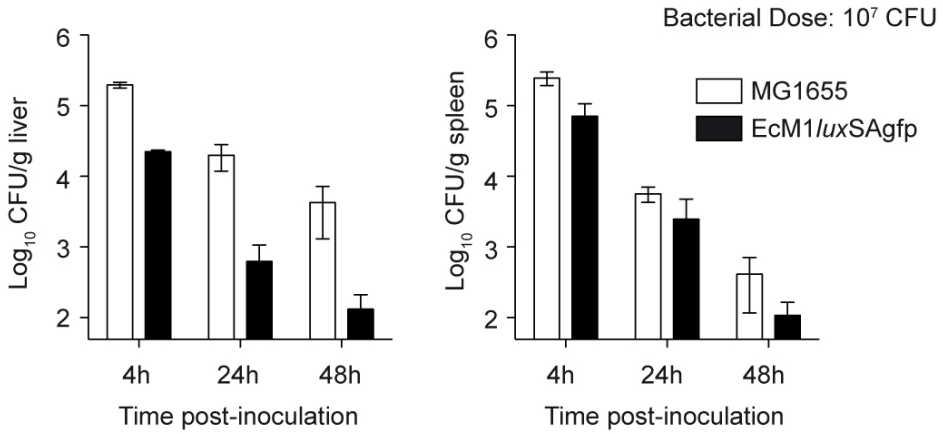

Figure 25. Low retention of the engineered *E. coli* strain in non-target organs. Bacterial titers (Log_{10} CFU/g) recovered from livers (left) and spleens (right) of tumor-less nude mice at 4, 24 and 48 h after intravenous administration of $1x10^7$ CFU of wild type *E. coli* K-12 (MG1655) or EcM1*lux*SAgfp, as indicated. Each bar represents the average CFU/g with standard deviation determined from three mice from each group at the indicated time post-inoculation.

The experiment revealed that, at all time points analyzed, the titers of the engineered *E. coli* strain in these organs were lower than those obtained in the case of wild type *E. coli.* The difference is especially remarkable in liver were the titers of engineered bacteria were ~10 to 30 times lower than those found for wild type *E. coli*, whereas in spleen the difference is around ~2 to 4 times.

Therefore, these data indicated that the engineered bacteria exhibit a lower retention in non-target organs that the wild type *E. coli* strain.

Chapter 4: Development and validation of a SA against tumor cells expressing EGFR, a therapeutically relevant marker.

4.1 Construction of a SA binding EGFR.

The modular architecture of SAs makes possible the modification of their specificity by an exchange of the VHH sequence. Thus, we decided to create SAs against clinically relevant tumor-associated antigens, such as the human Epidermal Growth Factor Receptor (EGFR). EGFR has been shown to be a valid target for antibody-based cancer therapy as its expression is upregulated in many tumors, especially those from epithelial origin, such as those found in the gastrointestinal tract (Cohen et al., 2006) or the urinary tract (Neal et al., 1990). Indeed, several anti-hEGFR monoclonal antibodies such as cetuximab or matuzumab are currently in use (Vacchelli et al., 2014). In addition, a VHH library has been created by immunization of llamas (*Llama glama*) with human tumor cells termed A431 that are derived from a cervix squamous cell carcinoma and overexpress EGFR (Roovers et al., 2007). Hence, the sequence coding for a VHH termed EGa1, which binds the extracellular domain of EGFR, was selected from the above-mentioned repertoire and cloned in the pGE suicide vector to create pGE*flu*-SAega plasmid. Integration of this construction in EcM1*lux* chromosome leads to the generation of EcM1*lux*SAega strain. Flow cytometry analysis demonstrated that SA against EGFR is displayed on the bacterial surface at levels close to the ones found for the SA against GFP (Fig. 26)

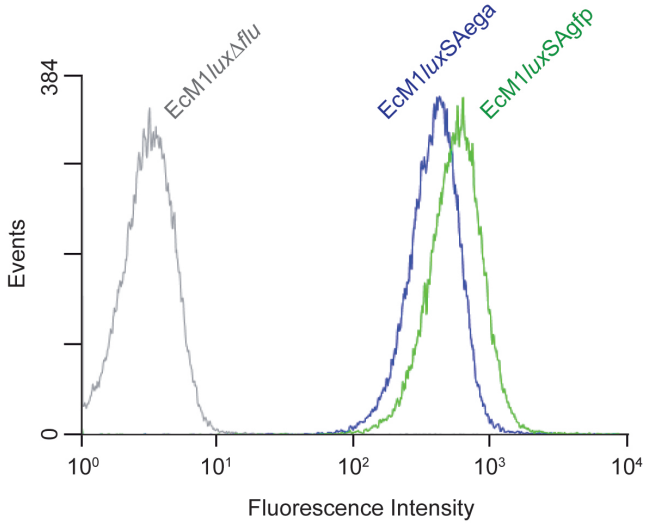

Figure 26. Display levels of the SA against EGFR. Flow cytometry analysis of *E. coli* EcM1*lux*SAega bacteria. EcM1*lux*Δ*flu* and EcM1*lux*SAgfp strains were also analyzed as negative and positive controls for SAs expression, respectively. Histograms show the fluorescence intensity of bacteria stained with anti-myc mAb and secondary anti-mouse IgG-Alexa 488.

4.2 Specific adhesion of the engineered strain to EGFR-positive tumor cells.

The ability of EcM1*lux*SAega bacteria to adhere specifically to tumor cells expressing EGFR on their surface was evaluated. To this end, two isogenic cell lines derived from the mouse fibroblast stable cell line NIH 3T3, termed 3T3#2.2 and Her14, were employed. 3T3#2.2 cells

are devoid of endogenous mouse EGFR expression, while Her14 cells are stable transfectants of 3T3#2.2 cells expressing human EGFR on their surface (Honegger et al., 1987). In addition, the cell line employed to immunize llamas for the VHH library construction (i.e. A431) was also tested.

Subsequently, *in vitro* adhesion assays with EcM1*lux*SAega strain (MOI 300:1) to 3T3#2.2, Her14 and A431 cells were performed as follows. After one hour of infection unbound bacteria were washed with PBS and samples were fixed and stained with anti-EGFR mAb, anti-*E. coli* polyclonal serum and DAPI. Images of the adhesion assay showed that cells positive for EGFR surface expression (i.e. Her14 and A431) (green fluorescence) were largely covered by EcM1*lux*SAega bacteria (red fluorescence), while in cells negative for EGFR expression (i.e. 3T3#2.2) no bound bacteria were detected (Fig. 27).

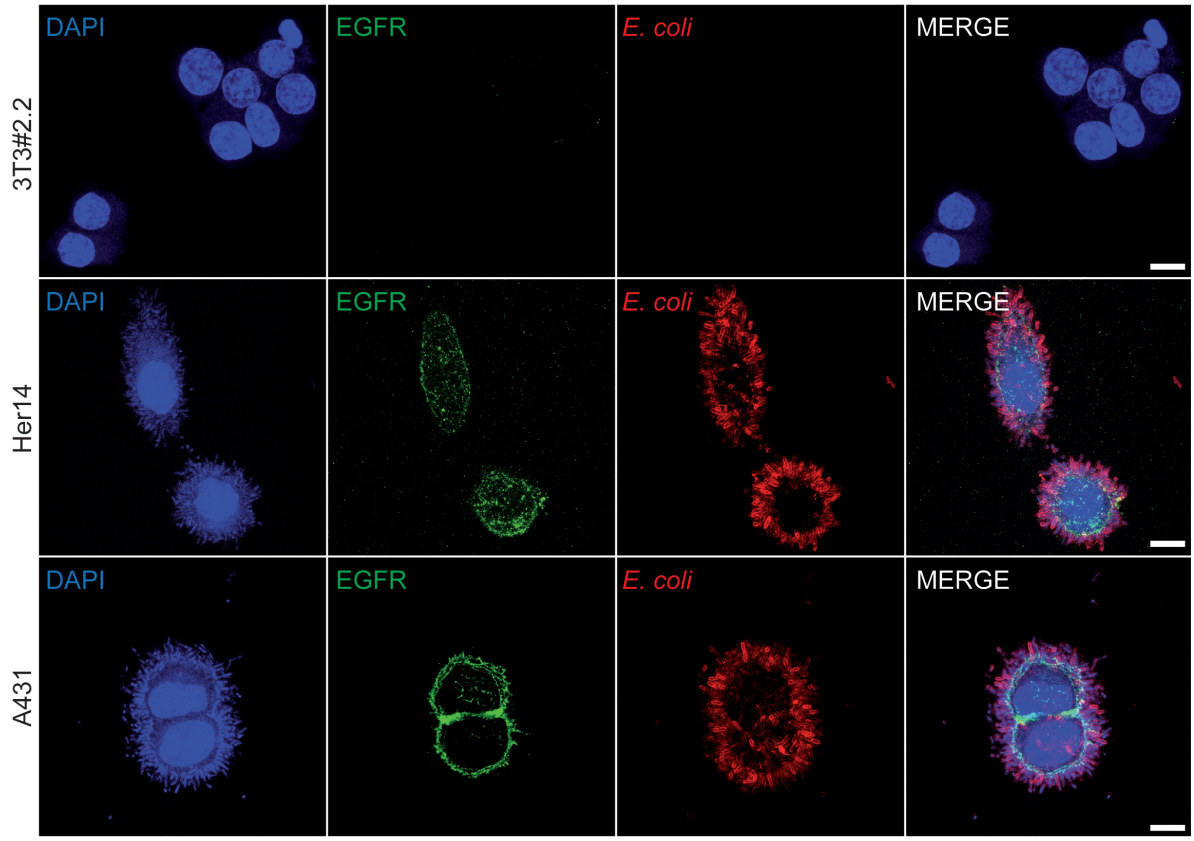

Figure 27. Anti-EGFR SAs drive the specific adhesion of engineered *E. coli* cells to EGFR positive cell lines. Confocal microscopy images of 3T3#2.2, Her14 and A431 cells infected with EcM1*lux*SAega strain. Bacteria were stained with anti-*E. coli* polyclonal serum and anti-rabbit IgG-Alexa-594 (red), EGFR was stained with anti-EGFR mAb and anti-mouse IgG-Alexa-488 (green), cell nuclei and bacterial chromosomes were stained with DAPI (blue). Scale bars (white lines) showed on the merge pictures represent 10 μm.

Therefore, these data demonstrate that SAs can target *E. coli* to tumor cells expressing on their surface EGFR, a therapeutically relevant tyrosine kinase receptor overexpressed on the cell surface of many human cancers of epithelial origin (Cohen et al., 2006; Neal et al., 1990).

Chapter 5: Transcriptional response of *E. coli* upon adhesion mediated by Synthetic Adhesins.

5.1 Experimental design.

The transcriptional response of *E. coli* upon adhesion to surfaces has been widely studied (Beloin et al., 2003; Bhomkar et al., 2010; Domka et al., 2007; Hancock and Klemm, 2007; Ren et al., 2004; Schembri et al., 2003). However, all these studies analyzed transcriptional changes that take place in *E. coli* after several hours or even days upon bacterial adhesion, which makes difficult to ensure that the transcriptional profile observed is developed in response to adhesion rather than in response to sessile life adaptation or even biofilm development. The extremely fast adhesion mediated by SAs could allow the study of those transcriptional changes that take place immediately upon adhesion. Moreover, SAs-mediated adhesion would also allow to perform a transcriptomic analysis of a more coordinated bacterial population, since all analyzed bacteria would have adhered in a short window of time, as opposed to the above-mentioned studies. In addition, our experimental model based on SAs-mediated adhesion to mammalian cells would allow to describe, for the first time, the transcriptional changes of *E. coli* upon adhesion to cells, instead of adhesion to abiotic surfaces. Hence, our objective was to test whether the binding mediated by SAs induces changes in the transcriptional profile of *E. coli* bacteria at a short time just after bacterial adhesion to target cells. We selected SAs-mediated adhesion to cells expressing GFP and EGFR on their surface, and 15 minutes as the time point after adhesion in which the transcriptional response would be analyzed.

Before performing the transcriptomic studies, we tested whether at the infection time selected (15 min) most of the adhered bacteria remain extracellular and therefore are under similar environmental stimuli.

To address this question we carried out *in vitro* adhesion assays of Her14 and HeLa-GFP-tm cells infected (MOI 100:1) with EcM1*lux*SAega and EcM1l*ux*SAgfp bacteria, respectively. After 15 min of infection, unbound bacteria were removed with PBS and samples were subjected to a double staining of bacteria before and after permeablization of the tumor cell plasma membrane, that allowed to distinguish between intracellular and extracellular bacteria.

Inspection of Her14 cells samples by confocal microscopy revealed that in most cells, all bound EcM1*lux*SAega bacteria remained extracellular (Fig. 28A). Exceptionally, we could detect some intracellular bacteria (ca. 1-2 per cell) in a small percentage of the Her14cells inspected (ca. 5%) (Fig. 28B). Similar results were obtained with HeLa-GFP-tm cells infected with EcM1*lux*SAgfp bacteria (Fig. 28CD).

Hence, in both experimental models (EGFR and GFP) most bacteria (>99%) remained extracellular at the time analyzed (15 min).

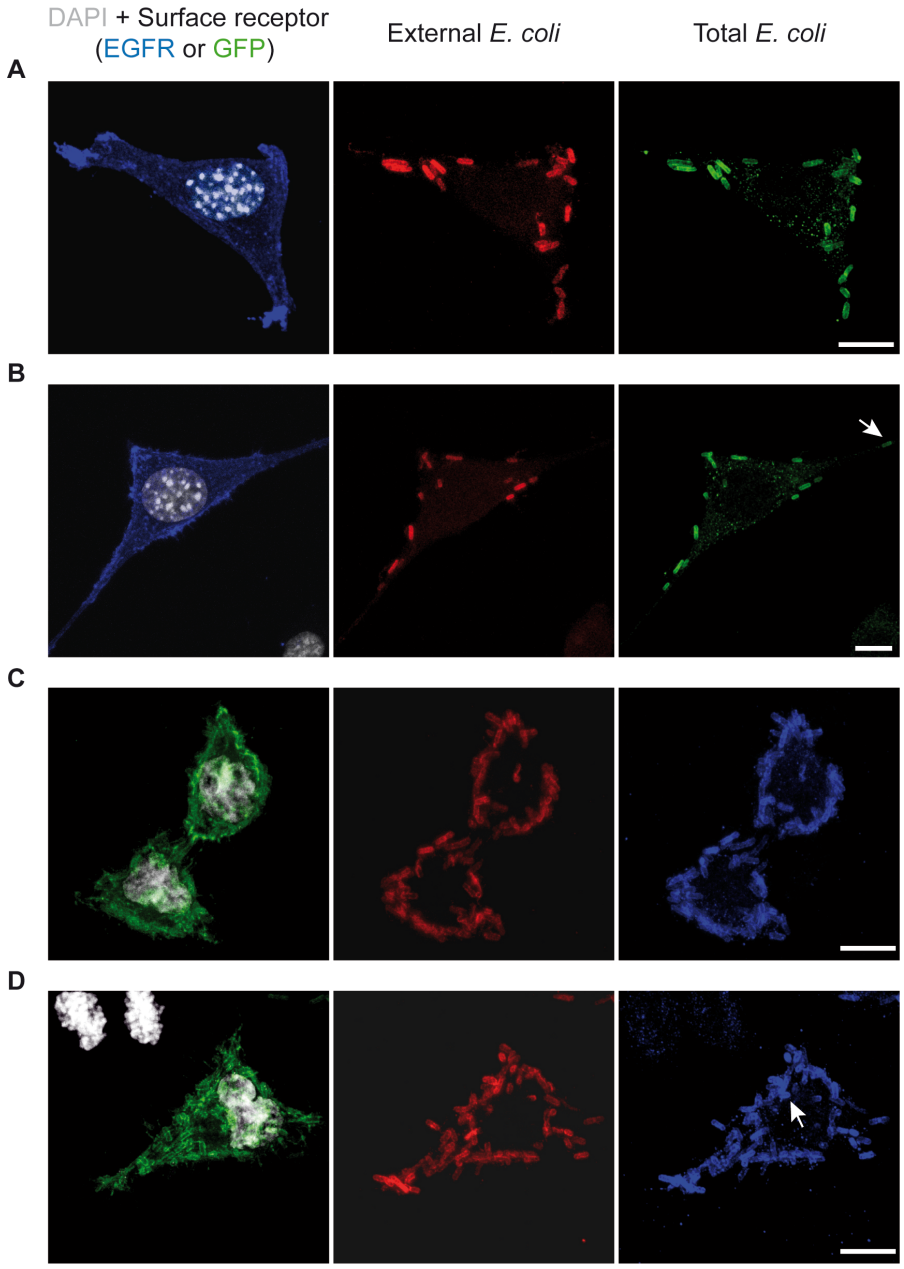

Figure 28. Bacterial internalization rate at the conditions determined for RNA extraction. Confocal microscopy images of Her14 cells infected with EcM1*lux*SAega (**A** and **B**) and HeLa-GFP-tm cells infected with EcM1*lux*SAgfp (**C** and **D**). A and C panels represent the situation found in most of the cells analyzed, whereas B and D panels show cells with internalized bacteria (marked with arrows) that were exceptionally found. Infections were carried out at a MOI 100:1 for 15 minutes. Prior to Triton-mediated membrane permeablization, external bacteria were stained with anti-*E. coli* polyclonal serum and anti-rabbit IgG-Alexa-594 (red). After triton-mediated permeablization total bacteria were stained with anti-*E. coli* polyclonal serum and anti-rabbit IgG-Alexa-488 (green) in A and B or with anti-*E. coli* polyclonal serum and anti-rabbit IgG-Alexa-647 (dark blue) in C and D. Cell nuclei and bacterial chromosomes were stained with DAPI (white). EGFR was stained with anti-EGFR mAb and anti-mouse IgG-Alexa-647 (dark blue) in A and B, while GFP was detected by its green fluorescent emission in C and D. Scale bars (white lines) showed on total bacteria pictures represent 10 μm.

5.2 Experimental conditions and samples for the transcriptomic analysis.

We performed *in vitro* adhesion assays in two different models involving bacterial adhesion to mammalian cells expressing EGFR and GFP-tm on their surface. After 15 min of infection adhered bacteria (i.e. EcM1*lux*SAega infecting Her14 cells, and EcM1*lux*SAgfp infecting HeLa-GFP-tm cells) and non-adhered bacteria (i.e. EcM1*lux*SAega bacteria infecting 3T3#2.2 cells and EcM1*lux*SAgfp bacteria infecting HeLa cells) were collected to isolate bacterial RNA. This experimental setup allowed us to compare the transcriptomic profile of one bacterial strain (i.e. EcM1*lux*SAega or EcM1*lux*SAgfp) under two different physiological states (i.e. adhered or non-adhered). The RNA samples were isolated from four independent *in vitro* adhesion assays for each bacterial strain.

After removal of ribosomal RNA (rRNA) each bacterial RNA sample was used to construct a cDNA library, which was massively sequenced by RNAseq, a sequencing based method that allows the entire transcriptome to be surveyed in a very high-throughput and quantitative manner (Wang et al., 2009). In this technique the number of reads for a given transcript is directly related with the number of mRNA molecules present at the isolation time point. The construction of cDNA libraries as well as the subsequent massive sequencing and statistical analyses of data were carried out at the Genopole platform from Institut Pasteur (France).

5.3 Genes upregulated upon adhesion to target mammalian cells.

According to the RNAseq data, adhesion of EcM1*lux*SAega bacteria to Her14 cells upregulated a set of 136 genes ($p \leq 0.05$) (original excel file available in the CD). Among them, 21 genes were upregulated more than two-fold (Table 1). On the other hand, adhesion of EcM1*lux*SAgfp bacteria to HeLa-GFP-tm cells upregulated a set of 58 genes ($p \leq 0.05$) (original excel file available in the CD), being 12 of them upregulated two-fold or more (Table 1).

		EcM1*lux*SAega		EcM1*lux*SAgfp	
Description	**gene**	**fold change**	**rank**	**fold change**	**rank**
Thiosulfate-binding protein, periplasmic	*cysP*	26,66	1	4,84	1
Inner membrane protein, encoded with predicted sulfurtransferase YeeD	*yeeE*	17,73	2	4	3
Sulfate adenylyltransferase subunit 2	*cysD*	17	3	4,42	2
Sulfite reductase [NADPH] flavoprotein alpha-component	*cysJ*	13,27	4	NSS	NSS
Predicted symporter, function unknown	*ydjN*	11,96	5	2,22	6
Sulfate/thiosulfate ABC transporter permease	*cysU*	6,57	6	NSS	NSS
Sulfate-binding protein, periplasmic	*sbp*	5,63	7	NSS	NSS
Function unknown	*ydjO*	5,4	8	NSS	NSS
cysteine desulfhydrase forms a bienzyme complex with CysE	*cysK*	4,78	9	1,57	43
D-lactate dehydrogenase, NAD-dependent	*ldhA*	4,31	10	3,19	5
Sulfate/thiosulfate ABC transporter permease	*cysW*	3,5	11	NSS	NSS
Glutaredoxin 1	*grxA*	3,49	12	NSS	NSS
L-rhamnose isomerase	*rhaA*	3	13	NSS	NSS
Inner membrane protein, function unknown	*ybjM*	2,87	14	2,1	8
Multiphosphoryl transfer protein: fructose PTS EIIA and FPr; MTP-Fru	*fruB*	2,81	15	3,66	4
Secreted protein, function unknown	*yfdX*	2,55	16	NSS	NSS
Thioredoxin 2, zinc-binding; Trx2	*trxC*	2,53	17	NSS	NSS
Ketol-acid reductoisomerase	*ilvC*	2,5	18	NSS	NSS
Lipoprotein-28, inner membrane protein, function unknown	*nlpA*	2,18	19	NSS	NSS
Arginine ABC transporter periplasmic binding protein	*artJ*	2,08	20	2,1	9
N-acetylglutamate kinase	*argB*	2,06	21	NSS	NSS
Galactitol-specific PTS system EIIB component	*gatB*	NSS	NSS	2,15	7
Phosphoglycerate mutase, Mn-dependent, cofactor-independent	*gpmM*	NSS	NSS	2,04	10
Function unknown, UPF0265 family	*yeeX*	NSS	NSS	2,03	11
Argininosuccinate lyase	*argH*	NSS	NSS	2	12

Table 1. List of genes upregulated upon adhesion more than two-fold in at least one bacterial strain. RNA from EcM1*lux*SAega and EcM1*lux*SAgfp bacteria was isolated at two different physiological states (i.e. adhered and non-adhered) and massively sequenced. In the list are showed those bacterial genes in which the number of reads at sequencing was at least 2 times higher for the adhered condition than for the non-adhered condition (Fold change) in at least one of the indicated strains. NSS is indicated when no statistically significant data was obtained for a gene when comparing adhered vs. non-adhered conditions.

Classification into functional categories revealed that most of the genes whose expression is upregulated upon adhesion are involved in the transport and metabolism of amino acids, carbohydrates and inorganic ions. However, the function of a significant number of upregulated genes remain to be elucidated and were therefore assigned to the unknown function functional category (Fig. 29).

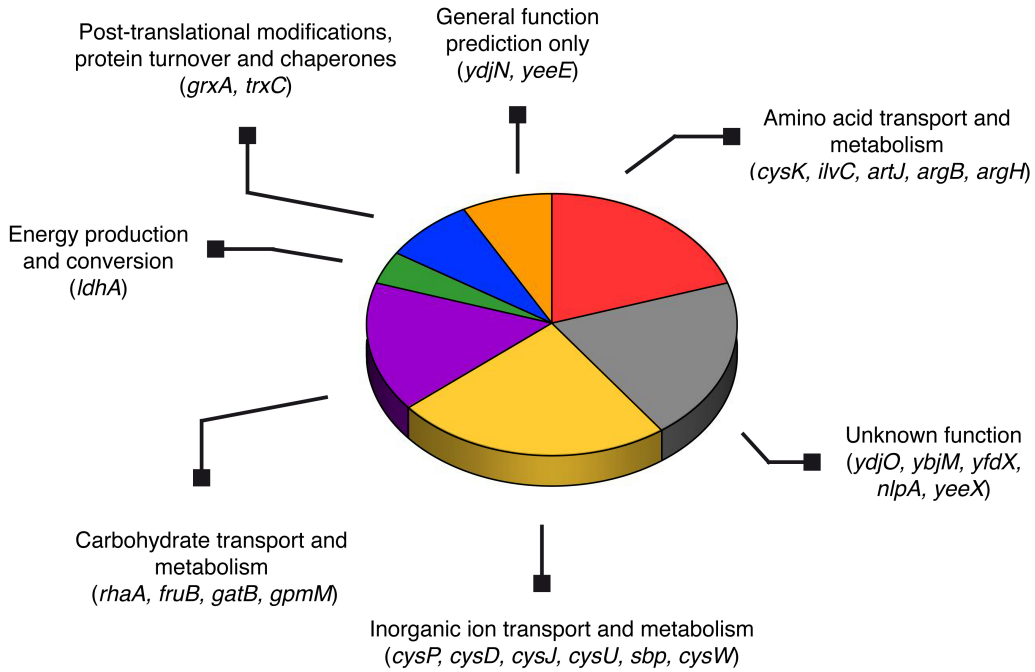

Figure 29. Functional categories of genes upregulated upon SAs-mediated adhesion to target cells. The figure summarizes the data showed in Table 1. The 25 genes were classified according to the cluster of orthologous groups (COG) functional categories annotation system.

Remarkably, we found that a set of eight genes showed an upregulation on their expression upon bacterial adhesion higher than two-fold in both, EcM1*lux*SAega and EcM1*lux*SAgfp strains, suggesting that the transcriptional change in response to adhesion was triggered regardless of the cellular receptor recognized (Table 2). The genes that are upregulated in common to both strains upon adhesion are mainly involved in sulfur uptake and metabolism.

To validate RNAseq data with a different technology, we performed a microarray analysis (Schena et al., 1995) with mRNA samples obtained from adhered and non-adhered EcM1*lux*SAega bacteria. The mRNA samples were used to synthesize two cDNA libraries labeled with two different fluorophores. Subsequently, the labeled cDNAs were mixed in equal proportions and hybridized on a chip containing complementary oligonucleotides probes corresponding to most *E. coli* ORFs (Agilent Microarray Design ID 020097). The fluorescence level of each fluorophore was determined in all the spots of the chip, providing a quantitative measure of how differentially expressed is a given gene (fold change) under the two conditions investigated (adhered vs. non-adhered). Hybrydization of the chip, as well as data recording and statistical analysis of the data, were carried out at the CNB-CSIC Genomic Platform.

Remarkably, the expression of seven out of the eight genes found upregulated by RNAseq analysis was also found upregulated according to the microarray analysis. (Table 2)

		EcM1*lux*SAega RNAseq		EcM1*lux*SAgfp RNAseq		EcM1*lux*SAega Microarray validation
Description	**gene**	**fold change**	**rank**	**fold change**	**rank**	**fold change**
Thiosulfate-binding protein, periplasmic	*cysP*	26,66	1	4,84	1	3,74
Inner membrane protein, encoded with predicted sulfurtransferase YeeD	*yeeE*	17,73	2	4	3	2,43
Sulfate adenylyltransferase subunit 2	*cysD*	17	3	4,42	2	1,95
Predicted symporter, function unknown	*ydjN*	11,96	5	2,22	6	4,42
D-lactate dehydrogenase, NAD-dependent	*ldhA*	4,31	10	3,19	5	2,07
Inner membrane protein, function unknown	*ybjM*	2,87	14	2,1	8	NSS
Multiphosphoryl transfer protein: fructose PTS EIIA and FPr	*fruB*	2,81	15	3,66	4	1,2
Arginine ABC transporter periplasmic binding protein	*artJ*	2,08	20	2,1	9	1,65

Table 2. List of genes upregulated upon adhesion common to both, EcM1*lux*SAega and EcM1*lux*SAgfp strains. The list shows the genes whose expression was upregulated at least two-fold in both strains. The table includes microarray data obtained for EcM1*lux*SAega strain. NSS is indicated when no statistically significant difference was obtained for a gene when its expression level was compared at the adhered and the non-adhered conditions.

5.4 Genes downregulated upon adhesion to target mammalian cells.

We also scrutinize transcriptomic data for those genes whose expression was repressed (downregulated) in the adhered condition. RNAseq data indicated that EcM1*lux*SAega bacteria downregulated a set of 125 genes ($p \leq 0.05$) after binding to Her14 cells (original excel file available in the CD), being 22 of them highly repressed (more than two-fold) Adhesion of EcM1*lux*SAgfp bacteria to HeLa-GFP-tm cells downregulated the expression of 85 genes ($p \leq 0.05$) (original excel file available in the CD) and 38 of them showed a repression higher than two-fold (Table 3).

		EcM1*lux*SAega		EcM1*lux*SAgfp	
description	**gene**	**fold change**	**rank**	**fold change**	**rank**
tryptophan transporter of high affinity	*mtr*	-10,38	1	-2,82	12
trp operon leader peptide	*trpL*	-9,14	2	NSS	NSS
component I of anthranilate synthase	*trpE*	-4,87	3	-2,33	22
Phosphonate ABC transporter periplasmic binding protein; phosphonate catabolism	*phnD*	-3,7	4	-1,9	42
glycerol-3-phosphate transporter subunit	*ugpE*	-3,6	5	-2,5	18
sn-Glycerol-3-phosphate ABC transporter permease	*ugpA*	-3,5	6	-2,69	13
D-ribose pyranase; interconverts beta-pyran and beta-furan forms of D-ribose	*rbsD*	-3,46	7	-3	9
Putative luciferase-like monooxygenase, function unknown	*yhbW*	-3,26	8	NSS	NSS
D-ribose ABC transporter ATPase	*rbsA*	-3,12	9	-3,4	4
Asparagine tRNA(GUU)	*asnU*	-2,9	10	NSS	NSS
sRNA activator of glmS mRNA, glmZ processing antagonist	*glmY*	-2,84	11	-2,61	16
Autogenously regulated tryptophan repressor protein; regulator of trp operon	*trpR*	-2,84	12	-1,98	40
ilvB operon leader peptid	*ivbL*	-2,59	13	-3,01	8
function unknown; predicted periplasmic location	*yfgI*	-2,4	14	NSS	NSS
Expressed protein, function unknown	*yrbN*	-2,3	15	NSS	NSS
Antisense sRNA regulator of toxic IbsD protein; in SIBd repeat	*sibD*	-2,3	16	-2,62	15
Aspartate tRNA(GUC)	*aspV*	-2,25	17	-2,02	35
Serine tRNA(GGA)	*serW*	-2,23	18	NSS	NSS
his operon leader peptide	*hisL*	-2,21	19	-1,82	49
IS150 transposase A	*insJ*	-2,2	20	-2,35	20
Putative ABC transporter ATPase	*ybhF*	-2,16	21	NSS	NSS
Antisense sRNA regulator of toxic IbsC protein; in SIBc repeat	*sibC*	-2,14	22	NSS	NSS
Predicted membrane fusion protein (MFP), function unknown; probable exporter	*ybhG*	-2,14	23	NSS	NSS
Transcriptional activator for the silent bgl operon	*bglJ*	-2,08	24	NSS	NSS
Serine tRNA(UGA) 1	*serT*	-2,05	25	NSS	NSS
C4-dicarboxylic acid, orotate and citrate transporter	*dctA*	-2,03	26	-2,26	25
sRNA affecting sensitivity to antimicrobial peptides	*mgrR*	-2	27	NSS	NSS
Succinate dehydrogenase (SQR) cytochrome b556; membrane anchor	*sdhC*	NSS	NSS	-3,95	1
L-lactate permease; also involved in glycolate uptake	*lldP*	NSS	NSS	-3,68	2
Tryptophan tRNA(CCA)	*trpT*	NSS	NSS	-3,47	3
encodes putative Tpr protein	*rttR*	NSS	NSS	-3,36	5
IS1 transposase B	*insB1*	NSS	NSS	-3,18	6
Putative inner membrane-bound redox modulator, alkali-induced riboswitch	*alx*	NSS	NSS	-3,13	7
Asparagine tRNA(GUU)	*asnT*	-1,93	28	-2,92	10
Succinate dehydrogenase (SQR) hydrophobic subunit	*sdhD*	NSS	NSS	-2,89	11
Chaperone, heat-inducible protein of HSP20 family	*ibpA*	NSS	NSS	-2,69	14
Inhibitor of the cpx response; periplasmic adaptor protein	*cpxP*	NSS	NSS	-2,56	17
Predicted inner membrane protein, DUF2754 family; function unknown	*yaiZ*	NSS	NSS	-2,4	19
Glycine tRNA(GCC)	*glyX*	NSS	NSS	-2,34	21
Aspartate tRNA(GUC)	*aspU*	NSS	NSS	-2,3	23
Chitosugar-induced verified lipoprotein	*chiQ*	NSS	NSS	-2,28	24
Valine tRNA(GAC)	*valV*	NSS	NSS	-2,25	26
Short chain acyltransferase	*yqeF*	NSS	NSS	-2,25	27
Predicted transporter, DcuC paralog, function unknown	*dcuD*	-1,84	36	-2,25	28
Succinate dehydrogenase (SQR) flavoprotein subunit	*sdhA*	NSS	NSS	-2,22	29
Glycine tRNA(GCC)	*glyV*	NSS	NSS	-2,11	30
Function unknown; Fur regulon	*yjjZ*	-1,89	33	-2,1	31
Maltose O-acetyltransferase	*maa*	NSS	NSS	-2,04	32
Putative amino acid:H+ symport permease, function unknown	*yhaO*	-1,92	30	-2,04	33
pyrBI operon regulatory leader peptide	*pyrL*	-1,44	85	-2,03	34
sn-Glycerol-3-phosphate ABC transporter periplasmic binding protein	*ugpB*	NSS	NSS	-2,01	36
ATP-dependent transcriptional activator for the mal regulon	*malT*	NSS	NSS	-2,01	37
Phenylacetate-coenzyme A ligase, phenylacetic acid degradation	*paaK*	NSS	NSS	-2	38

Table 3. List of genes downregulated upon adhesion more than two-fold in at least one bacterial strain. In the list are showed those bacterial genes in which the number of reads by RNAseq at least two times higher for the non-adhered condition than for the adhered condition (Fold change) in at least one of the indicated strains. NSS is indicated when no statistically significant difference was obtained the expression of a gene when comparing adhered vs. non-adhered conditions.

Analysis of the functional categories in which the downregulated genes were classified showed that most of these genes are involved in energy production and conversion and transcription and carbohydrate transport and metabolism in a lesser extent. However, again a significant number of downregulated genes were assigned to the unknown function functional category (Fig. 30).

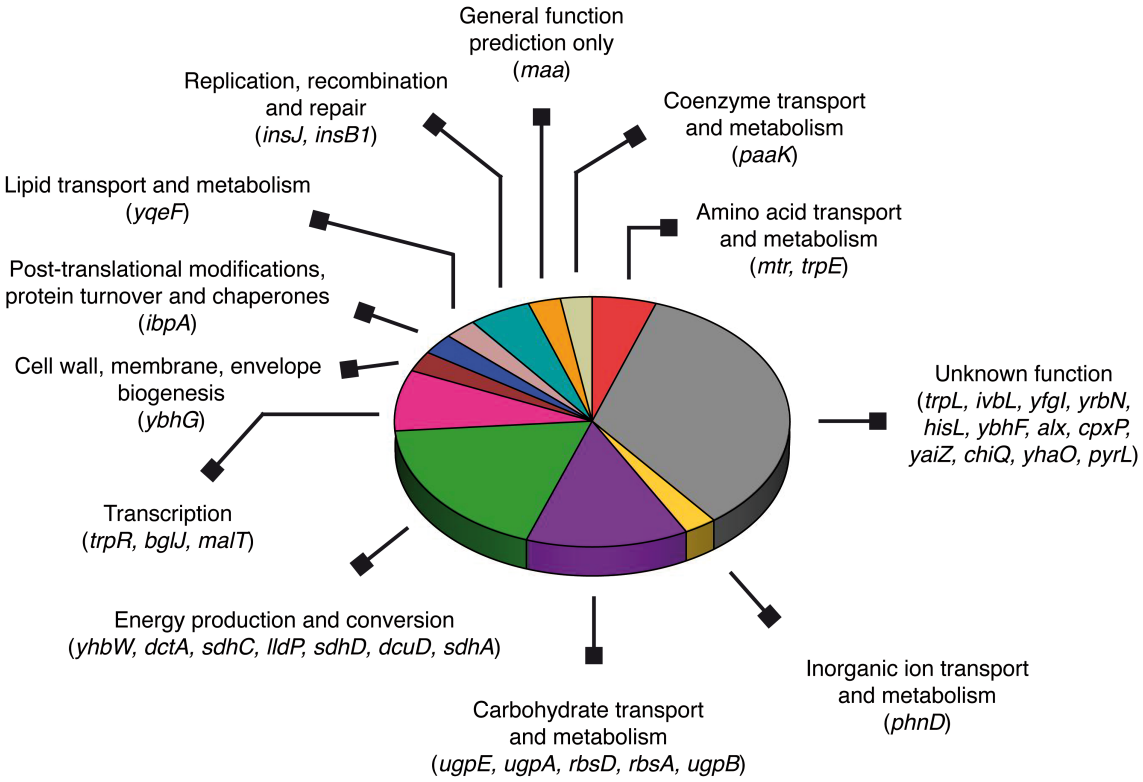

Figure 30. Functional categories of genes downregulated upon SAs-mediated adhesion to target cells. The figure summarizes the data showed in Table 3. The 37 protein-coding genes were classified according to the cluster of orthologous groups (COG) functional categories annotation system.

As shown in Table 3, the expression of 12 genes was highly repressed (fold change <-2) upon adhesion to the target cell in both strains, suggesting a programmed genetic repression profile in response to adhesion that is independent of the antigen that is recognized. The transcriptional downregulation of six of these genes was also validated for EcM1*lux*SAega bacteria by microarray analysis (Table 4).

		EcM1*lux*SAega RNAseq		EcM1*lux*SAgfp RNAseq		EcM1*lux*SAega Microarray validation
description	**gene**	**fold change**	**rank**	**fold change**	**rank**	**fold change**
tryptophan transporter of high affinity	*mtr*	-10,38	1	-2,82	12	-5,7
component I of anthranilate synthase	*trpE*	-4,87	3	-2,33	22	-2,05
glycerol-3-phosphate transporter subunit	*ugpE*	-3,6	5	-2,5	18	-1,28
sn-Glycerol-3-phosphate ABC transporter permease	*ugpA*	-3,5	6	-2,69	13	-1,53
D-ribose pyranase; interconverts beta-pyran and beta-furan forms of D-ribose	*rbsD*	-3,46	7	-3	9	-1,6
D-ribose ABC transporter ATPase	*rbsA*	-3,12	9	-3,4	4	NSS
sRNA activator of glmS mRNA, glmZ processing antagonist	*glmY*	-2,84	11	-2,61	16	NPA
ilvB operon leader peptid	*ivbL*	-2,59	13	-3,01	8	NPA
Antisense sRNA regulator of toxic IbsD protein; in SIBd repeat	*sibD*	-2,3	16	-2,62	15	NPA
Aspartate tRNA(GUC)	*aspV*	-2,25	17	-2,02	35	NPA
IS150 transposase A	*insJ*	-2,2	20	-2,35	20	NSS
C4-dicarboxylic acid, orotate and citrate transporter	*dctA*	-2,03	26	-2,26	25	-1,12

Table 4. List of genes downregulated upon adhesion common to both, EcM1*lux*SAega and EcM1*lux*SAgfp strains. In the list are showed the genes that are downregulated upon adhesion in both strains, at least two times. Results were validated by microarray for EcM1*lux*SAega strain. NSS is indicated when no statistically significant difference was obtained when the expression level of that gene was compared at the adhered and the non-adhered situations. NPA is indicated when in the chip no probe was available for that gene.

The above data showed that upon adhesion both strains mainly repress the transcription of genes involved in the transport of some carbohydrates (e.g. D-ribose, citrate etc.) and genes involved in the transport and synthesis of tryptophane.

5.5 Adhesion-dependent promoters.

The finding that the expression of certain genes is upregulated upon the adhesion of *E. coli* to mammalian cells mediated by SAs, prompted us to investigate whether the activation of these promoters could be used as a signal of bacterial adhesion. This will allow the coupling of a stimulus (i.e. adhesion to a target cell) to a response (i.e. production of a reporter or therapeutic protein)

To this end, we amplified 500 bp DNA fragments containing the promoter and the upstream region of *cysP, cysD, yeeE, ydjN, ldhA* and *fruB* genes, whose expression was found upregulated upon adhesion in both, EcM1*lux*SAega and EcM1*lux*SAgfp strains (Table 2). These promoter regions were cloned in pGE suicide plasmids upstream of the Shine-Dalgarno and coding sequence of mCherry fluorescent protein (Fig. 31) (Shaner et al., 2004). The resulting suicide plasmids were used to transform EcM1*lux*SAega strain. Interestingly, co-integrants obtained after transformation of these plasmids in EcM1*lux*SAega strain, showed a duplication of the corresponding promoter region, in which one copy drives the expression of the natural gene, whereas the other regulates the expression of mCherry gene (Fig. 31).

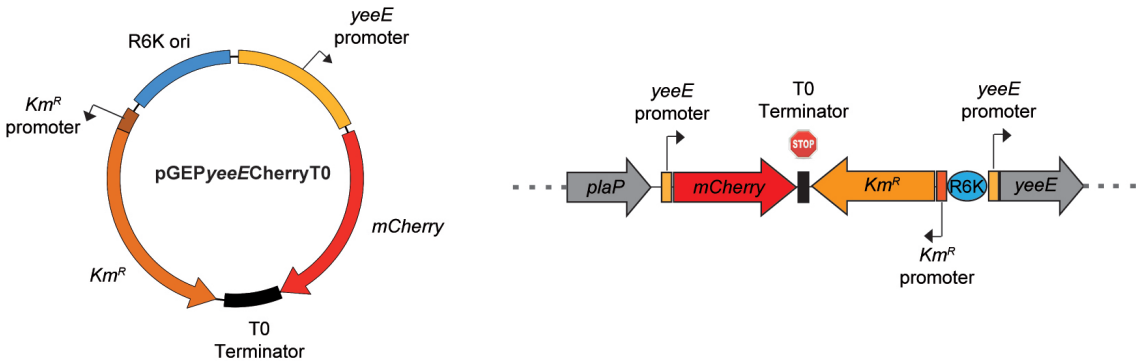

Figure 31. Constructions to test adhesion-dependent promoters. Schematic representation of *yeeE* promoter as an example of the constructions generated to test adhesion-dependent promoters. mCherry gene was cloned between the promoter region of *yeeE* gene, and the lambda t0 derived transcriptional termination region, in the pGE suicide vector (left). Chromosomal integration takes place by homologous recombination in the *yeeE* gene promoter region present in both EcM1*lux*SAega chromosome and pGEP*yeeE*CherryT0 plasmid. Cointegrants selected by Kanamycin resistance, have two copies of the *yeeE* promoter, one that controls *yeeE* gene transcription and other that controls mCherry gene transcription

Following this strategy, we generated six reporter strains that have mCherry gene under the control of *cysP, cysD, yeeE, ydjN, ldhA or fruB* promoter regions. Next their activation was tested *in vitro* by infecting Her14 and control 3T3#2.2 cells with the reporter strains (MOI 100:1). After 15 minutes of infection (identical time that the one of RNA isolation), Her14 cells were washed to remove unbound bacteria and then incubated for 2 additional hours at 37ºC to leave enough time for mCherry protein translation, maturation and accumulation. On the other hand, 3T3#2.2 cells were infected for 2 hours, and after that, the medium in which the infection took place was collected and centrifuged to obtain non-adhered bacteria that were fixed and prepared for microscopy visualization. Inspection of the samples by light and fluorescence microscopy revealed that most reporter strains did not express detectable levels of mCherry protein (red fluorescence) neither at the non-adhered condition, nor at the adhered situation (Fig. 32, *cysD* gene promoter as example).

Interestingly, the reporter strain used to test the *yeeE* gene promoter expressed detectable levels of mCherry protein when it was incubated with Her14 cells and not with 3T3#2.2 cells. However, the expression of mCherry protein in response to adhesion was not homogeneous across the entire bacterial population, and only some of the adhered bacteria expressed mCherry protein upon binding to target cells (Fig. 32). Taken together these results indicated that the *yeeE* gene promoter acts as an adhesion-responsive promoter in at least some bacteria adhered to the target cell.

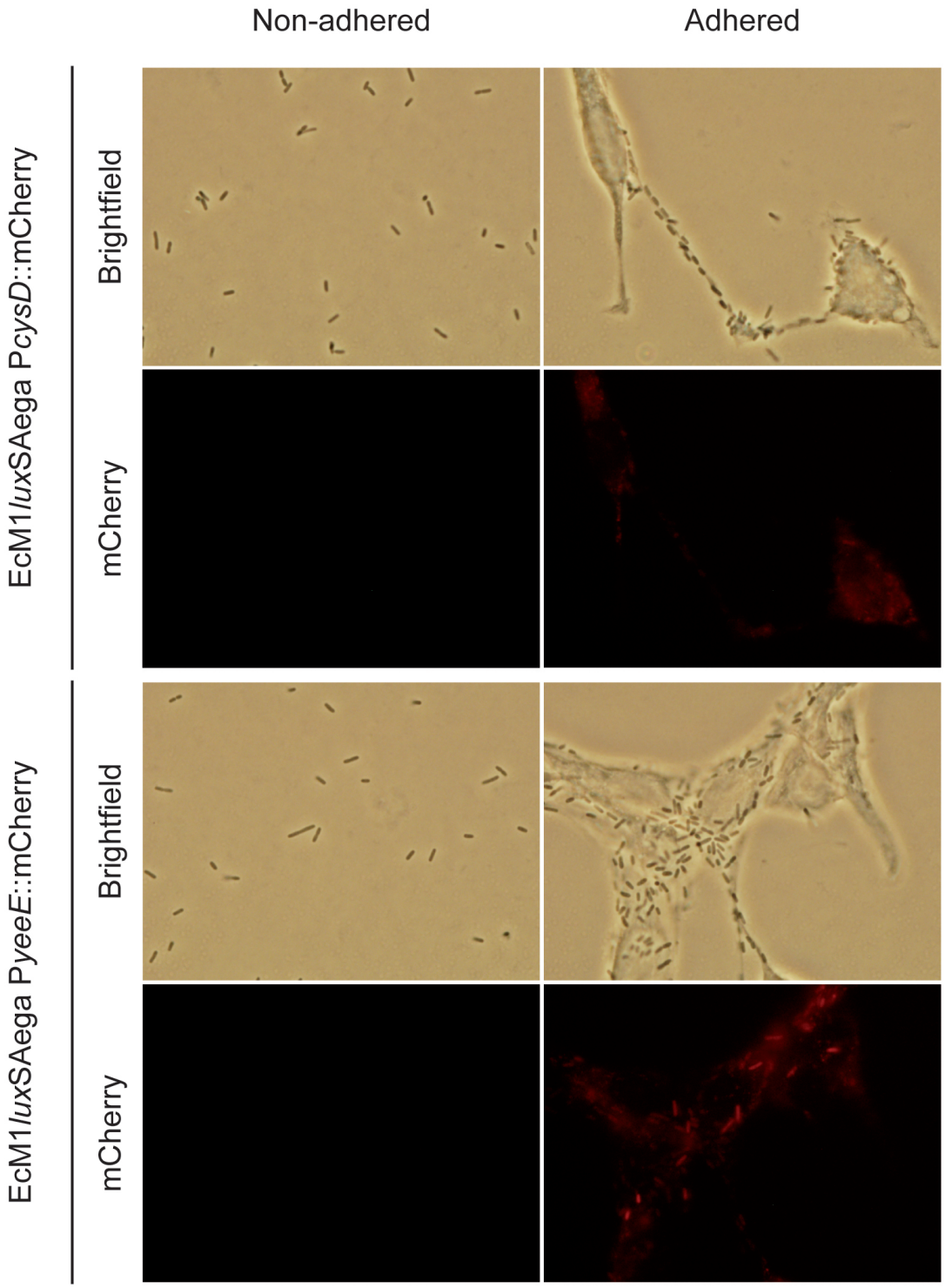

Figure 32. Adhesion-dependent promoters. The indicated reporter strains derived from EcM1*lux*SAega strain were used to infect Her14 cells (adhered panels), and 3T3#2.2 cells (non-adhered panels). After 15 minutes of infection, Her14 cells were washed to remove unbound bacteria and then incubated for 2 hours before fixation. Infection of 3T3#2.2 cells was carried out for two hours and after that bacteria in media were collected and fixed. Samples were analyzed by light (brightfield panels) and fluorescence microscopy (mCherry panels) to test whether an upregulation in mCherry expression take place upon adhesion.

Chapter 6: SAs to drive the adhesion of minicells.

6.1 Minicells producer strains generation.

Nano-sized vehicles have attracted the attention of researchers as tools for the specific delivery of therapeutic compounds to target cells (Malam et al., 2009). We wanted to test whether SAs could drive the adhesion of non-live bacterial nanoparticles derived from *E. coli,* termed minicells or nanocells. These minicells are bacterial-derived anucleate nanoparticles produced as a result of inactivating the *minCD* genes that control septum positioning during bacterial cell division (Adler et al., 1967). Minicells obtained from *Salmonella enterica* serovar Typhimurium have been used as nano-vehicles for the *in vivo* delivery of chemotherapeutic agents, cell-cycle inhibitors and vectors encoding for siRNAs (MacDiarmid et al., 2009; MacDiarmid et al., 2007a; MacDiarmid et al., 2007b). To date, targeting of minicells to specific cell-types (i.e. tumor cells) has been achieved using bispecific antibodies, in which one arm recognizes a component of the minicell surface (i.e. LPS), and the other a cell surface receptor specific for the targeted mammalian cell (i.e. EGFR). However, this system suffers an important limitation because bispecific antibodies have to be designed, expressed, purified and chemically linked to the minicells, which leads to a time consuming and expensive procedure.

These reports prompted us to investigate whether the expression of SAs could be maintained on the surface of *E. coli* minicells. In addition, we wanted to generate minicell producer strains with reduced immunogenicity, in order to create safer minicells for therapeutic purposes. To this end, we selected the EcM1Δ*fli* strain as minicell-producer strain, since it is deficient for the expression of FimH and flagellar proteins FliC (flagellin) and FliD (flagellar cap protein), which are major inducers of innate immunity against bacteria through the activation of Toll-like receptors 4 (FimH) (Mossman et al., 2008) and 5 (FliC) (Hayashi et al., 2001). To further reduce immunogenicity, we also deleted the *msbB (lpxM)* gene from the chromosome of EcM1Δ*fli* strain, using the suicide plasmid pGEmsbB. Inactivation of *msbB (lpxM)* gene results in the synthesis of an altered LPS with a penta-acylated lipid A that has a reduced ability to stimulate innate immunity through the activation of Toll like receptor 4 (Somerville et al., 1999). The *msbB (lpxM)* gene deletion in EcM1Δ*fli* bacteria generated a strain termed in EcM1Δ*fli* Δ*msbB*. Subsequently, the acylation pattern found in the lipid A of purified LPS samples from EcM1Δ*fli* Δ*msbB* and EcM1Δ*fli* strains was compared by mass spectrometry (Fig. 33). Results showed a decrease in the mass of lipid A purified from EcM1Δ*fli* Δ*msbB* strain, compatible with the predicted penta-acylated lipid A caused by *msbB (lpxM)* gene deletion, instead of the hexa-acylated lipid A found in EcM1Δ*fli* bacteria. Mass spectrometry analyses were carried out in collaboration with the group of Prof. Jose Antonio Bengoechea at the Fundación Caubet-Cimera, Mallorca, Spain.

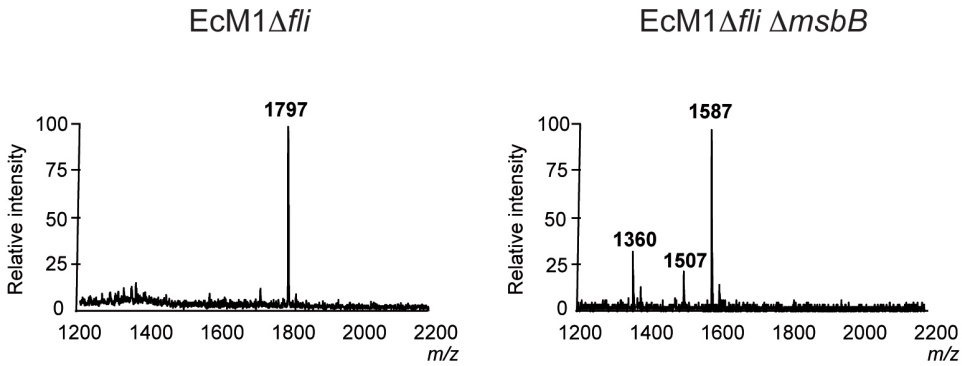

Figure 33. Mass spectrometry analysis of purified lipid A from EcM1Δ*fli* and EcM1Δ*fli* Δ*msbB* strains. Negative ion MALDI-TOF mass spectrometry spectra of lipid A purified from the indicated strains. The results are representative of three independent lipid A extractions.

To obtain a minicell-producer strain, the genes *minCD* were deleted from the chromosome of EcM1Δ*fli* Δ*msbB* strain using the suicide vector pGEminCD-AmpFRT. The *minC* and *minD* genes together with *minE*, whose deletion results lethal for *E. coli*, conform the Min system, which drives the position of the Z ring at midcell, inhibiting the formation of division septum away from there (Lutkenhaus, 2007). The minicell-producer strain derived from of EcM1Δ*fli* Δ*msbB* bacteria was termed EcMini. In addition, the plasmid pGEminCD-AmpFRT was also recombined in wildtype *E. coli* MG1655 to generate the strain EcMini-WT.

6.2 Purification of minicells and expression of SAs on their surface.

SAs binding GFP and EGFR were integrated in the chromosome of the minicell-producer strain EcMini, using vectors pGE*flu*-SAgfp and pGE*flu*-SAega respectively. The final minicell-producer strains that constitutively produce SAs against GFP or EGFR were named EcMini-SAgfp and EcMini-SAega, respectively.

Minicells were purified from cultures of EcMini-WT, EcMini-SAgfp and EcMini-SAega strains by mean of procedure consisting mainly in several differential centrifugations and density gradient centrifugations that isolate minicells (Fig. 34A), followed by a short gentamicin treatment to kill any residual bacteria.

Purified minicells were free of viable bacteria as no CFU was detected after plating purified minicell samples (data not shown). Importantly, minicells purified from EcMini-SAgfp and EcMini-SAega strains maintained the expression of SAs on their surface, as was demonstrated by immunofluorescence with anti-myc mAb and anti-mouse IgG-Alexa 488 (Fig. 34B).

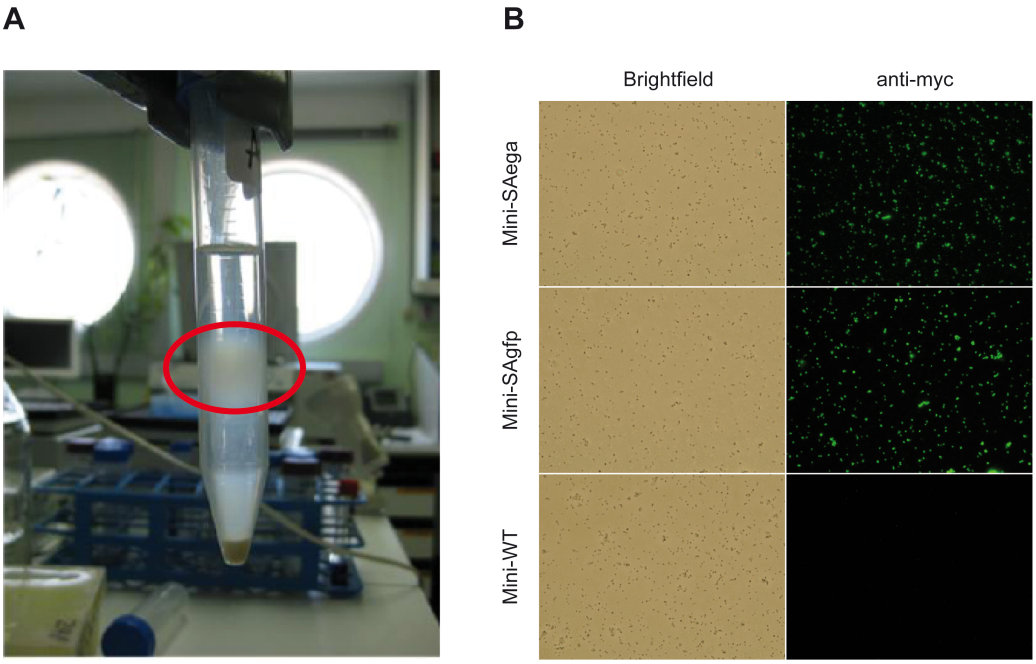

Figure 34. Purification of minicells displaying SAs on their surface. (**A**) Density gradient centrifugation of a minicell enriched culture of EcMini-SAega. The fraction containing minicells is marked with a red circle. (**B**) Brightfield and fluorescence images of purified minicells Mini-WT, Mini-SAgfp and Mini-SAega purified minicells. After their purification minicells were stained with anti-myc mAb and anti-mouse IgG-Alexa488 to demonstrate the expression of SAs on their surface.

Minicell purifications from EcMini-WT and EcMini-SAgfp cultures were analyzed by transmission electron microscopy (TEM). Inspection of the samples revealed the massive presence of fimbrial and flagellar contaminants in the minicells obtained from EcMini-WT strain, whereas minicells obtained from EcMini-SAgfp strain were free of fimbriae and flagellar debris (Fig. 35).

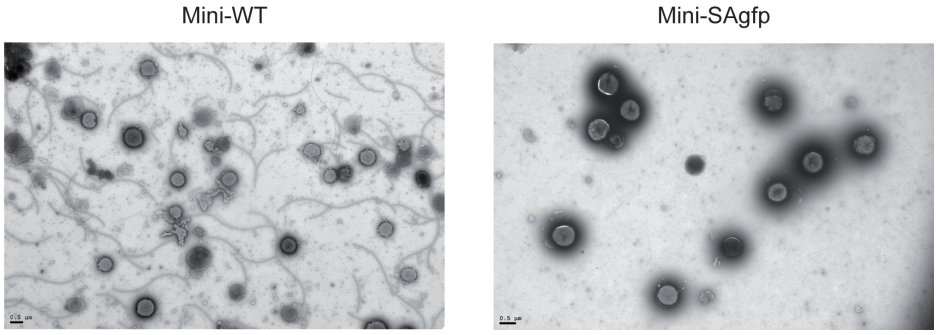

Figure 35. TEM images of Mini-WT and Mini-SAgfp minicells. Purified minicells from EcMini-WT (left) and EcMini-SAgfp (right) bacterial strains were mounted in copper-collodion grids and stained with phosphotungstic acid for TEM.

6.3 Adhesion of engineered minicells to target tumor cells.

We tested whether SAs expressed on minicells could drive their adhesion to target tumor cells expressing on their surface the antigen recognized by the SA. To this end, we performed *in vitro* assays, in which Her14 cells (EGFR positive) were incubated with Mini-SAega or Mini-

SAgfp minicells (MOI 1000:1). After 4 h of incubation at 37 ºC, unbound minicells were washed with PBS and samples were fixed and stained with anti-*E. coli* polyclonal antibodies, anti-EGFR mAb, and DAPI for its visualization by fluorescence microscopy. The experiment showed high numbers of Mini-SAega minicells (red fluorescence) adhered to Her14 cells expressing human EGFR (green fluorescence), whereas only few Mini-SAgfp minicells were visualized on the surface of these cells (Fig. 36A).

Additionally, as a control for specificity 3T3#2.2 cells (negative for EGFR) were incubated as above with Mini-SAega minicells. Inspection of the sample revealed few minicells (red fluorescence) on the surface of 3T3#2.2 cells (Fig. 36B).

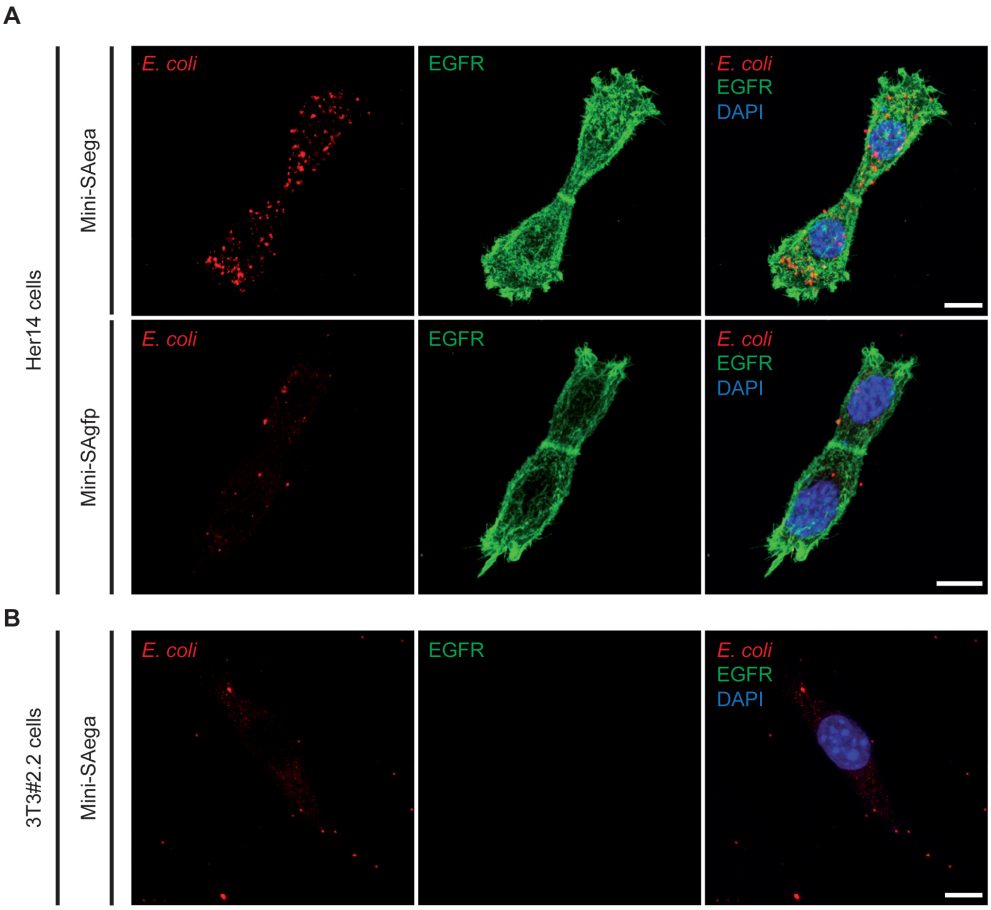

Figure 36. Specific adhesion of minicells expressing SAs to target tumor cells. (A) Confocal microscopy images of Her14 cells incubated for 4 h at 37 ºC with Mini-SAega (top panels) or Mini-SAgfp (bottom panels) (MOI 1000:1). Minicells were stained with anti-*E. coli* polyclonal serum and anti-rabbit IgG-Alexa594 (red), EGFR was stained with anti-EGFR mAb and anti-mouse IgG-Alexa-488 (green), cell nuclei and bacterial chromosomes were stained with DAPI (blue). **(B)** Confocal microscopy images of 3T3 #2.2 cells incubated with Mini-SAega minicells and stained as in A. Scale bars (white lines) showed on merge pictures represent 10 μm.

Taken together, these results demonstrated that minicells purified expressing functional SAs on their surface are able to adhere to target tumor cells.

DISCUSSION

Bacterial adhesion mediated by SAs.

Programming adhesion capacities of engineered microorganisms is an important aspect for synthetic biology (Moe-Behrens et al., 2013). In this work we took advantage of the fact that antibodies and bacterial adhesins share a common folding structure based on Ig domains (Bodelon et al., 2012) to anchor antibody fragments to the surface of *E. coli* as SAs. Antibody surface display has been employed to create and adhesion module that directs *E. coli* adhesion at will, and fulfills most of the desirable conditions for a genetic module or device (Porcar et al., 2011).

We have engineered a stable and specific adhesion of *E. coli* bacteria with SAs based on the β-domain of Intimin (Fairman et al., 2012) and the Ig-domain from VHHs (Muyldermans, 2013). Importantly constitutive expression of SAs from the chromosome did not affect growth and viability of the engineered *E. coli* strain, being stably maintained and inherited through multiple bacterial generations without selection pressure. In addition the modular architecture of SAs makes possible a simple modification of their specificity by an exchange of the VHH sequence, which can be selected from repertoires employing phage and cell display technologies in *E. coli* (Muyldermans, 2013; Salema et al., 2013). This allows the generation of SAs against virtually any antigen of interest, enabling the design of a programmable *E. coli* adhesion to any chosen surface or cell. Previous works have displayed antibody fragments on the surface of *E. coli* with various systems (Bodelon et al., 2012) such as lipoprotein fusions (Francisco et al., 1993) or β-domains of autotransporters (Marin et al., 2010) with the objective of screening libraries of antibody-fragments and the subsequent identification of high affinity clones against an antigen of interest. Nevertheless, programmable adhesion of *E. coli* bacteria to target surfaces or cells has not been reported with those systems. Lipoprotein fusions severely disturb the integrity of bacterial OM causing significant leakiness that threat bacterial viability (Georgiou et al., 1996), whereas β-domains of autotransporters are prone to proteolysis as part of their secretion system. In contrast, the expression of SAs reported in this work is well-tolerated by *E. coli* through multiple generations and the components selected for SAs construction (i.e. β-domain of Intimin and VHHs) are resistant to proteases and denaturant agents (e.g. SDS, urea, temperature) (Bodelon et al., 2009; Muyldermans, 2013). Altogether these properties make SAs extremely robust, inducing the stable attachment of a great number of *E. coli* bacteria to the targeted surface or cell.

Adhesion mediated by SAs is a fast and effective process that in most cases takes place in less than 30 s from the initial contact of a swimming bacterium with the target cell. After this contact, bacteria move and tumble close to the target cell surface, which resembles a “scanning” process, until active movement is stopped and a phenotype of permanent attachment to the cell

is established. In contrast, when the initial contact is made with a non-target cell, the scanning process ends with the bacterium swimming in a different direction away from the cell.

Interestingly, the bacterial behavior observed upon SAs-mediated adhesion to target cells suggests that engineered bacteria are able to sense the productive adhesion and transduce that signal to stop flagella, mimicking what happens in natural adhesion processes. It is clear that motility and adhesion are mutually exclusive events. Although the mechanism by which microbes sense and respond to the contact with a cell or surface are poorly understood, it is widely accepted that transition from motile to sessile bacteria is a fast process, that therefore is probably mediated by post-translational mechanisms. In fact c-di-GMP, a global second messenger in bacteria, has been proposed as a key factor in the switching between motile to sessile lifestyles (Boyd and O'Toole, 2012). Current hypothesis propose that enzymes that maintain steady state levels of c-di-GMP somehow sense that bacteria are in close proximity to a cell or surface, which leads to an increase in intracellular c-di-GMP levels and impairment of flagellar rotation mediated by YcgR bound to c-di-GMP. Several studies have tried to determine the exact flagellar component that interacts with YcgR, and how this interaction affects motility (Boehm et al., 2010; Fang and Gomelsky, 2010; Paul et al., 2010). However the role of the interaction between YcgR and flagellar components in the development of a stable adhesive phenotype has not been demonstrated. We hypothesized that a strain lacking *ycgR* gene might show an impaired adhesion, since although it would sense proximity to target cells, it might be unable to stop flagella. However, our data showed that adhesion to target cells of *E. coli* expressing SAs but lacking YcgR is not impaired, suggesting that, at least in *E. coli,* other proteins should be involved in the arrest of bacterial motility upon adhesion. Indeed, it has been demonstrated that, at least in *Salmonella*, the cellulose synthesized by BcsA protein interfere with flagellum functionality through steric hindrance in a c-di-GMP dependent manner (Zorraquino et al., 2013), given that BcsA together with YcgR seems to be the only proteins found in enterobacteria that have a conserved c-di-GMP binding domain (i.e. PilZ) (Amikam and Galperin, 2006). However this second mechanism inhibiting flagellar motility in the transition between motile and sessile lifestyles it is likely to need more time to be effective than that observed in our experiments. Therefore we believe that additional mechanisms might be controlling the initial bacterial response to adhesion and the arrest of motility.

The fast and efficient adhesive phenotype conferred by SAs expression was also used to evaluate the influence that active motility has during the adhesion of bacteria to target cells. Our data indicated that active motility dramatically improves the adhesive phenotype of engineered bacteria. The number of bacteria adhered to target cells was determined for two isogenic *E. coli* strains that only differs in the expression of FliC and FliD flagellar components. Engineered *E. coli* strain lacking FliC and FliD showed a reduced adhesion to target cells compared with the isogenic *E. coli* strain producing functional flagella. Since our experiment

was carried out under static conditions the differences found could be assignable to a positive effect of motility for contacting a target cell. However a study of bacterial adhesion to glass surfaces under continuous flow conditions, which ensured similar scanned area for both motile and non-motile bacteria, revealed that non-motile bacteria adhered in a rate five times slower than the one found for motile bacteria (McClaine and Ford, 2002). These data suggest that active bacterial motility mediated by flagellar rotation may have a positive role in the development of an efficient adhesion phenotype, not only by increasing the possibilities to find a target, but also by strengthening the interaction between bacteria and target cell.

Tumor targeting capabilities improved by SAs expression.

We have demonstrated the functionality of SAs to drive the adhesion of *E. coli* to antigen-coated surfaces and mammalian cells *in vitro*. Further, we have demonstrated the functionality of SAs *in vivo* showing that the engineered *E. coli* strain with SAs colonizes more efficiently solid tumors expressing a target cell surface antigen. Interestingly, in our study a clear improvement in tumor colonization was observed when bacteria are administered at low doses (i.e. 10^5 CFU) and carry SAs against antigens present on the surface of tumor cells. However, 4 days post-infection all tumors that were colonized by bacteria, irrespective of the dose or the administered strain, showed similar bacterial titers and intra-tumoral distribution. These data suggest that bacteria expressing SAs have and advantage to colonize tumors at the initial stages of colonization, likely by adhering to tumor cells, but once bacteria succeed at this early stage of colonization SAs appear to have less influence in the replication and intra-tumoral distribution of bacteria at later stages of colonization.

The natural ability of bacteria for tumor colonization has encouraged the development of several bacterial therapies to treat tumors (Lee, 2012). Indeed, an attenuated *Salmonella* strain termed VNP-2009, was administered sistemically to treat melanoma patients in a phase I clinical trial (Toso et al., 2002). Unfortunately, the study highlighted the trade-off between safe and effective dose, since at the highest dose that was well tolerated, less than 20% of patients showed tumor colonization by VNP-2009, whereas the use of higher doses was associated with side-effects such as anemia, hyperbilirubinemia, thrombocytopenia, diarrhea and nausea among others. In our work, the higher efficiency in tumor colonization showed by bacteria expressing SAs allowed a significant reduction (ca. two-orders of magnitude) of the bacterial dose needed for optimal tumor colonization *in vivo.* In addition, we have found that the engineered *E. coli* strain is retained at lower levels than the wild-type strain in non-target organs such as liver or spleen. This phenotype might be due to due to the deletion of natural adhesins in the engineered strain (i.e. Type 1 fimbriae, Antigen 43 and Mat fimbriae) that have the potential to bind receptors (e.g. glycan residues) widely expressed on the surface of several host tissues (Kline et al., 2009). Hence, expression of SAs into an *E. coli* chassis lacking a set

of natural adhesins generates engineered bacteria with selective adhesion to target tissues and lower adhesion to healthy non-target organs. This approach could solve some limitations in terms of biosafety and tumor colonization effectiveness that came up in clinical trials with *Salmonella* strains. In addition, other bacterial-based therapeutic approaches for tumor therapy could benefit from SAs, such as the expression of therapeutic proteins within the tumor (Ganai et al., 2009), the localized conversion of prodrugs to drugs (Cheng et al., 2008), or the delivery of plasmids for gene therapy (Xiang et al., 2006). We think that although intravenous administration of bacteria to treat tumors has reached clinical trials, other routes of bacterial administration could be more suitable to carry out an effective cancer therapy, such as oral administration for gastrointestinal tumors or urethral administration for bladder cancer. The utility of SAs in bacteria administered in any of these ways probably overcomes the one showed for intravenous administration since without blood flux, active adhesion seems to be a key factor for tumor colonization.

Currently, intra-vesicle administration of BCG bacteria is approved as an standard treatment for high-grade, non-muscle invasive bladder cancer (Gandhi et al., 2013). Apparently, the presence of BCG in bladder triggers a strong local immunological response leading to tumor cells destruction. However, BCG therapy is not free of undesired side-effects ranging from discomfort, ache, fever and hematuria to life-threatening by fatal sepsis (Lamm et al., 1992). It is likely that a more targeted therapy based on SAs against specific markers on bladder tumor cells could improve current treatment of bladder cancer.

Tumor cells often deregulate the expression and/or post-translational modification of cell surface proteins (e.g. growth factor receptors, mucins) (Hanahan and Weinberg, 2011), allowing their use as specific targets for therapeutic antibodies (Vacchelli et al., 2014). Hence, SAs could be constructed against these validated targets in order to improve the colonization of specific tumors by engineered *E. coli* strains.

During the development of this work, a modified *Salmonella* strain termed AT-*Salmonella* displaying a VHH against CD20 antigen marker of lymphomas was reported (Massa et al., 2013). The strain also expressed HSV-TK in order to locally convert ganciclovir into a GTP analogue that induces apoptosis once it is incorporated in DNA. It should be mentioned the VHH against CD20 was obtained from a naïve library (i.e. constructed from non-immunized animals) (Monegal et al., 2009), without any step of affinity maturation, which resulted in the isolation of a clone that binds CD20 with low affinity as can be inferred from the weak bacterial adhesion observed in *in vitro* adhesion assays to target cells. In addition, the display of the VHH molecule was achieved by fusion to a truncated version of OprL lipoprotein, lacking the characteristic stability whole β-barrels OMPs. The reported toxicity exerted by the expression of this truncated lipoprotein (Cote-Sierra et al., 1998), could be responsible of the diminished ability of AT-*Salmonella*-CD20 strain to adhere and invade non-target cells *in vitro*, compared to

the parental AT-*Salmonella* strain. Lastly, expression of both VHH-lipoprotein and HSV-TK was controlled from inducible plasmids that could be lost during *in vivo* experiments. In spite of all these limitations, AT-*Salmonella*-CD20 strain expressing HSV-TK was quite successful in mediating significant reduction in tumor volume when coadministered with ganciclovir. Therefore, it is likely that a better targeting based on SAs might improve this therapy.

Short-term transcriptional response of E. coli upon adhesion mediated by SAs.

We also investigated the global transcriptional response of *E. coli* in the transition from motile to sessile lifestyle in a model of adhesion to tumor cells. In addition to the basic interest for understanding bacterial adhesion to mammalian cells our study could be of interest for biotechnological applications (e.g. specific activation of therapeutic or reporter genes in the bacteria upon specific cell contact). We took advantage of the fast, specific and efficient adhesive phenotype exhibited by bacteria expressing SAs to analyze which transcriptional changes take place immediately after adhesion of *E. coli* bacteria to target tumor cells.

Several groups have studied long-term transcriptional response upon bacterial adhesion, in order to understand bacterial adaptation to biofilm development (Beloin et al., 2003; Domka et al., 2007; Hancock and Klemm, 2007; Ren et al., 2004; Schembri et al., 2003). However, to our best knowledge only a single study had addressed the short-term impact that *E. coli* adhesion mediated by Type 1 fimbriae has in global gene regulation, using as substrate for adhesion agarose beads coated with mannose and setting 1 hour as the time-point analyzed (Bhomkar et al., 2010).

In our study we analyzed the transcriptional response of *E. coli* bacteria after infecting mammalian cells for 15 minutes. The time point selected for the analysis allows to measure early transcriptional responses related with adhesion rather than with first stages of biofilm development. This short time may also help to obtain a more homogeneous transcriptional response in the bacterial population. Given the massive adhesion phenotype of *E. coli* with SAs we employed a lower MOI (i.e. 100:1) to minimize transcriptional changes in response to bacterial density instead of adhesion.

In our study, analysis of the transcriptional response of bacteria was performed in two different experimental models involving adhesion to mammalian cells that express human EGFR (i.e. Her14 cell line) or GFP-tm (i.e. HeLa-GFP-tm cells) on their surface. The combination of both models allowed the finding of the transcriptional program that bacteria activate upon binding, independently of the recognized receptor or the origin of the mammalian cell line (murine or human).

Our data showed that most of the genes that are upregulated upon binding are common to both experimental models, supporting the existence of a genetic program that is activated upon binding independently of the target. Most of the upregulated genes (i.e. *cysP, cysD, yeeE*) are

involved in the assimilatory reduction of sulfate, which probably leads to an increased production of the amino acid cysteine. Production of the tripeptide glutathione (γ–glutamyl-cysteine-glycine) is limited by the availability of its three amino acids components. Glutathione is essential to maintain the redox balance of the bacteria since glutaredoxin use reduced glutathione (GSH) as cofactor to reduce oxidized proteins. Thus, it seems that adhesion to target cells triggers a state of oxidative stress in bacteria that is balanced through the overexpression of genes involved in Glutathione biosynthesis. Interestingly, expression of gene encoding for glutaredoxin 1 (*grxA*) was also upregulated in the model involving adhesion to EGFR, and this upregulation was also found in the DNA microarray validation (data not shown). No statistical significant data was obtained for this gene in the model involving adhesion to GFP. Glutaredoxin 1 catalyzes the reduction of oxidized proteins in a Glutathione dependent manner and its expression is regulated by the OxyR cysteine-based redox sensor. Therefore upregulation of *grxA* gene agrees with the oxidative stress that seems to take place upon bacterial adhesion. Actually, it is known that *E. coli* as well as many other bacteria have mechanosensitive channels that adopt distinct conformational states in response to applied tension in the membrane (Busscher and van der Mei, 2012). In fact, it has been proposed that bacterial adhesion leads to a membrane stress that triggers a switch from the close to the open conformational state of mechanosensitive channels, allowing in that way the flow of solutes across the membrane in a tension-dependent manner (Haswell et al., 2011). Thus, it is likely that this transitory flow of solutes could disbalance the bacterial redox state of bacteria, which could explain the transcriptional changes observed in *E. coli* upon adhesion. Alternatively, the fact that tumor cells have increased levels of reactive oxygen species (ROS) (Nogueira and Hay, 2013) might also explain the oxidative stress that seems to take place in *E. coli* upon adhesion to target tumor cells. However, this second hypothesis seems less feasible since bacterial adhesion to mannose-coated agarose beads instead of tumor cells also induce the upregulation of genes involved in the assimilatory reduction of sulfate (i.e. *cysD, yeeE*) and reduction of oxidized proteins (i.e. *grxA*) (Bhomkar et al., 2010).

Our data also showed that the expression of some genes is inhibited upon contact, however this downregulation in gene expression does not seem to be as homogenous as the upregulation is, since both experimental models show modest overlapping. Among the genes whose expression appear to be downregulated in response to adhesion independently of the experimental model analyzed, we found genes involved in tryptophan synthesis and transport, as well as genes encoding for IM transporters of several carbohydrates, such as glycerol, ribose, citrate and C4 dicarboxilic acids. *dctA* gene encodes for a transporter protein that mediates the uptake of orotate, an intermediary metabolite of the pyrimidines synthesis pathway, as well as citrate and several C4 dicarboxilic acids (i.e. malate, fumarate) that could act as intermediary metabolites of the Krebs cycle. *dctA* gene product mediates transport of

these molecules under aerobic conditions since an alternative transport system termed Dcu is employed under anaerobic conditions (Davies et al., 1999). Ugp operon includes genes involved in the uptake of glycerol-3-phosphate (G3P) and glycerophosphodiesters that can be later degrade to G3P an essential precursor for de novo synthesis of glycerophospholipids that constitute membranes (Ohshima et al., 2008). *rbsA* gene encodes for a ATPase that transports ribose across the IM (Lopilato et al., 1984).

Interestingly, most of the genes whose expression is altered upon adhesion to mammalian cells are associated with metabolic activities rather than with cell surface or cell structure composition. This might be explained by the fact that bacterial adhesion involves loss of cell mobility and a reduction in the bacterial surface area available to interact with the environment. Together, these 2 events, that are inherent to bacterial adhesion, limit bacterial capacity to uptake oxygen and nutrients, which may exert a pressure to modify some metabolic pathways.

Congruently with our vision of synthetic biology and bacterial engineering, we wanted to test whether the identified promoters responding to adhesion may help us to develop a genetic circuit able to program bacterial behavior in response to adhesion. Common inducible promoters respond to nutrients (e.g. PBAD by Arabinose) (Guzman et al., 1995), nutrient analogues (Ptac/Plac by IPTG) (de Boer et al., 1983), antibiotics analogues (Ptet by anhydrotetracycline) (Skerra, 1994) or small molecules (Psal by salycilate) (Royo et al., 2007). However it is noticeably the lack of promoters that are induced by a switch in the physiological state of bacteria as for instance, the transition from motile to sessile bacteria. Promoters upregulated in the adhered bacteria could represent the basis for the generation of a genetic circuit responding to this transition. We constructed six strains carrying SAs against EGFR and having the mCherry gene cloned downstream the promoter regions of six genes whose expression was found upregulated upon adhesion (i.e. *ldhA*, *yeeE*, *cysP*, *cysD*, *fruB* and *ydjN*). The strategy followed allowed site-specific integration of the reporter gene, maintaining a wild type copy of the gene. One of the reporter strains constructed (i.e. *yeeE* gene promoter reporter strain) showed an specific induction of mCherry gene expression upon adhesion to mammalian cells, although the induction was detectable only in a small percentage of bacteria. The rest of the reporter strains did not show any detectable expression of mCherry upon adhesion. Despite these data, it cannot be discarded that an induction of mCherry expression is taking place upon adhesion, since the selected promoters could be controlling the expression of genes that are naturally transcribed at low rates. An increased transcription from these promoters after adhesion, may lead to the generation of an insufficient number of mCherry molecules to obtain a detectable fluorescent signal. The reporter strain carrying the genetic fusion P*yeeE*::mCherry show an adhesion-dependent increase of red fluorescence. However the behavior was not homogenous in all bacterial population, as only a small percentage of adhered bacteria showed red fluorescence. These data might be revealing a major limitation of

massive transcriptional analysis such as RNAseq or microarrays since both techniques provides a huge amount of data that represents the mean of all analyzed bacteria. Upregulations or downregulations in gene expression found by these techniques, explain the global behavior of the whole bacterial population, missing valuable information about heterogeneity in bacterial responses.

Minicells adhesion directed by SAs.

We have demonstrated that SAs are also effective to drive the adhesion of non-live nanoparticles derived from bacteria (i.e. minicells) toward target cells. Previously, minicells derived from *Salmonella enterica* serovar typhimurium were used for the localized delivery of chemotherapeutics (MacDiarmid et al., 2007b), cell cycle inhibitors (MacDiarmid et al., 2007a), or siRNAs (MacDiarmid et al., 2009) to tumor target cells. The Australian company EnGeneIC (http://www.engeneic.com/index.html) has recently completed a Phase I first-in-man clinical trial that proved the safety of minicells as therapy vehicles. A weak point in the development of these minicells is that the tumor targeting was carried out using bispecific antibodies, in which one arm recognize the surface of the minicell and the other an antigen expressed on the surface of the tumor cell. This requires a complex composition, with at least three molecular entities that should be combined, which turns the production into a costly and difficult process.

In our work we have improved the production of minicells generated from an *E. coli* strain devoid of major immunogenic components (i.e. Type 1 fimbriae, flagellin, hexa-acylated lipid A) that is endogenously expressing SAs against EGFR on the surface. Minicells purified from this strain are free of major bacterial components causing immunogenic response in patients and in addition carry functional SAs that bind tumor cells expressing EGFR. However, although an effective targeting of EGFR+ tumor cells was achieved with minicells, it required the use of longer infection times (4 h) and higher infective dose (MOI 1000:1) than those used with live bacteria. Likely this limitation is related with the non-motile phenotype of minicells that limits the possibilities to contact with a target cell. In fact this low level adhesion phenotype was also observed with non-motile live bacteria, as discussed above.

To conclude, in this work we have designed SAs that drive the adhesion of live *E. coli* and derived nanoparticles at will. Additionally, we have characterized the transcriptomic response of *E. coli* in response to adhesion. Given the modularity of SAs and the possibility of generate VHHs against different targets (De Meyer et al., 2014; Vincke et al., 2012), this technology offers multiple potential applications beyond the improved tumor targeting that has been demonstrated *in vivo*.

For instance, SAs could help in the localized delivery of antigens to specific immune cells or tissues (Owen et al., 2013) for more effective vaccines based on bacterial vectors (Bolhassani

and Zahedifard, 2012). Tailored probiotics could be constructed with SAs, facilitating the therapeutic intervention of bacteria (Sartor, 2005). In addition SAs could be targeted to antigens expressed by viral and bacterial pathogens on their own surface or on the surface of infected cells, facilitating the intervention of engineered bacteria against pathogens (Hwang et al., 2013). Industrial applications could be also envisioned for SAs technology, such as the generation of defined bacterial consortia for certain industrial processes (Minty et al., 2013). In addition adhesion of bacteria to metal plastics and other abiotic surfaces could improve the development of biosensors (Park et al., 2013), as well as more efficient bioreactors retaining bacterial biomass (Kalyanpur, 2002).

Given the conservation of cellular machineries used for folding and insertion of β-barrel OM proteins (Noinaj et al., 2013), it is likely that SAs could be functional in other Gram-negative bacterial species, including alternative non-pathogenic bacterial chassis commonly used in synthetic biology such as *Pseudomonas putida* (Martinez-Garcia and de Lorenzo, 2011). In conclusion, future work on SAs technology should expand its use in *E. coli* and other bacterial chassis for specialized biomedical, industrial and environmental applications.

CONCLUSIONS

1- Synthetic Adhesins that are able to drive an effective and specific adhesion of *E. coli* bacteria to a target surface or cell, can be constructed as protein fusions between the outer membrane anchoring β-domain of Intimin, residues 1 to 659 of wild type Intimin from EHEC, and one adhesive Ig domain based on VHHs from camelid heavy-chain antibodies recognizing a specific antigen on the target surface or cell. The modular structure of the SAs enables to program the adhesion of *E. coli* toward different target surfaces or cells by the simple exchange of the VHH sequence, which can be selected with the desired specificity from large VHH repertoires cloned in *E. coli*.

2- Constitutive expression of SAs from the chromosome of *E. coli* does not affect bacterial growth or viability, being stable maintained through multiple bacterial generations. The expression of SAs in an *E. coli* strain having deletions in several major natural adhesins (i.e. Type 1 fimbriae, Antigen 43 and Mat fimbriae) allows the specific adhesion of *E. coli* bacteria to target cells expressing a specific protein antigen on their surface.

3- Adhesion of *E. coli* mediated by SAs is a fast and very effective process that, at least *in vitro,* is enhanced by the presence of active bacterial motility. We have observed that, immediately upon contact with the target cell surface, the active motility mediated by flagella is stopped by an uncharacterized signaling mechanism that does not require the presence of YcgR protein.

4- Functionality of SAs *in vivo* was demonstrated by testing the efficiency of *E. coli* wild type strain and engineered strains expressing SAs, in the colonization of solid tumors implanted subcutaneously in mice. After systemic administration of different bacterial doses in tumor-bearing mice, we showed that the engineered *E. coli* strain, lacking major natural adhesins and expressing SAs, efficiently colonized solid tumors expressing on the surface of the tumor cells an antigen recognized by the SA. Significant lower doses of the engineered strain were required to colonize >90% of the target tumors (i.e. 2% of the dose required for the same level of tumor colonization with wild type *E. coli* strain or an engineered strain expressing a control SA that does not recognize the tumor cell).

5- The engineered *E. coli* strain expressing SAs and lacking natural adhesins is retained at lower levels in non-target organs such as liver and spleen, increasing the specificity and biosafety of its systemic administration.

6- The fast and specific adhesion of engineered *E. coli* bacteria expressing SAs allowed us to characterize by RNAseq the global transcriptomic changes taking place in *E. coli* after 15 min of adhesion to target tumor cells, which revealed a common transcriptional response independently of the recognized target. We found that genes related to sulfur uptake and its metabolism (e.g. *cysD, yeeE* etc) are upregulated upon bacterial adhesion, whereas genes encoding transporters of amino acids (i.e. *mtr*), of carbohydrates (i.e. *ugpE, rbsA* etc) and of intermediary metabolites of the Krebs cycle (i.e. *dctA*) are downregulated.

7- Gene fusion between the mCherry reporter gene and the promoter region of *yeeE* gene, integrated in the chromosome of *E. coli,* allowed us to confirm the activation of this promoter upon bacterial adhesion to target tumor cells. Activation of this promoter upon adhesion could provide the basis for the generation of an *E. coli* genetic circuit responding to specific adhesion.

8- We have produced and purified non live bacterial nanoparticles termed minicells, derived from an *E. coli minCD* mutant strain lacking major immunogenic antigens (i.e. Type 1 fimbriae, flagellar filament and hexa-acylated lipid A), which express functional SAs on their surface. SAs against a relevant therapeutic target (i.e. EGFR) allowed the specific adhesion of these nanoparticles to target tumor cells.

1- Adhesinas sintéticas capaces de dirigir de manera efectiva y específica la adhesión de *E. coli* hacia superficies o células diana, pueden ser construidas como proteínas de fusión entre el dominio β de anclaje a membrana externa de Intimina (aminoácidos 1-659 de la secuencia nativa de Intimina en EHEC) y un dominio Ig adhesivo basado en moléculas VHH, presentes en los anticuerpos de cadena pesada de los camélidos, que reconozcan de manera específica un antígeno presente en la superficie o célula diana. La estructura modular de las adhesinas sintéticas permite programar la adhesión de *E. coli* a diferentes superficies o células diana mediante el intercambio de secuencias VHH, que pueden ser seleccionadas con la especificidad deseada desde repertorios de VHH clonados en *E. coli.*

2- La expresión constitutiva de adhesinas sintéticas desde el cromosoma de *E. coli* no afecta el crecimiento bacteriano ni su viabilidad, y se mantiene estable durante múltiples generaciones bacterianas. La expresión de las adhesinas sintéticas en una cepa de *E. coli* que carece de varias adhesinas naturales conservadas (fimbrias tipo 1, Antígeno 43 y fimbrias Mat) permite la adhesión específica de esta cepa a células diana que expresan en su superficie un antígeno proteico específico.

3- La adhesión de *E. coli* mediada por adhesinas sintéticas es un proceso muy rápido y efectivo que, al menos *in vitro*, se ve potenciado por la presencia de un sistema de motilidad bacteriana activo. Además hemos observado que inmediatamente después del contacto con la superficie de una célula diana, la motilidad bacteriana mediada por el flagelo se detiene mediante un mecanismo de señalización no caracterizado, que no requiere la presencia de la proteína YcgR.

4- La funcionalidad *in vivo* de las adhesinas sintéticas fue demostrada comparando la eficiencia de la cepa silvestre y las cepas modificadas de *E. coli*, en la colonización de tumores sólidos implantados subcutáneamente en ratones. Tras la administración sistémica de distintas dosis bacterianas a ratones portadores de tumores comprobamos que la cepa modificada de *E. coli*, carente de muchas de las principales adhesinas naturales y que expresaba adhesinas sintéticas, colonizaba de modo muy eficiente tumores sólidos que expresaban en la superficie de sus células el antígeno reconocido por la adhesina sintética. Para obtener una colonización efectiva en mas del 90% de los tumores se requirió una dosis bacteriana de la cepa modificada significativamente menor (2%) que la requerida para alcanzar un eficiencia similar de colonización con la cepa silvestre de *E. coli* o con una cepa control que expresaba adhesinas sintéticas frente a otro antígeno no expresado por el tumor.

5- La cepa de *E. coli* modificada, carente de las principales adhesinas naturales y que expresa las adhesinas sintéticas, presenta *in vivo* una menor tasa de retención en órganos no diana como el hígado o el bazo, incrementando de este modo la especificidad y la bioseguridad de su administración sistémica.

6- La rápida y específica adhesión mostrada por las cepas modificas de *E. coli* que expresaban adhesinas sintéticas, nos permitió caracterizar mediante secuenciación masiva de ARN los cambios transcripcionales que ocurren en *E. coli* tras 15 minutos de adhesión a células tumorales diana, revelando una respuesta trancripcional común, independientemente del receptor reconocido. Encontramos que genes relacionados con la asimilación y el metabolismo del sulfato (p.ej. *cysD, yeeE. etc.*) se sobreexpresan en respuesta a la adhesión, mientras que la expresión de genes que codifican para transportadores de aminoácidos (*mtr*), de carbohidratos (*ugpE, rbsA*) y de intermediarios del ciclo de Krebs (*dctA*) se ve reducida tras la adhesión.

7- La fusión entre el gen de la proteína roja fluorescente mCherry y la región promotora del gen *yeeE* integrada en el cromosoma de *E. coli,* nos permitió confirmar la activación de este promotor tras la adhesión bacteriana a células tumorales diana. La activación de este promotor tras la adhesión puede suponer el punto de partida para la generación de un circuito genético en *E. coli* que responda específicamente a la adhesión.

8- Hemos producido y purificado nanopartículas bacterianas no vivas llamadas minicélulas desde una cepa de *E. coli* mutante para los genes *minCD* y carente de los principales antígenos que desencadenan una respuesta inmunológica (fimbrias tipo 1, el filamento flagelar, y el lípido A hexa-acilado), que expresan adhesinas sintéticas funcionales en su superficie. Las adhesinas sintéticas frente un marcador terapéuticamente relevante (EGFR), permitieron la adhesión específica de estas nanopartículas a células tumorales diana.

REFERENCES

- Adler, H.I., Fisher, W.D., Cohen, A., and Hardigree, A.A. (1967). MINIATURE escherichia coli CELLS DEFICIENT IN DNA. Proceedings of the National Academy of Sciences of the United States of America *57*, 321-326.
- Ai, H.W., Olenych, S.G., Wong, P., Davidson, M.W., and Campbell, R.E. (2008). Hue-shifted monomeric variants of Clavularia cyan fluorescent protein: identification of the molecular determinants of color and applications in fluorescence imaging. BMC biology *6*, 13.
- Amikam, D., and Galperin, M.Y. (2006). PilZ domain is part of the bacterial c-di-GMP binding protein. Bioinformatics *22*, 3-6.
- Anders, S., and Huber, W. (2010). Differential expression analysis for sequence count data. Genome biology *11*, R106.
- Anderson, J.L., Edney, R.J., and Whelan, K. (2012). Systematic review: faecal microbiota transplantation in the management of inflammatory bowel disease. Alimentary pharmacology & therapeutics *36*, 503-516.
- Annaluru, N., Muller, H., Mitchell, L.A., Ramalingam, S., Stracquadanio, G., Richardson, S.M., Dymond, J.S., Kuang, Z., Scheifele, L.Z., Cooper, E.M.*, et al.* (2014). Total synthesis of a functional designer eukaryotic chromosome. Science *344*, 55-58.
- Arrach, N., Zhao, M., Porwollik, S., Hoffman, R.M., and McClelland, M. (2008). Salmonella promoters preferentially activated inside tumors. Cancer research *68*, 4827-4832.
- Aureli, P., Capurso, L., Castellazzi, A.M., Clerici, M., Giovannini, M., Morelli, L., Poli, A., Pregliasco, F., Salvini, F., and Zuccotti, G.V. (2011). Probiotics and health: an evidence-based review. Pharmacological research : the official journal of the Italian Pharmacological Society *63*, 366-376.
- Beloin, C., Roux, A., and Ghigo, J.M. (2008). Escherichia coli biofilms. Current topics in microbiology and immunology *322*, 249-289.
- Beloin, C., Valle, J., Latour-Lambert, P., Faure, P., Kzreminski, M., Balestrino, D., Haagensen, J.A.J., Molin, S., Prensier, G., Arbeille, B.*, et al.* (2003). Global impact of mature biofilm lifestyle on Escherichia coli K-12 gene expression. Molecular microbiology *51*, 659-674.
- Benjamini, Y. Controlling the false discovery rate: a practical and powerful approach to multiple testing.
- Better, M., Chang, C.P., Robinson, R.R., and Horwitz, A.H. (1988). Escherichia coli secretion of an active chimeric antibody fragment. Science *240*, 1041-1043.
- Bhomkar, P., Materi, W., Semenchenko, V., and Wishart, D.S. (2010). Transcriptional response of E. coli upon FimH-mediated fimbrial adhesion. Gene regulation and systems biology *4*, 1-17.
- Bian, Z., Brauner, A., Li, Y., and Normark, S. (2000). Expression of and cytokine activation by Escherichia coli curli fibers in human sepsis. The Journal of infectious diseases *181*, 602-612.
- Bird, R.E., and Walker, B.W. (1991). Single chain antibody variable regions. Trends in biotechnology *9*, 132-137.
- Blattner, F.R. (1997). The Complete Genome Sequence of Escherichia coli K-12. Science *277*, 1453-1462.
- Blount, B.A., Weenink, T., Vasylechko, S., and Ellis, T. (2012). Rational diversification of a promoter providing fine-tuned expression and orthogonal regulation for synthetic biology. PloS one *7*, e33279.

- Bodelon, G., Marin, E., and Fernandez, L.A. (2009). Role of periplasmic chaperones and BamA (YaeT/Omp85) in folding and secretion of intimin from enteropathogenic Escherichia coli strains. Journal of bacteriology *191*, 5169-5179.
- Bodelon, G., Palomino, C., and Fernandez, L.A. (2012). Immunoglobulin domains in E. coli and other enterobacteria: from pathogenesis to applications in antibody technologies. FEMS microbiology reviews.
- Boehm, A., Kaiser, M., Li, H., Spangler, C., Kasper, C.A., Ackermann, M., Kaever, V., Sourjik, V., Roth, V., and Jenal, U. (2010). Second messenger-mediated adjustment of bacterial swimming velocity. Cell *141*, 107-116.
- Bolhassani, A., and Zahedifard, F. (2012). Therapeutic live vaccines as a potential anticancer strategy. International journal of cancer Journal international du cancer *131*, 1733-1743.
- Borody, T.J., and Khoruts, A. (2012). Fecal microbiota transplantation and emerging applications. Nature reviews Gastroenterology & hepatology *9*, 88-96.
- Boyd, C.D., and O'Toole, G.A. (2012). Second messenger regulation of biofilm formation: breakthroughs in understanding c-di-GMP effector systems. Annual review of cell and developmental biology *28*, 439-462.
- Braat, H., Rottiers, P., Hommes, D.W., Huyghebaert, N., Remaut, E., Remon, J.P., van Deventer, S.J., Neirynck, S., Peppelenbosch, M.P., and Steidler, L. (2006). A phase I trial with transgenic bacteria expressing interleukin-10 in Crohn's disease. Clinical gastroenterology and hepatology : the official clinical practice journal of the American Gastroenterological Association *4*, 754-759.
- Bridier, A., Briandet, R., Thomas, V., and Dubois-Brissonnet, F. (2011). Resistance of bacterial biofilms to disinfectants: a review. Biofouling *27*, 1017-1032.
- Brunner, M., and Bujard, H. (1987). Promoter recognition and promoter strength in the Escherichia coli system. EMBO J *6*, 3139-3144.
- Busscher, H.J., and van der Mei, H.C. (2012). How do bacteria know they are on a surface and regulate their response to an adhering state? PLoS pathogens *8*, e1002440.
- Cabilly, S., Riggs, A.D., Pande, H., Shively, J.E., Holmes, W.E., Rey, M., Perry, L.J., Wetzel, R., and Heyneker, H.L. (1984). Generation of antibody activity from immunoglobulin polypeptide chains produced in Escherichia coli. Proceedings of the National Academy of Sciences of the United States of America *81*, 3273-3277.
- Campuzano, S., Salema, V., Moreno-Guzman, M., Gamella, M., Yanez-Sedeno, P., Fernandez, L.A., and Pingarron, J.M. (2014). Disposable amperometric magnetoimmunosensors using nanobodies as biorecognition element. Determination of fibrinogen in plasma. Biosensors & bioelectronics *52*, 255-260.
- Carleton, H.A., Lara-Tejero, M., Liu, X., and Galan, J.E. (2013). Engineering the type III secretion system in non-replicating bacterial minicells for antigen delivery. Nature communications *4*, 1590.
- Chao, G., Lau, W.L., Hackel, B.J., Sazinsky, S.L., Lippow, S.M., and Wittrup, K.D. (2006). Isolating and engineering human antibodies using yeast surface display. Nature protocols *1*, 755-768.
- Chen, Y.J., Liu, P., Nielsen, A.A., Brophy, J.A., Clancy, K., Peterson, T., and Voigt, C.A. (2013). Characterization of 582 natural and synthetic terminators and quantification of their design constraints. Nature methods *10*, 659-664.
- Cheng, C.M., Lu, Y.L., Chuang, K.H., Hung, W.C., Shiea, J., Su, Y.C., Kao, C.H., Chen, B.M., Roffler, S., and Cheng, T.L. (2008). Tumor-targeting prodrug-activating bacteria for cancer therapy. Cancer gene therapy *15*, 393-401.

- Cherepanov, P.P., and Wackernagel, W. (1995). Gene disruption in Escherichia coli: TcR and KmR cassettes with the option of Flp-catalyzed excision of the antibiotic-resistance determinant. Gene *158*, 9-14.
- Claesson, M.J., Jeffery, I.B., Conde, S., Power, S.E., O'Connor, E.M., Cusack, S., Harris, H.M., Coakley, M., Lakshminarayanan, B., O'Sullivan, O.*, et al.* (2012). Gut microbiota composition correlates with diet and health in the elderly. Nature *488*, 178-184.
- Coburn, B., Sekirov, I., and Finlay, B.B. (2007). Type III secretion systems and disease. Clinical microbiology reviews *20*, 535-549.
- Cohen, G., Mustafi, R., Chumsangsri, A., Little, N., Nathanson, J., Cerda, S., Jagadeeswaran, S., Dougherty, U., Joseph, L., Hart, J.*, et al.* (2006). Epidermal growth factor receptor signaling is up-regulated in human colonic aberrant crypt foci. Cancer research *66*, 5656-5664.
- Coley, W.B. (1910). The Treatment of Inoperable Sarcoma by Bacterial Toxins (the Mixed Toxins of the Streptococcus erysipelas and the Bacillus prodigiosus). Proceedings of the Royal Society of Medicine *3*, 1-48.
- Connell, I., Agace, W., Klemm, P., Schembri, M., Marild, S., and Svanborg, C. (1996). Type 1 fimbrial expression enhances Escherichia coli virulence for the urinary tract. Proceedings of the National Academy of Sciences of the United States of America *93*, 9827-9832.
- Cote-Sierra, J., Jongert, E., Bredan, A., Gautam, D.C., Parkhouse, M., Cornelis, P., De Baetselier, P., and Revets, H. (1998). A new membrane-bound OprI lipoprotein expression vector. High production of heterologous fusion proteins in gram (-) bacteria and the implications for oral vaccination. Gene *221*, 25-34.
- Csorgo, B., Feher, T., Timar, E., Blattner, F.R., and Posfai, G. (2012). Low-mutation-rate, reduced-genome Escherichia coli: an improved host for faithful maintenance of engineered genetic constructs. Microbial cell factories *11*, 11.
- Datsenko, K.A., and Wanner, B.L. (2000). One-step inactivation of chromosomal genes in Escherichia coli K-12 using PCR products. Proceedings of the National Academy of Sciences of the United States of America *97*, 6640-6645.
- Davies, S.J., Golby, P., Omrani, D., Broad, S.A., Harrington, V.L., Guest, J.R., Kelly, D.J., and Andrews, S.C. (1999). Inactivation and regulation of the aerobic C(4)-dicarboxylate transport (dctA) gene of Escherichia coli. Journal of bacteriology *181*, 5624-5635.
- de Boer, H.A., Comstock, L.J., and Vasser, M. (1983). The tac promoter: a functional hybrid derived from the trp and lac promoters. Proceedings of the National Academy of Sciences of the United States of America *80*, 21-25.
- De Meyer, T., Muyldermans, S., and Depicker, A. (2014). Nanobody-based products as research and diagnostic tools. Trends in biotechnology *32*, 263-270.
- Desvaux, M., Hebraud, M., Talon, R., and Henderson, I.R. (2009). Secretion and subcellular localizations of bacterial proteins: a semantic awareness issue. Trends in microbiology *17*, 139-145.
- Diaz Heijtz, R., Wang, S., Anuar, F., Qian, Y., Bjorkholm, B., Samuelsson, A., Hibberd, M.L., Forssberg, H., and Pettersson, S. (2011). Normal gut microbiota modulates brain development and behavior. Proceedings of the National Academy of Sciences of the United States of America *108*, 3047-3052.
- Dimitrov, D.S., and Marks, J.D. (2009). Therapeutic antibodies: current state and future trends--is a paradigm change coming soon? Methods in molecular biology (Clifton, NJ) *525*, 1-27, xiii.

- Domka, J., Lee, J., Bansal, T., and Wood, T.K. (2007). Temporal gene-expression in Escherichia coli K-12 biofilms. Environmental microbiology *9*, 332-346.
- Duan, F., and March, J.C. (2010). Engineered bacterial communication prevents Vibrio cholerae virulence in an infant mouse model. Proceedings of the National Academy of Sciences of the United States of America *107*, 11260-11264.
- Egbert, R.G., and Klavins, E. (2012). Fine-tuning gene networks using simple sequence repeats. Proceedings of the National Academy of Sciences of the United States of America *109*, 16817-16822.
- El Hamidi, A., Tirsoaga, A., Novikov, A., Hussein, A., and Caroff, M. (2005). Microextraction of bacterial lipid A: easy and rapid method for mass spectrometric characterization. Journal of lipid research *46*, 1773-1778.
- Ellis, T.N., and Kuehn, M.J. (2010). Virulence and immunomodulatory roles of bacterial outer membrane vesicles. Microbiology and molecular biology reviews : MMBR *74*, 81-94.
- Fairman, J.W., Dautin, N., Wojtowicz, D., Liu, W., Noinaj, N., Barnard, T.J., Udho, E., Przytycka, T.M., Cherezov, V., and Buchanan, S.K. (2012). Crystal structures of the outer membrane domain of intimin and invasin from enterohemorrhagic E. coli and enteropathogenic Y. pseudotuberculosis. Structure *20*, 1233-1243.
- Fairman, J.W., Noinaj, N., and Buchanan, S.K. (2011). The structural biology of beta-barrel membrane proteins: a summary of recent reports. Current opinion in structural biology *21*, 523-531.
- Fang, X., and Gomelsky, M. (2010). A post-translational, c-di-GMP-dependent mechanism regulating flagellar motility. Molecular microbiology *76*, 1295-1305.
- Fanning, L.J., Connor, A.M., and Wu, G.E. (1996). Development of the immunoglobulin repertoire. Clinical immunology and immunopathology *79*, 1-14.
- Feldhaus, M.J., and Siegel, R.W. (2004). Yeast display of antibody fragments: a discovery and characterization platform. Journal of immunological methods *290*, 69-80.
- Fernandez, L.A. (2004). Prokaryotic expression of antibodies and affibodies. Current opinion in biotechnology *15*, 364-373.
- Forbes, N.S. (2010). Engineering the perfect (bacterial) cancer therapy. Nature reviews Cancer *10*, 785-794.
- Forbes, N.S., Munn, L.L., Fukumura, D., and Jain, R.K. (2003). Sparse initial entrapment of systemically injected Salmonella typhimurium leads to heterogeneous accumulation within tumors. Cancer research *63*, 5188-5193.
- Francisco, J.A., Campbell, R., Iverson, B.L., and Georgiou, G. (1993). Production and fluorescence-activated cell sorting of Escherichia coli expressing a functional antibody fragment on the external surface. Proceedings of the National Academy of Sciences of the United States of America *90*, 10444-10448.
- Frankel, G., Phillips, A.D., Trabulsi, L.R., Knutton, S., Dougan, G., and Matthews, S. (2001). Intimin and the host cell--is it bound to end in Tir(s)? Trends in microbiology *9*, 214-218.
- Fu, W., Chu, L., Han, X., Liu, X., and Ren, D. (2008). Synergistic antitumoral effects of human telomerase reverse transcriptase-mediated dual-apoptosis-related gene vector delivered by orally attenuated Salmonella enterica Serovar Typhimurium in murine tumor models. The journal of gene medicine *10*, 690-701.
- Ganai, S., Arenas, R.B., and Forbes, N.S. (2009). Tumour-targeted delivery of TRAIL using Salmonella typhimurium enhances breast cancer survival in mice. British journal of cancer *101*, 1683-1691.

- Gandhi, N.M., Morales, A., and Lamm, D.L. (2013). Bacillus Calmette-Guerin immunotherapy for genitourinary cancer. BJU international *112*, 288-297.
- Garnett, J.A., Martinez-Santos, V.I., Saldana, Z., Pape, T., Hawthorne, W., Chan, J., Simpson, P.J., Cota, E., Puente, J.L., Giron, J.A.*, et al.* (2012). Structural insights into the biogenesis and biofilm formation by the Escherichia coli common pilus. Proceedings of the National Academy of Sciences of the United States of America *109*, 3950-3955.
- Georgiou, G., Stephens, D.L., Stathopoulos, C., Poetschke, H.L., Mendenhall, J., and Earhart, C.F. (1996). Display of beta-lactamase on the Escherichia coli surface: outer membrane phenotypes conferred by Lpp'-OmpA'-beta-lactamase fusions. Protein engineering *9*, 239-247.
- Gerber, G.K. (2014). The dynamic microbiome. FEBS letters.
- Gerlach, R.G., and Hensel, M. (2007). Protein secretion systems and adhesins: the molecular armory of Gram-negative pathogens. International journal of medical microbiology : IJMM *297*, 401-415.
- Gibson, D.G., Benders, G.A., Andrews-Pfannkoch, C., Denisova, E.A., Baden-Tillson, H., Zaveri, J., Stockwell, T.B., Brownley, A., Thomas, D.W., Algire, M.A.*, et al.* (2008). Complete chemical synthesis, assembly, and cloning of a Mycoplasma genitalium genome. Science *319*, 1215-1220.
- Gibson, D.G., Glass, J.I., Lartigue, C., Noskov, V.N., Chuang, R.Y., Algire, M.A., Benders, G.A., Montague, M.G., Ma, L., Moodie, M.M.*, et al.* (2010). Creation of a bacterial cell controlled by a chemically synthesized genome. Science *329*, 52-56.
- Goeddel, D.V., Kleid, D.G., Bolivar, F., Heyneker, H.L., Yansura, D.G., Crea, R., Hirose, T., Kraszewski, A., Itakura, K., and Riggs, A.D. (1979). Expression in Escherichia coli of chemically synthesized genes for human insulin. Proceedings of the National Academy of Sciences of the United States of America *76*, 106-110.
- Green, L.L., Hardy, M.C., Maynard-Currie, C.E., Tsuda, H., Louie, D.M., Mendez, M.J., Abderrahim, H., Noguchi, M., Smith, D.H., Zeng, Y.*, et al.* (1994). Antigen-specific human monoclonal antibodies from mice engineered with human Ig heavy and light chain YACs. Nature genetics *7*, 13-21.
- Gujrati, V., Kim, S., Kim, S.H., Min, J.J., Choy, H.E., Kim, S.C., and Jon, S. (2014). Bioengineered bacterial outer membrane vesicles as cell-specific drug-delivery vehicles for cancer therapy. ACS nano *8*, 1525-1537.
- Gutierrez, C., and Schiff, R. (2011). HER2: biology, detection, and clinical implications. Archives of pathology & laboratory medicine *135*, 55-62.
- Guzman, L.M., Belin, D., Carson, M.J., and Beckwith, J. (1995). Tight regulation, modulation, and high-level expression by vectors containing the arabinose PBAD promoter. Journal of bacteriology *177*, 4121-4130.
- Hamers-Casterman, C., Atarhouch, T., Muyldermans, S., Robinson, G., Hamers, C., Songa, E.B., Bendahman, N., and Hamers, R. (1993). Naturally occurring antibodies devoid of light chains. Nature *363*, 446-448.
- Han, H.J., Park, S.G., Kim, S.H., Hwang, S.Y., Han, J., Traicoff, J., Kho, W.G., and Chung, J.Y. (2004). Epidermal growth factor-like motifs 1 and 2 of Plasmodium vivax merozoite surface protein 1 are critical domains in erythrocyte invasion. Biochemical and biophysical research communications *320*, 563-570.
- Hanahan, D., and Weinberg, R.A. (2011). Hallmarks of cancer: the next generation. Cell *144*, 646-674.

- Hancock, V., and Klemm, P. (2007). Global gene expression profiling of asymptomatic bacteriuria Escherichia coli during biofilm growth in human urine. Infection and immunity *75*, 966-976.
- Hannon, G.J. (2002). RNA interference. Nature *418*, 244-251.
- Harvey, B.R., Georgiou, G., Hayhurst, A., Jeong, K.J., Iverson, B.L., and Rogers, G.K. (2004). Anchored periplasmic expression, a versatile technology for the isolation of high-affinity antibodies from Escherichia coli-expressed libraries. Proceedings of the National Academy of Sciences of the United States of America *101*, 9193-9198.
- Hasty, J. (2012). Engineered microbes for therapeutic applications. ACS synthetic biology *1*, 438-439.
- Haswell, E.S., Phillips, R., and Rees, D.C. (2011). Mechanosensitive channels: what can they do and how do they do it? Structure *19*, 1356-1369.
- Hayashi, F., Smith, K.D., Ozinsky, A., Hawn, T.R., Yi, E.C., Goodlett, D.R., Eng, J.K., Akira, S., Underhill, D.M., and Aderem, A. (2001). The innate immune response to bacterial flagellin is mediated by Toll-like receptor 5. Nature *410*, 1099-1103.
- He, M., and Khan, F. (2005). Ribosome display: next-generation display technologies for production of antibodies in vitro. Expert review of proteomics *2*, 421-430.
- Henderson, I.R., Navarro-Garcia, F., Desvaux, M., Fernandez, R.C., and Ala'Aldeen, D. (2004). Type V protein secretion pathway: the autotransporter story. Microbiology and molecular biology reviews : MMBR *68*, 692-744.
- Hengge, R. (2009). Principles of c-di-GMP signalling in bacteria. Nature reviews Microbiology *7*, 263-273.
- Herrero, M., de Lorenzo, V., and Timmis, K.N. (1990). Transposon vectors containing non-antibiotic resistance selection markers for cloning and stable chromosomal insertion of foreign genes in gram-negative bacteria. Journal of bacteriology *172*, 6557-6567.
- Herring, C.D., Glasner, J.D., and Blattner, F.R. (2003). Gene replacement without selection: regulated suppression of amber mutations in Escherichia coli. Gene *311*, 153-163.
- Hess, J., Gentschev, I., Miko, D., Welzel, M., Ladel, C., Goebel, W., and Kaufmann, S.H. (1996). Superior efficacy of secreted over somatic antigen display in recombinant Salmonella vaccine induced protection against listeriosis. Proceedings of the National Academy of Sciences of the United States of America *93*, 1458-1463.
- Hoiby, N., Bjarnsholt, T., Givskov, M., Molin, S., and Ciofu, O. (2010). Antibiotic resistance of bacterial biofilms. International journal of antimicrobial agents *35*, 322-332.
- Hommais, F., Gouriou, S., Amorin, C., Bui, H., Rahimy, M.C., Picard, B., and Denamur, E. (2003). The FimH A27V Mutation Is Pathoadaptive for Urovirulence in Escherichia coli B2 Phylogenetic Group Isolates. Infection and immunity *71*, 3619-3622.
- Honegger, A.M., Dull, T.J., Felder, S., Van Obberghen, E., Bellot, F., Szapary, D., Schmidt, A., Ullrich, A., and Schlessinger, J. (1987). Point mutation at the ATP binding site of EGF receptor abolishes protein-tyrosine kinase activity and alters cellular routing. Cell *51*, 199-209.
- Huh, J.H., Kittleson, J.T., Arkin, A.P., and Anderson, J.C. (2013). Modular design of a synthetic payload delivery device. ACS synthetic biology *2*, 418-424.

- Huibregtse, I.L., Zaat, S.A., Kapsenberg, M.L., Sartori da Silva, M.A., Peppelenbosch, M.P., van Deventer, S.J., and Braat, H. (2012). Genetically Modified Lactococcus lactis for Delivery of Human Interleukin-10 to Dendritic Cells. Gastroenterology research and practice *2012*, 639291.
- Hwang, I.Y., Tan, M.H., Koh, E., Ho, C.L., Poh, C.L., and Chang, M.W. (2013). Reprogramming Microbes to Be Pathogen-Seeking Killers. ACS synthetic biology.
- Jenal, U., and Malone, J. (2006). Mechanisms of cyclic-di-GMP signaling in bacteria. Annual review of genetics *40*, 385-407.
- Jiang, S.N., Phan, T.X., Nam, T.K., Nguyen, V.H., Kim, H.S., Bom, H.S., Choy, H.E., Hong, Y., and Min, J.J. (2010). Inhibition of tumor growth and metastasis by a combination of Escherichia coli-mediated cytolytic therapy and radiotherapy. Molecular therapy : the journal of the American Society of Gene Therapy *18*, 635-642.
- Jordan, M., Schallhorn, A., and Wurm, F.M. (1996). Transfecting mammalian cells: optimization of critical parameters affecting calcium-phosphate precipitate formation. Nucleic acids research *24*, 596-601.
- Jurado, P., de Lorenzo, V., and Fernandez, L.A. (2006). Thioredoxin fusions increase folding of single chain Fv antibodies in the cytoplasm of Escherichia coli: evidence that chaperone activity is the prime effect of thioredoxin. Journal of molecular biology *357*, 49-61.
- Jurado, P., Ritz, D., Beckwith, J., de Lorenzo, V.c., and Fernández, L.A. (2002). Production of Functional Single-Chain Fv Antibodies in the Cytoplasm of Escherichia coli. Journal of molecular biology *320*, 1-10.
- Kalyanpur, M. (2002). Downstream processing in the biotechnology industry. Molecular biotechnology *22*, 87-98.
- Kasinskas, R.W., and Forbes, N.S. (2006). Salmonella typhimurium specifically chemotax and proliferate in heterogeneous tumor tissue in vitro. Biotechnology and bioengineering *94*, 710-721.
- Kelly, D.F., Moxon, E.R., and Pollard, A.J. (2004). Haemophilus influenzae type b conjugate vaccines. Immunology *113*, 163-174.
- Kenny, B., DeVinney, R., Stein, M., Reinscheid, D.J., Frey, E.A., and Finlay, B.B. (1997). Enteropathogenic E. coli (EPEC) transfers its receptor for intimate adherence into mammalian cells. Cell *91*, 511-520.
- King, I., Bermudes, D., Lin, S., Belcourt, M., Pike, J., Troy, K., Le, T., Ittensohn, M., Mao, J., Lang, W*., et al.* (2002). Tumor-targeted Salmonella expressing cytosine deaminase as an anticancer agent. Human gene therapy *13*, 1225-1233.
- Kirkpatrick, C.L., and Viollier, P.H. (2012). Reflections on a sticky situation: how surface contact pulls the trigger for bacterial adhesion. Molecular microbiology *83*, 7-9.
- Kline, K.A., Falker, S., Dahlberg, S., Normark, S., and Henriques-Normark, B. (2009). Bacterial adhesins in host-microbe interactions. Cell host & microbe *5*, 580-592.
- Korea, C.G., Badouraly, R., Prevost, M.C., Ghigo, J.M., and Beloin, C. (2010). Escherichia coli K-12 possesses multiple cryptic but functional chaperone-usher fimbriae with distinct surface specificities. Environmental microbiology *12*, 1957-1977.
- Korea, C.G., Ghigo, J.M., and Beloin, C. (2011). The sweet connection: Solving the riddle of multiple sugar-binding fimbrial adhesins in Escherichia coli: Multiple E. coli fimbriae form a versatile arsenal of sugar-binding lectins potentially involved in surface-colonisation and tissue tropism. BioEssays : news and reviews in molecular, cellular and developmental biology *33*, 300-311.

- Kulp, A., and Kuehn, M.J. (2010). Biological functions and biogenesis of secreted bacterial outer membrane vesicles. Annual review of microbiology *64*, 163-184.
- Lagenaur, L.A., Sanders-Beer, B.E., Brichacek, B., Pal, R., Liu, X., Liu, Y., Yu, R., Venzon, D., Lee, P.P., and Hamer, D.H. (2011). Prevention of vaginal SHIV transmission in macaques by a live recombinant Lactobacillus. Mucosal immunology *4*, 648-657.
- Lamm, D.L., van der Meijden, P.M., Morales, A., Brosman, S.A., Catalona, W.J., Herr, H.W., Soloway, M.S., Steg, A., and Debruyne, F.M. (1992). Incidence and treatment of complications of bacillus Calmette-Guerin intravesical therapy in superficial bladder cancer. The Journal of urology *147*, 596-600.
- Langmead, B., Trapnell, C., Pop, M., and Salzberg, S.L. (2009). Ultrafast and memory-efficient alignment of short DNA sequences to the human genome. Genome biology *10*, R25.
- Lee, C.H. (2012). Engineering bacteria toward tumor targeting for cancer treatment: current state and perspectives. Applied microbiology and biotechnology *93*, 517-523.
- Lee, C.H., Wu, C.L., and Shiau, A.L. (2004). Endostatin gene therapy delivered by Salmonella choleraesuis in murine tumor models. The journal of gene medicine *6*, 1382-1393.
- Lee, E.C., Liang, Q., Ali, H., Bayliss, L., Beasley, A., Bloomfield-Gerdes, T., Bonoli, L., Brown, R., Campbell, J., Carpenter, A*., et al.* (2014). Complete humanization of the mouse immunoglobulin loci enables efficient therapeutic antibody discovery. Nature biotechnology *32*, 356-363.
- Lee, J.S., Poo, H., Han, D.P., Hong, S.P., Kim, K., Cho, M.W., Kim, E., Sung, M.H., and Kim, C.J. (2006). Mucosal immunization with surface-displayed severe acute respiratory syndrome coronavirus spike protein on Lactobacillus casei induces neutralizing antibodies in mice. Journal of virology *80*, 4079-4087.
- Leffler, H. Chemical identification of a glycosphingolipid receptor for Escherichia coli attaching to human urinary tract epithelial cells and agglutinating human erythrocytes.
- Lehouritis, P., Springer, C., and Tangney, M. (2013). Bacterial-directed enzyme prodrug therapy. Journal of controlled release : official journal of the Controlled Release Society *170*, 120-131.
- Lehti, T.A., Bauchart, P., Heikkinen, J., Hacker, J., Korhonen, T.K., Dobrindt, U., and Westerlund-Wikstrom, B. (2010). Mat fimbriae promote biofilm formation by meningitis-associated Escherichia coli. Microbiology *156*, 2408-2417.
- Leo, J.C., Grin, I., and Linke, D. (2012). Type V secretion: mechanism(s) of autotransport through the bacterial outer membrane. Philosophical transactions of the Royal Society of London Series B, Biological sciences *367*, 1088-1101.
- Leyton, D.L., Rossiter, A.E., and Henderson, I.R. (2012). From self sufficiency to dependence: mechanisms and factors important for autotransporter biogenesis. Nature reviews Microbiology *10*, 213-225.
- Li, T., Xu, L., Ren, G., Yin, C., Zhou, B., Ye, X., Li, Q., Li, N., and Li, D. (2013). A neutralization scFv antibody against IL-1beta isolated from a NIPA-based bacterial display library. Current pharmaceutical biotechnology *14*, 571-581.
- Lindberg, U., Hanson, L.A., Jodal, U., Lidin-Janson, G., Lincoln, K., and Olling, S. (1975). Asymptomatic bacteriuria in schoolgirls. II. Differences in escherichia coli causing asymptomatic bacteriuria. Acta paediatrica Scandinavica *64*, 432-436.
- Loeffler, M., Le'Negrate, G., Krajewska, M., and Reed, J.C. (2007). Attenuated Salmonella engineered to produce human cytokine LIGHT inhibit tumor growth.

Proceedings of the National Academy of Sciences of the United States of America *104*, 12879-12883.

- Loeffler, M., Le'Negrate, G., Krajewska, M., and Reed, J.C. (2008). Inhibition of tumor growth using salmonella expressing Fas ligand. Journal of the National Cancer Institute *100*, 1113-1116.
- Lopilato, J.E., Garwin, J.L., Emr, S.D., Silhavy, T.J., and Beckwith, J.R. (1984). D-ribose metabolism in Escherichia coli K-12: genetics, regulation, and transport. Journal of bacteriology *158*, 665-673.
- Lutkenhaus, J. (2007). Assembly dynamics of the bacterial MinCDE system and spatial regulation of the Z ring. Annual review of biochemistry *76*, 539-562.
- MacDiarmid, J.A., Amaro-Mugridge, N.B., Madrid-Weiss, J., Sedliarou, I., Wetzel, S., Kochar, K., Brahmbhatt, V.N., Phillips, L., Pattison, S.T., Petti, C.*, et al.* (2009). Sequential treatment of drug-resistant tumors with targeted minicells containing siRNA or a cytotoxic drug. Nature biotechnology *27*, 643-651.
- MacDiarmid, J.A., Madrid-Weiss, J., Amaro-Mugridge, N.B., Phillips, L., and Brahmbhatt, H. (2007a). Bacterially-derived nanocells for tumor-targeted delivery of chemotherapeutics and cell cycle inhibitors. Cell Cycle *6*, 2099-2105.
- MacDiarmid, J.A., Mugridge, N.B., Weiss, J.C., Phillips, L., Burn, A.L., Paulin, R.P., Haasdyk, J.E., Dickson, K.A., Brahmbhatt, V.N., Pattison, S.T.*, et al.* (2007b). Bacterially derived 400 nm particles for encapsulation and cancer cell targeting of chemotherapeutics. Cancer Cell *11*, 431-445.
- Macdonald, L.E., Karow, M., Stevens, S., Auerbach, W., Poueymirou, W.T., Yasenchak, J., Frendewey, D., Valenzuela, D.M., Giallourakis, C.C., Alt, F.W.*, et al.* (2014). Precise and in situ genetic humanization of 6 Mb of mouse immunoglobulin genes. Proceedings of the National Academy of Sciences of the United States of America *111*, 5147-5152.
- Maeda, H. (2013). The link between infection and cancer: tumor vasculature, free radicals, and drug delivery to tumors via the EPR effect. Cancer science *104*, 779-789.
- Majander, K., Anton, L., Antikainen, J., Lang, H., Brummer, M., Korhonen, T.K., and Westerlund-Wikstrom, B. (2005). Extracellular secretion of polypeptides using a modified Escherichia coli flagellar secretion apparatus. Nature biotechnology *23*, 475-481.
- Malam, Y., Loizidou, M., and Seifalian, A.M. (2009). Liposomes and nanoparticles: nanosized vehicles for drug delivery in cancer. Trends in pharmacological sciences *30*, 592-599.
- Maltby, R., Leatham-Jensen, M.P., Gibson, T., Cohen, P.S., and Conway, T. (2013). Nutritional basis for colonization resistance by human commensal Escherichia coli strains HS and Nissle 1917 against E. coli O157:H7 in the mouse intestine. PloS one *8*, e53957.
- Marin, E., Bodelon, G., and Fernandez, L.A. (2010). Comparative analysis of the biochemical and functional properties of C-terminal domains of autotransporters. Journal of bacteriology *192*, 5588-5602.
- Martin, R., Miquel, S., Ulmer, J., Kechaou, N., Langella, P., and Bermudez-Humaran, L.G. (2013). Role of commensal and probiotic bacteria in human health: a focus on inflammatory bowel disease. Microbial cell factories *12*, 71.
- Martinez-Garcia, E., and de Lorenzo, V. (2011). Engineering multiple genomic deletions in Gram-negative bacteria: analysis of the multi-resistant antibiotic profile of Pseudomonas putida KT2440. Environmental microbiology *13*, 2702-2716.

- Massa, P.E., Paniccia, A., Monegal, A., de Marco, A., and Rescigno, M. (2013). Salmonella engineered to express CD20-targeting antibodies and a drug-converting enzyme can eradicate human lymphomas. Blood.
- Mazor, Y., Van Blarcom, T., Mabry, R., Iverson, B.L., and Georgiou, G. (2007). Isolation of engineered, full-length antibodies from libraries expressed in Escherichia coli. Nature biotechnology *25*, 563-565.
- McCafferty, J., Griffiths, A.D., Winter, G., and Chiswell, D.J. (1990). Phage antibodies: filamentous phage displaying antibody variable domains. Nature *348*, 552-554.
- McClaine, J.W., and Ford, R.M. (2002). Characterizing the adhesion of motile and nonmotile Escherichia coli to a glass surface using a parallel-plate flow chamber. Biotechnology and bioengineering *78*, 179-189.
- Min, J.J., Kim, H.J., Park, J.H., Moon, S., Jeong, J.H., Hong, Y.J., Cho, K.O., Nam, J.H., Kim, N., Park, Y.K.*, et al.* (2008). Noninvasive real-time imaging of tumors and metastases using tumor-targeting light-emitting Escherichia coli. Molecular imaging and biology : MIB : the official publication of the Academy of Molecular Imaging *10*, 54-61.
- Minty, J.J., Singer, M.E., Scholz, S.A., Bae, C.H., Ahn, J.H., Foster, C.E., Liao, J.C., and Lin, X.N. (2013). Design and characterization of synthetic fungal-bacterial consortia for direct production of isobutanol from cellulosic biomass. Proceedings of the National Academy of Sciences of the United States of America *110*, 14592-14597.
- Moe-Behrens, G.H., Davis, R., and Haynes, K.A. (2013). Preparing synthetic biology for the world. Frontiers in microbiology *4*, 5.
- Monegal, A., Ami, D., Martinelli, C., Huang, H., Aliprandi, M., Capasso, P., Francavilla, C., Ossolengo, G., and de Marco, A. (2009). Immunological applications of single-domain llama recombinant antibodies isolated from a naive library. Protein engineering, design & selection : PEDS *22*, 273-280.
- Mossman, K.L., Mian, M.F., Lauzon, N.M., Gyles, C.L., Lichty, B., Mackenzie, R., Gill, N., and Ashkar, A.A. (2008). Cutting Edge: FimH Adhesin of Type 1 Fimbriae Is a Novel TLR4 Ligand. The Journal of Immunology *181*, 6702-6706.
- Munera, D., Palomino, C., and Fernandez, L.A. (2008). Specific residues in the N-terminal domain of FimH stimulate type 1 fimbriae assembly in Escherichia coli following the initial binding of the adhesin to FimD usher. Molecular microbiology *69*, 911-925.
- Murphy, A.J., Macdonald, L.E., Stevens, S., Karow, M., Dore, A.T., Pobursky, K., Huang, T.T., Poueymirou, W.T., Esau, L., Meola, M.*, et al.* (2014). Mice with megabase humanization of their immunoglobulin genes generate antibodies as efficiently as normal mice. Proceedings of the National Academy of Sciences of the United States of America *111*, 5153-5158.
- Muyldermans, S. (2013). Nanobodies: natural single-domain antibodies. Annual review of biochemistry *82*, 775-797.
- Neal, D.E., Sharples, L., Smith, K., Fennelly, J., Hall, R.R., and Harris, A.L. (1990). The epidermal growth factor receptor and the prognosis of bladder cancer. Cancer *65*, 1619-1625.
- Nelson, A.L. (2010). Antibody fragments: hope and hype. mAbs *2*, 77-83.
- Nogueira, V., and Hay, N. (2013). Molecular pathways: reactive oxygen species homeostasis in cancer cells and implications for cancer therapy. Clinical cancer

research : an official journal of the American Association for Cancer Research *19*, 4309-4314.

- Noinaj, N., Kuszak, A.J., Gumbart, J.C., Lukacik, P., Chang, H., Easley, N.C., Lithgow, T., and Buchanan, S.K. (2013). Structural insight into the biogenesis of beta-barrel membrane proteins. Nature *501*, 385-390.
- Ohshima, N., Yamashita, S., Takahashi, N., Kuroishi, C., Shiro, Y., and Takio, K. (2008). Escherichia coli cytosolic glycerophosphodiester phosphodiesterase (UgpQ) requires Mg2+, Co2+, or Mn2+ for its enzyme activity. Journal of bacteriology *190*, 1219-1223.
- Olsen, A., Wick, M.J., Morgelin, M., and Bjorck, L. (1998). Curli, fibrous surface proteins of Escherichia coli, interact with major histocompatibility complex class I molecules. Infection and immunity *66*, 944-949.
- Otto, K., and Silhavy, T.J. (2002). Surface sensing and adhesion of Escherichia coli controlled by the Cpx-signaling pathway. Proceedings of the National Academy of Sciences of the United States of America *99*, 2287-2292.
- Owen, J.L., Sahay, B., and Mohamadzadeh, M. (2013). New generation of oral mucosal vaccines targeting dendritic cells. Current opinion in chemical biology *17*, 918-924.
- Park, M., Tsai, S.L., and Chen, W. (2013). Microbial biosensors: engineered microorganisms as the sensing machinery. Sensors (Basel) *13*, 5777-5795.
- Paton, A.W., Morona, R., and Paton, J.C. (2000). A new biological agent for treatment of Shiga toxigenic Escherichia coli infections and dysentery in humans. Nature medicine *6*, 265-270.
- Paukner, S., Kudela, P., Kohl, G., Schlapp, T., Friedrichs, S., and Lubitz, W. (2005). DNA-loaded bacterial ghosts efficiently mediate reporter gene transfer and expression in macrophages. Molecular therapy : the journal of the American Society of Gene Therapy *11*, 215-223.
- Paul, K., Nieto, V., Carlquist, W.C., Blair, D.F., and Harshey, R.M. (2010). The c-di-GMP binding protein YcgR controls flagellar motor direction and speed to affect chemotaxis by a "backstop brake" mechanism. Molecular cell *38*, 128-139.
- Pawelek, J.M., Low, K.B., and Bermudes, D. (1997). Tumor-targeted Salmonella as a novel anticancer vector. Cancer research *57*, 4537-4544.
- Perez-Gutierrez, C., Llobet, E., Llompart, C.M., Reines, M., and Bengoechea, J.A. (2010). Role of lipid A acylation in Yersinia enterocolitica virulence. Infection and immunity *78*, 2768-2781.
- Perna, N.T., Plunkett, G., 3rd, Burland, V., Mau, B., Glasner, J.D., Rose, D.J., Mayhew, G.F., Evans, P.S., Gregor, J., Kirkpatrick, H.A*., et al.* (2001). Genome sequence of enterohaemorrhagic Escherichia coli O157:H7. Nature *409*, 529-533.
- Pessi, T., Sutas, Y., Hurme, M., and Isolauri, E. (2000). Interleukin-10 generation in atopic children following oral Lactobacillus rhamnosus GG. Clinical and experimental allergy : journal of the British Society for Allergy and Clinical Immunology *30*, 1804-1808.
- Pizarro-Cerda, J., and Cossart, P. (2006). Bacterial adhesion and entry into host cells. Cell *124*, 715-727.
- Pizza, M., Covacci, A., Bartoloni, A., Perugini, M., Nencioni, L., De Magistris, M.T., Villa, L., Nucci, D., Manetti, R., Bugnoli, M*., et al.* (1989). Mutants of pertussis toxin suitable for vaccine development. Science *246*, 497-500.

- Porcar, M., Danchin, A., de Lorenzo, V., Dos Santos, V.A., Krasnogor, N., Rasmussen, S., and Moya, A. (2011). The ten grand challenges of synthetic life. Systems and synthetic biology *5*, 1-9.
- Posfai, G., Kolisnychenko, V., Bereczki, Z., and Blattner, F.R. (1999). Markerless gene replacement in Escherichia coli stimulated by a double-strand break in the chromosome. Nucleic acids research *27*, 4409-4415.
- Posfai, G., Plunkett, G., 3rd, Feher, T., Frisch, D., Keil, G.M., Umenhoffer, K., Kolisnychenko, V., Stahl, B., Sharma, S.S., de Arruda, M.*, et al.* (2006). Emergent properties of reduced-genome Escherichia coli. Science *312*, 1044-1046.
- Pouttu, R., Westerlund-Wikstrom, B., Lang, H., Alsti, K., Virkola, R., Saarela, U., Siitonen, A., Kalkkinen, N., and Korhonen, T.K. (2001). matB, a common fimbrillin gene of Escherichia coli, expressed in a genetically conserved, virulent clonal group. Journal of bacteriology *183*, 4727-4736.
- Pulido, J., Kottke, T., Thompson, J., Galivo, F., Wongthida, P., Diaz, R.M., Rommelfanger, D., Ilett, E., Pease, L., Pandha, H.*, et al.* (2012). Using virally expressed melanoma cDNA libraries to identify tumor-associated antigens that cure melanoma. Nature biotechnology *30*, 337-343.
- Qin, J., Li, Y., Cai, Z., Li, S., Zhu, J., Zhang, F., Liang, S., Zhang, W., Guan, Y., Shen, D.*, et al.* (2012). A metagenome-wide association study of gut microbiota in type 2 diabetes. Nature *490*, 55-60.
- Ren, D., Bedzyk, L.A., Thomas, S.M., Ye, R.W., and Wood, T.K. (2004). Gene expression in Escherichia coli biofilms. Applied microbiology and biotechnology *64*, 515-524.
- Rendon, M.A., Saldana, Z., Erdem, A.L., Monteiro-Neto, V., Vazquez, A., Kaper, J.B., Puente, J.L., and Giron, J.A. (2007). Commensal and pathogenic Escherichia coli use a common pilus adherence factor for epithelial cell colonization. Proceedings of the National Academy of Sciences of the United States of America *104*, 10637-10642.
- Romling, U., Gomelsky, M., and Galperin, M.Y. (2005). C-di-GMP: the dawning of a novel bacterial signalling system. Molecular microbiology *57*, 629-639.
- Roovers, R.C., Laeremans, T., Huang, L., De Taeye, S., Verkleij, A.J., Revets, H., de Haard, H.J., and van Bergen en Henegouwen, P.M. (2007). Efficient inhibition of EGFR signaling and of tumour growth by antagonistic anti-EFGR Nanobodies. Cancer immunology, immunotherapy : CII *56*, 303-317.
- Rothbauer, U., Zolghadr, K., Muyldermans, S., Schepers, A., Cardoso, M.C., and Leonhardt, H. (2008). A versatile nanotrap for biochemical and functional studies with fluorescent fusion proteins. Molecular & cellular proteomics : MCP *7*, 282-289.
- Royo, J.L., Becker, P.D., Camacho, E.M., Cebolla, A., Link, C., Santero, E., and Guzman, C.A. (2007). In vivo gene regulation in Salmonella spp. by a salicylate-dependent control circuit. Nature methods *4*, 937-942.
- Ryjenkov, D.A., Simm, R., Romling, U., and Gomelsky, M. (2006). The PilZ domain is a receptor for the second messenger c-di-GMP: the PilZ domain protein YcgR controls motility in enterobacteria. The Journal of biological chemistry *281*, 30310-30314.
- Saldana, Z., Erdem, A.L., Schuller, S., Okeke, I.N., Lucas, M., Sivananthan, A., Phillips, A.D., Kaper, J.B., Puente, J.L., and Giron, J.A. (2009). The Escherichia coli common pilus and the bundle-forming pilus act in concert during the formation of localized adherence by enteropathogenic E. coli. Journal of bacteriology *191*, 3451-3461.

- Salema, V., Marin, E., Martinez-Arteaga, R., Ruano-Gallego, D., Fraile, S., Margolles, Y., Teira, X., Gutierrez, C., Bodelon, G., and Fernandez, L.A. (2013). Selection of single domain antibodies from immune libraries displayed on the surface of E. coli cells with two beta-domains of opposite topologies. PloS one *8*, e75126.
- Sartor, R.B. (2005). Role of commensal enteric bacteria in the pathogenesis of immune-mediated intestinal inflammation: lessons from animal models and implications for translational research. Journal of pediatric gastroenterology and nutrition *40 Suppl 1*, S30-31.
- Sauer, F.G., Pinkner, J.S., Waksman, G., and Hultgren, S.J. (2002). Chaperone priming of pilus subunits facilitates a topological transition that drives fiber formation. Cell *111*, 543-551.
- Schembri, M.A., Kjaergaard, K., and Klemm, P. (2003). Global gene expression in Escherichia coli biofilms. Molecular microbiology *48*, 253-267.
- Schena, M., Shalon, D., Davis, R.W., and Brown, P.O. (1995). Quantitative monitoring of gene expression patterns with a complementary DNA microarray. Science *270*, 467-470.
- Schroeder, H.W., Jr., and Cavacini, L. (2010). Structure and function of immunoglobulins. The Journal of allergy and clinical immunology *125*, S41-52.
- Schultz, M. (2008). Clinical use of E. coli Nissle 1917 in inflammatory bowel disease. Inflammatory bowel diseases *14*, 1012-1018.
- Schwan, W.R., Beck, M.T., Hultgren, S.J., Pinkner, J., Woolever, N.L., and Larson, T. (2005). Down-regulation of the kps region 1 capsular assembly operon following attachment of Escherichia coli type 1 fimbriae to D-mannose receptors. Infection and immunity *73*, 1226-1231.
- Seo, E.J., Weibel, S., Wehkamp, J., and Oelschlaeger, T.A. (2012). Construction of recombinant E. coli Nissle 1917 (EcN) strains for the expression and secretion of defensins. International journal of medical microbiology : IJMM *302*, 276-287.
- Shaner, N.C., Campbell, R.E., Steinbach, P.A., Giepmans, B.N., Palmer, A.E., and Tsien, R.Y. (2004). Improved monomeric red, orange and yellow fluorescent proteins derived from Discosoma sp. red fluorescent protein. Nature biotechnology *22*, 1567-1572.
- Silva-Rocha, R., Martinez-Garcia, E., Calles, B., Chavarria, M., Arce-Rodriguez, A., de Las Heras, A., Paez-Espino, A.D., Durante-Rodriguez, G., Kim, J., Nikel, P.I.*, et al.* (2013). The Standard European Vector Architecture (SEVA): a coherent platform for the analysis and deployment of complex prokaryotic phenotypes. Nucleic acids research *41*, D666-675.
- Skerra, A. (1994). Use of the tetracycline promoter for the tightly regulated production of a murine antibody fragment in Escherichia coli. Gene *151*, 131-135.
- Smith, G.P. (1985). Filamentous fusion phage: novel expression vectors that display cloned antigens on the virion surface. Science *228*, 1315-1317.
- Smith, K., McCoy, K.D., and Macpherson, A.J. (2007). Use of axenic animals in studying the adaptation of mammals to their commensal intestinal microbiota. Seminars in immunology *19*, 59-69.
- Smyth, G.K. (2004). Linear models and empirical bayes methods for assessing differential expression in microarray experiments. Statistical applications in genetics and molecular biology *3*, Article3.
- Sokol, H., Pigneur, B., Watterlot, L., Lakhdari, O., Bermudez-Humaran, L.G., Gratadoux, J.J., Blugeon, S., Bridonneau, C., Furet, J.P., Corthier, G.*, et al.* (2008). Faecalibacterium prausnitzii is an anti-inflammatory commensal bacterium identified

by gut microbiota analysis of Crohn disease patients. Proceedings of the National Academy of Sciences of the United States of America *105*, 16731-16736.
- Somerville, J.E., Jr., Cassiano, L., and Darveau, R.P. (1999). Escherichia coli msbB gene as a virulence factor and a therapeutic target. Infection and immunity *67*, 6583-6590.
- Stalker, D.M., Kolter, R., and Helinski, D.R. (1982). Plasmid R6K DNA replication. I. Complete nucleotide sequence of an autonomously replicating segment. Journal of molecular biology *161*, 33-43.
- Sunden, F., Hakansson, L., Ljunggren, E., and Wullt, B. (2006). Bacterial interference--is deliberate colonization with Escherichia coli 83972 an alternative treatment for patients with recurrent urinary tract infection? International journal of antimicrobial agents *28 Suppl 1*, S26-29.
- Taniguchi, T., Matsui, H., Fujita, T., Takaoka, C., Kashima, N., Yoshimoto, R., and Hamuro, J. (1983). Structure and expression of a cloned cDNA for human interleukin-2. Nature *302*, 305-310.
- Toso, J.F., Gill, V.J., Hwu, P., Marincola, F.M., Restifo, N.P., Schwartzentruber, D.J., Sherry, R.M., Topalian, S.L., Yang, J.C., Stock, F.*, et al.* (2002). Phase I study of the intravenous administration of attenuated Salmonella typhimurium to patients with metastatic melanoma. Journal of clinical oncology : official journal of the American Society of Clinical Oncology *20*, 142-152.
- Turnbaugh, P.J., Hamady, M., Yatsunenko, T., Cantarel, B.L., Duncan, A., Ley, R.E., Sogin, M.L., Jones, W.J., Roe, B.A., Affourtit, J.P.*, et al.* (2009). A core gut microbiome in obese and lean twins. Nature *457*, 480-484.
- Tzschaschel, B.D., Guzman, C.A., Timmis, K.N., and de Lorenzo, V. (1996). An Escherichia coli hemolysin transport system-based vector for the export of polypeptides: export of Shiga-like toxin IIeB subunit by Salmonella typhimurium aroA. Nature biotechnology *14*, 765-769.
- Uhlich, G.A., Cooke, P.H., and Solomon, E.B. (2006). Analyses of the red-dry-rough phenotype of an Escherichia coli O157:H7 strain and its role in biofilm formation and resistance to antibacterial agents. Applied and environmental microbiology *72*, 2564-2572.
- Vacchelli, E., Aranda, F., Eggermont, A., Galon, J., Sautes-Fridman, C., Zitvogel, L., Kroemer, G., and Galluzzi, L. (2014). Trial Watch: Tumor-targeting monoclonal antibodies in cancer therapy. Oncoimmunology *3*, e27048.
- van der Linden, R.H., Frenken, L.G., de Geus, B., Harmsen, M.M., Ruuls, R.C., Stok, W., de Ron, L., Wilson, S., Davis, P., and Verrips, C.T. (1999). Comparison of physical chemical properties of llama VHH antibody fragments and mouse monoclonal antibodies. Biochimica et biophysica acta *1431*, 37-46.
- van der Woude, M.W., and Henderson, I.R. (2008). Regulation and function of Ag43 (flu). Annual review of microbiology *62*, 153-169.
- van Diemen, P.M., Dziva, F., Stevens, M.P., and Wallis, T.S. (2005). Identification of enterohemorrhagic Escherichia coli O26:H- genes required for intestinal colonization in calves. Infection and immunity *73*, 1735-1743.
- van Nood, E., Vrieze, A., Nieuwdorp, M., Fuentes, S., Zoetendal, E.G., de Vos, W.M., Visser, C.E., Kuijper, E.J., Bartelsman, J.F., Tijssen, J.G.*, et al.* (2013). Duodenal infusion of donor feces for recurrent Clostridium difficile. The New England journal of medicine *368*, 407-415.
- Vandenbroucke, K., de Haard, H., Beirnaert, E., Dreier, T., Lauwereys, M., Huyck, L., Van Huysse, J., Demetter, P., Steidler, L., Remaut, E.*, et al.* (2010). Orally

administered L. lactis secreting an anti-TNF Nanobody demonstrate efficacy in chronic colitis. Mucosal immunology *3*, 49-56.

- Veiga, E., de Lorenzo, V., and Fernandez, L.A. (2004). Structural tolerance of bacterial autotransporters for folded passenger protein domains. Molecular microbiology *52*, 1069-1080.
- Vieira, J., and Messing, J. (1982). The pUC plasmids, an M13mp7-derived system for insertion mutagenesis and sequencing with synthetic universal primers. Gene *19*, 259-268.
- Vincke, C., Gutierrez, C., Wernery, U., Devoogdt, N., Hassanzadeh-Ghassabeh, G., and Muyldermans, S. (2012). Generation of single domain antibody fragments derived from camelids and generation of manifold constructs. Methods in molecular biology (Clifton, NJ) *907*, 145-176.
- Wang, Z., Gerstein, M., and Snyder, M. (2009). RNA-Seq: a revolutionary tool for transcriptomics. Nature reviews Genetics *10*, 57-63.
- Weibel, S., Stritzker, J., Eck, M., Goebel, W., and Szalay, A.A. (2008). Colonization of experimental murine breast tumours by Escherichia coli K-12 significantly alters the tumour microenvironment. Cellular microbiology *10*, 1235-1248.
- Welch, R.A., Burland, V., Plunkett, G., 3rd, Redford, P., Roesch, P., Rasko, D., Buckles, E.L., Liou, S.R., Boutin, A., Hackett, J.*, et al.* (2002). Extensive mosaic structure revealed by the complete genome sequence of uropathogenic Escherichia coli. Proceedings of the National Academy of Sciences of the United States of America *99*, 17020-17024.
- Westphal, K., Leschner, S., Jablonska, J., Loessner, H., and Weiss, S. (2008). Containment of tumor-colonizing bacteria by host neutrophils. Cancer research *68*, 2952-2960.
- Whitman, W.B., Coleman, D.C., and Wiebe, W.J. (1998). Prokaryotes: the unseen majority. Proceedings of the National Academy of Sciences of the United States of America *95*, 6578-6583.
- Wolfe, A.J., and Visick, K.L. (2008). Get the message out: cyclic-Di-GMP regulates multiple levels of flagellum-based motility. Journal of bacteriology *190*, 463-475.
- Xiang, S., Fruehauf, J., and Li, C.J. (2006). Short hairpin RNA-expressing bacteria elicit RNA interference in mammals. Nature biotechnology *24*, 697-702.
- Yang, N., Zhu, X., Chen, L., Li, S., and Ren, D. (2008). Oral administration of attenuated S. typhimurium carrying shRNA-expressing vectors as a cancer therapeutic. Cancer biology & therapy *7*, 145-151.
- Yokota, T., Milenic, D.E., Whitlow, M., and Schlom, J. (1992). Rapid tumor penetration of a single-chain Fv and comparison with other immunoglobulin forms. Cancer research *52*, 3402-3408.
- Yuhua, L., Kunyuan, G., Hui, C., Yongmei, X., Chaoyang, S., Xun, T., and Daming, R. (2001). Oral cytokine gene therapy against murine tumor using attenuated Salmonella typhimurium. International journal of cancer Journal international du cancer *94*, 438-443.
- Zhang, J.P., and Normark, S. (1996). Induction of gene expression in Escherichia coli after pilus-mediated adherence. Science *273*, 1234-1236.
- Zorraquino, V., Garcia, B., Latasa, C., Echeverz, M., Toledo-Arana, A., Valle, J., Lasa, I., and Solano, C. (2013). Coordinated cyclic-di-GMP repression of Salmonella motility through YcgR and cellulose. Journal of bacteriology *195*, 417-428.

ANNEXURES